# EVOLUTION AND TAXONOMY OF THE SILURIAN CONODONT *PTEROSPATHODUS*

*by* PEEP MÄNNIK

ABSTRACT. New data indicate that *Carniodus* is not a separate taxon but the elements considered to belong to it in reality formed a part of the *Pterospathodus* apparatus. The latter contains 14 elements: Pa, $Pb_1$, $Pb_2$, Pc, $M_1$ ($+M_2$ in *P. pennatus procerus*), $Sc_1$, $Sc_2$, $Sc_3$, $Sb_1$, $Sb_2$, Sa, carnuliform with five morphs, carniciform, and curved element with three morphs. Two ecologically distinct lineages existed and evolved separately. One lineage (*P. amorphognathoides angulatus* – *P. amorphognathoides lennarti* ssp. nov. – *P. a. lithuanicus* – *P. a. amorphognathoides*) dominated open shelf carbonate-terrigeneous environments and the other (*P. pennatus pennatus* – *P. p. procerus*) the deeper basinal, graptolite-bearing facies. Both lineages evidently originated from a common ancestral taxon at the top of the *P. eopennatus* Biozone. Three main evolutionary intervals, separated by levels at which the most distinct morphological changes to the elements took place, have been recognized in the *Pterospathodus* sequence. Evolution was more rapid, and the morphological variation within each population considerably higher, in the *P. amorphognathoides* lineage.

*P. a. angulatus* and *P. p. pennatus* are recognized as separate taxa. *P. celloni* has a short range and originated from the *P. pennatus* lineage. Five morphologically distinct chronological populations are recognized in the *P. a. amorphognathoides* range.

*PTEROSPATHODUS* is one of the dominant taxa in Telychian conodont faunas, and Walliser (1964) based the first conodont zonation of this interval on *Pterospathodus* species. The genus has been subsequently widely recognized (for summary see Jeppsson 1987). However, although more than 30 years have passed since the first descriptions of *Pterospathodus*, and although its species have been widely used in stratigraphy, knowledge of this genus is still poor. The limitations of existing knowledge of apparatus structure, taxonomic composition, ecology and evolution of *Pterospathodus* have resulted in many different taxonomic and stratigraphical interpretations (Walliser 1964; Barrick and Klapper 1976; Jeppsson 1979; Mabillard and Aldridge 1983; Bischoff 1986; Männik and Aldridge 1989; etc.). Männik and Aldridge (1989) discussed the evolution and relationships within *Pterospathodus* and documented sequential changes shown by populations. They recognized morphological differences between sinistral and dextral Pa elements, and concluded that pennate forms (with a single unbranched or branched lateral process) and non-pennate forms (without a lateral process), previously treated as separate taxa (*P. angulatus*, *P. pennatus* and *P. celloni*), are conspecific. They assigned all these morphotypes to *P. celloni*.

Now, study of rich and well preserved collections (CAI = 1) from Estonia and Gotland, Sweden (Text-fig. 1; Appendix) has provided detailed information about *Pterospathodus* necessitating a re-evaluation of existing ideas about the taxonomy, evolution and ecology of the genus.

## APPARATUS

The structure of the *Pterospathodus* apparatus is evidently much more complicated than previous studies suggested. The co-occurrence, similarities in evolutionary patterns and in ecology of *Pterospathodus* and *Carniodus* indicate that both sets of elements belonged to the same apparatus.

*Pterospathodus* was originally reconstructed as a bimembrate apparatus (Walliser 1964), and later as a quadrimembrate apparatus including Pa, Pb, M and Sc elements (Barrick and Klapper 1976). Mabillard and Aldridge (1983) recognized a fifth – Sa/Sb – element, although it appeared to be

[Palaeontology, Vol. 41, Part 5, 1998, pp. 1001–1050, 6 pls] 

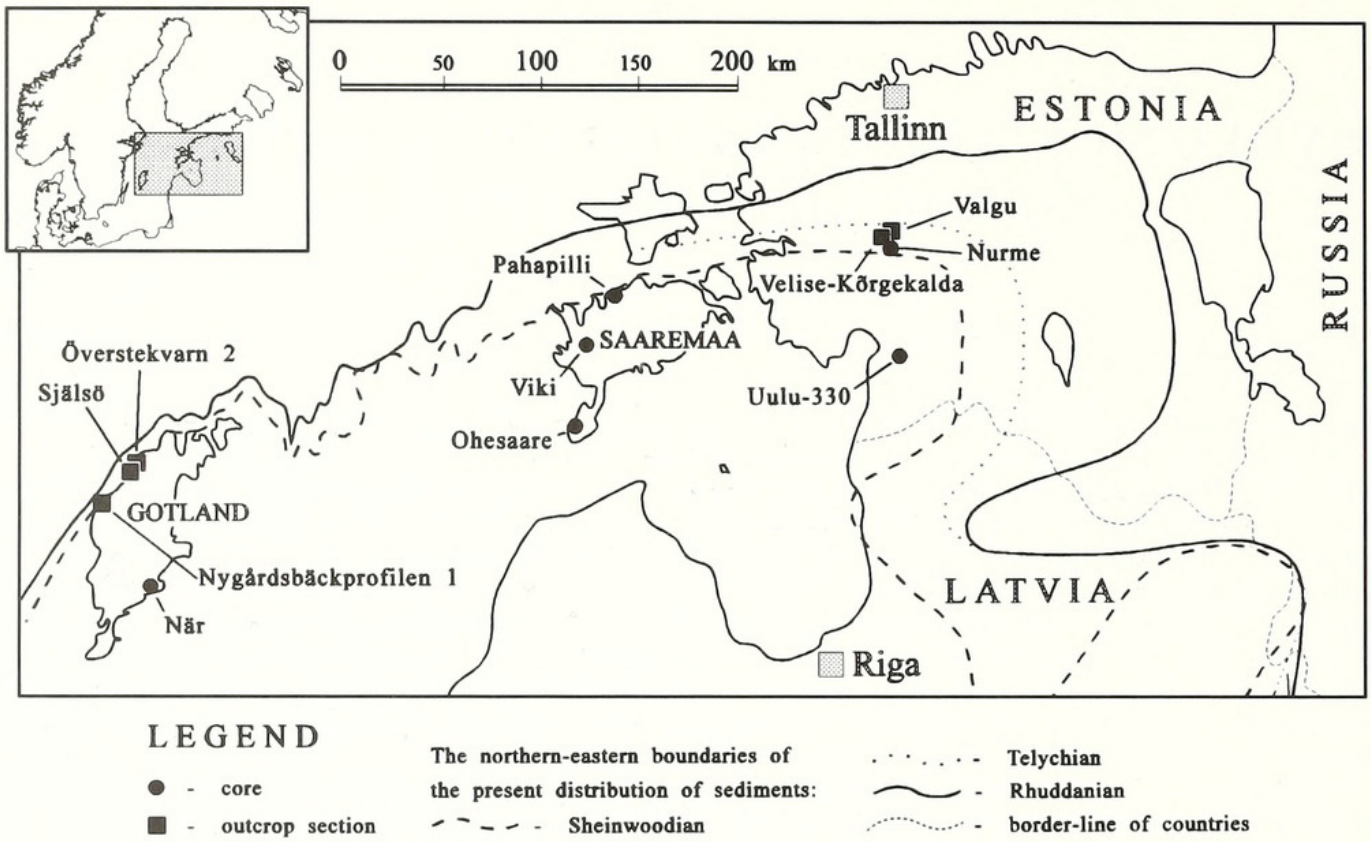


TEXT-FIG. 1. Location of studied sections (for details see Appendix).

morphologically almost identical to its analogue in the *Carniodus* apparatus as reconstructed by Barrick and Klapper (1976). Later, the Sc element of Barrick and Klapper (1976) was re-interpreted to be a Pc element by Aldridge (*in* Männik and Aldridge 1989).

Jeppsson (1979) was the first to propose that elements considered to belong to *Carniodus* in reality formed a part of the *Pterospathodus* apparatus. The main argument against Jeppsson's idea – the difference in stratigraphical ranges (see Männik and Aldridge 1989, pp. 894–895) – has lost its validity in the light of my new information: *Carniodus* has exactly the same stratigraphical range as *Pterospathodus* (Männik 1992). The absence or extreme rarity of *Carniodus* elements in collections from the lowermost part of the *Pterospathodus* range in many sections is most probably caused by their very small size. Small specimens are the most likely to be dissolved or washed away during the laboratory processing of samples.

Each taxon of *Pterospathodus* is associated with a distinct set of elements of *Carniodus* type, and the two sets display parallel evolutionary patterns (see below). It is concluded that *Carniodus* did not exist as a separate apparatus but represents elements of the *Pterospathodus* apparatus, mostly from its primary symmetry transition series. All of the elements (except the Sa) in the *Pterospathodus* apparatus are represented by sinistral and dextral forms, but some of them – $Pb_2$, $Sc_3$, carnuliform (morphs a, b, and short morph) – evidently also include symmetrical forms. Elements are morphologically variable and several morphs can be recognized in all of them. All morphs of the same element are closely related to each other and intermediate morphologies between them exist. Only the most distinctive and stratigraphically valuable morphs are described. Below, the elements are characterized briefly and the possible position of them in the apparatus indicated (Text-fig. 2; the main shape categories of elements according to Sweet 1981, 1988).

1. Pa element – carminate, pastinate and stellate (rare) elements in older strata, stelliscaphate and pastiniscaphate elements in younger strata. Originally described as *Pterospathodus amorphognathoides* s.f., *Spathognathodus celloni* s.f. and *S. pennatus* s.f. (Walliser 1964).

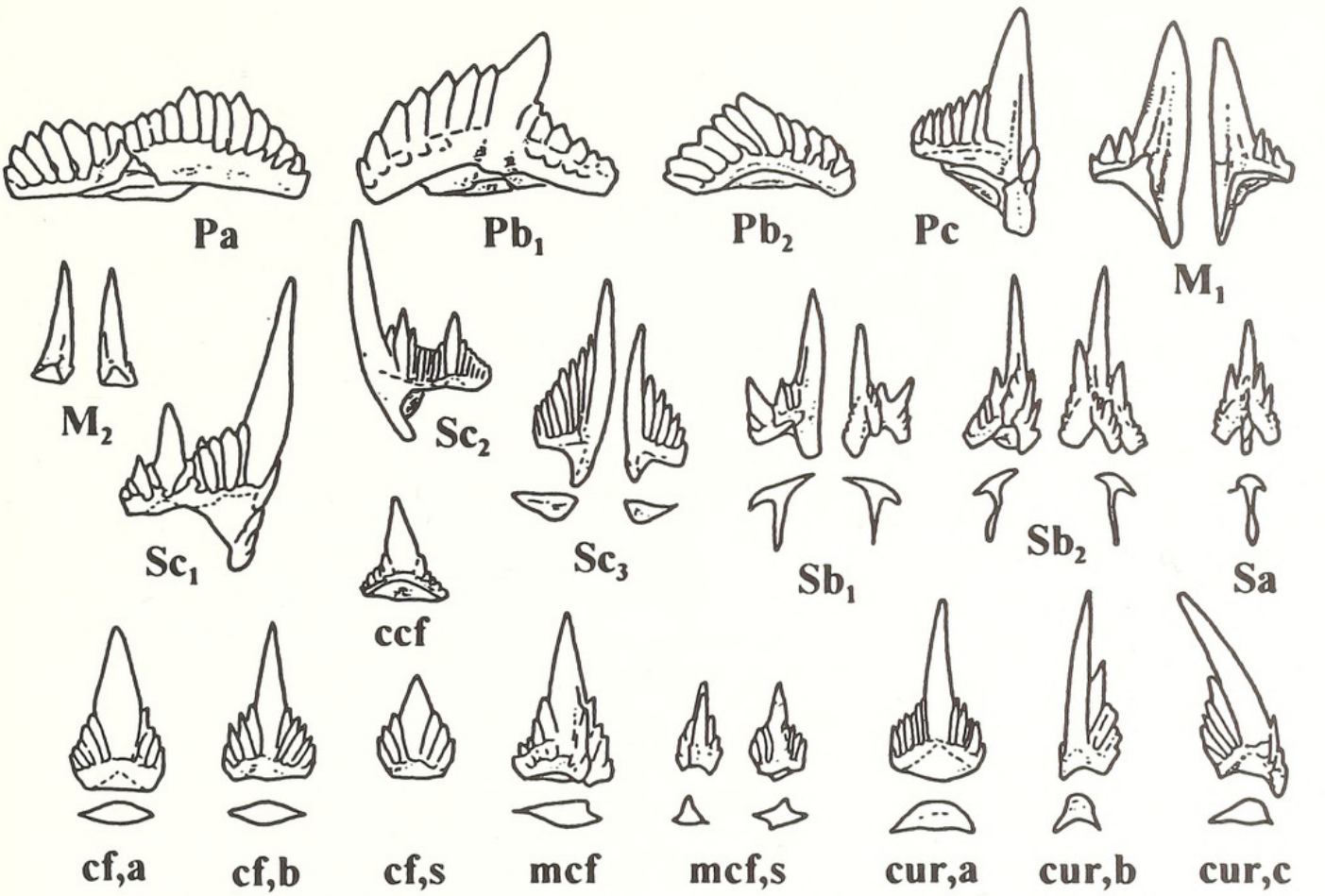


TEXT-FIG. 2. Elements in the *Pterospathodus* apparatus: ccf – carniciform element; cf, a – carnuliform element, morph a; cf, b – carnuliform element, morph b; cf, s – carnuliform element, short morph; mcf – modified carnuliform element; mcf, s – modified carnuliform element, short morph; cur, a – curved element, morph a; cur, b – curved element, morph b; cur, c – curved element, morph c.

2. $Pb_1$ element – angulate (in older strata) to anguliscaphate (in younger strata), with distinct cusp. Originally described as *Ozarkodina adiutricis* s.f. and *O. gaertneri* s.f. (Walliser 1964).
3. $Pb_2$ element – dolobrate (in *P. eopennatus*), angulate (in *P. pennatus* and older part of the *P. a. amorphognathoides* lineage) to anguliscaphate (in *P. a. amorphognathoides*), with poorly developed cusp. Originally described as *Carniodus carinthiacus* s.f. (Walliser 1964).
4. Pc element – pastinate, with short anterior and outer lateral, and longer posterior processes. Originally described as *Neoprioniodus costatus* s.f. (Walliser 1964).
5. $M_1$ element – dolabrate, with short undenticulated anterior (anticusp) and inner lateral processes, and short denticulated posterior process. Originally described as *N. triangularis* s.f. (Walliser 1964).
6. $M_2$ element – dolabrate, similar to $M_1$ but is slender, less curved inside, with shorter processes and without anticusp. Recognized only in the *P. pennatus procerus* apparatus.
7. $Sc_1$ element – bipennate, relatively short anterior process directed steeply downwards and turned only slightly to inner side; longer posterior process almost straight. Originally described as *C. carnus* s.f. (Walliser 1964).
8. $Sc_2$ element – dolabrate, anterior process directed downwards as a well-developed anticusp; denticulated posterior process relatively long. Originally described as *N. subcarnus* s.f. (Walliser 1964).
9. $Sc_3$ element – dolabrate, similar to $Sc_2$ but anticusp is poorly developed; posterior process is short and with denticles which rapidly decrease in size distally. Appears in the *P. eopennatus* ssp. nov. 2 apparatus.

10. $Sb_1$ element – tertiopedate, outer lateral process denticulated, inner one undenticulated (or with few small denticles) and directed steeply downwards as an anticusp; posterior process denticulated and straight. In *P. eopennatus* ssp. nov. 1, *P. eopennatus* ssp. nov. 2 and *P. p. procerus* the distal part of the outer lateral process is bifurcated. Originally described as *Roudya latialata* s.f. (Walliser 1964, pl. 31, fig. 13).
11. $Sb_2$ element – tertiopedate, similar to Sa, but lateral processes are asymmetrical and the posterior process is curved sigmoidally to the outer side. In *P. eopennatus* ssp. nov. 1, *P. eopennatus* ssp. nov. 2 and *P. p. procerus* the distal part of the outer lateral process is bifurcated. Originally described as *R. latialata* s.f. (Walliser 1964, pl. 6, fig. 15; pl. 31, figs 11–12).
12. Sa element – alate, all processes denticulated, lateral processes situated symmetrically. Originally described as *R. latialata* s.f. (Walliser 1964)?
13. Carnuliform element, morph a – angulate to carminate, elements with high base and short processes with few relatively wide short denticles. Elements highly variable, forming a transition series of morphologies from elements with almost symmetrically situated anterior and posterior processes and a vertical cusp at one end of the series to strongly posteriorly inclined elements at the other. The latter type possesses a denticulated posterior process but only a single denticle (or none) anterior to the cusp. Based on the form of the cusp and the curvature of processes sinistral, dextral and symmetrical forms can be recognized. Position in apparatus unknown. Originally described as *C. carnulus* s.f. (Walliser 1964).
14. Carnuliform element, morph b – angulate to carminate, carnuliform element with densely denticulated processes. Denticles higher, thinner and more numerous than those on morph a. Forms a morphology transition series similar to that of morph a. Specimens morphologically intermediate between morphs a and b have been found. Sinistral, dextral and symmetrical elements are recognized. Position in apparatus unknown.
15. Carnuliform element, short morph – angulate to carminate, similar to morph a but with short cusp. Less common than morphs a and b. Sinistral, dextral and probably also symmetrical elements exist. Position in apparatus unknown. Appears in the *P. amorphognathoides lennarti* ssp. nov. apparatus.
16. Modified carnuliform element – pastinate, carnuliform element with short straight denticulated outer lateral process. Position in apparatus unknown.
17. Modified carnuliform element, short morph – pastinate and stellate, short morph of carnuliform element with short denticulated lateral process on one or both sides of the element. Position in apparatus unknown. Appears in the *P. amorphognathoides lennarti* ssp. nov. apparatus.
18. Carniciform element – angulate to carminate, elements relatively short, triangular in lateral view, with cusp strongly curved to the inner side. Forms a transition series of morphology from elements with almost symmetrically situated processes and vertical (in lateral view) cusp to those with the cusp moderately inclined posteriorly. Position in apparatus unknown.
19. Curved element, morph a – angulate to carminate, element with high base, high vertical cusp and densely denticulated lateral processes considerably turned to inner side. The length of the processes varies. Position in apparatus unknown.
20. Curved element, morph b – angulate, similar to morph a of curved element but processes shorter and strongly turned to the inner side. Position in apparatus unknown.
21. Curved element, morph c – angulate, resembles morph a of curved element but differs by having fewer and larger denticles on the processes. As a rule the cusp is inclined posteriorly. Position in apparatus unknown. Appears in the *P. amorphognathoides lithuanicus* apparatus.

Hence, the *Pterospathodus* apparatus is probably made of 14 different elements: Pa, $Pb_1$, $Pb_2$, Pc, $M_1$ (joined by the $M_2$ element in the *P. pennatus procerus* apparatus), $Sc_1$, $Sc_2$, $Sc_3$, $Sb_1$, $Sb_2$, Sa and three main groups (carnuliform, carniciform and curved) of highly variable elements with unknown positions in the apparatus. This is many more than is usually recognized in Ordovician and Silurian conodonts. No apparatus known so far from a natural, bedding plane assemblage has so many elements. However, it is quite possible that the carnuliform element at least instead of occupying a

separate position in the apparatus in reality belonged to some of the S elements and its morphology transition series formed continuations of the (posterior) processes of the S elements. The positions of elements, identified here as $Pb_2$, $M_2$ and $Sc_3$, and not known in any other apparatus, are still problematical. The notation used for them in this paper only indicates that, morphologically, these elements are closest to those traditionally considered to occupy the Pb, M and Sc positions respectively in the conodont apparatuses.

## SYSTEMATIC PALAEONTOLOGY

Considerable revisions of the taxonomy of *Pterospathodus* are required by the new data. Contrary to the conclusions of Männik and Aldridge (1989), *P. angulatus* and *P. pennatus* are here recognized as separate taxa belonging to different lineages. *P. pennatus* is represented by two chronological subspecies: *P. p. pennatus* and *P. p. procerus*. *P. angulatus* is recognized as the oldest representative of the *P. amorphognathoides* lineage: *P. a. angulatus*.

It appears that the fauna from the Jõhve core discussed in Männik and Aldridge (1989, text-fig. 2) represents only a part (from the *A. kuehni* Subzone to Population 3 of the *P. a. amorphognathoides* Zone above; see Text-fig. 3 and Männik 1995) of the range of *Pterospathodus* in Estonia. No elements of *P. celloni s.s.* were found during a restudy of the Jõhve core collection. The form, identified previously as *P. celloni* in Estonia (and probably also in many collections from other regions of the world – restudy of collections is needed) appears to be multitaxonomic. It is here reidentified as *P. eopennatus* ssp. nov. 1, *P. eopennatus* ssp. nov. 2, *P. a. angulatus* and *P. a. lennarti* ssp. nov.

In the descriptions below only brief characterizations of the morphological features essential to identify each taxon are given.

Figured specimens from Estonia are deposited in the Institute of Geology, Tallinn Technical University, Tallinn, Estonia, and those from Gotland in the Department of Historical Geology and Palaeontology, Lund University, Lund, Sweden.

### Genus PTEROSPATHODUS Walliser, 1964

*Type species. Pterospathodus amorphognathoides* Walliser, 1964, from the Telychian, Cellon, Austria.

*Remarks. Pterospathodus* is a morphologically complicated genus which evolved rapidly. Eight taxa, representing three distinct lineages (treated here as species) – *P. eopennatus*, *P. pennatus* and *P. amorphognathoides* – are recognized in the Estonian sequence.

In many regions (Alaska – Savage 1985; Australia – Bischoff 1986; north-western Canada – Over and Chatterton 1987; McCracken 1991; Greenland – Armstrong 1990) *P. rhodesi*, all elements of which are characterized by extremely wide platforms/platform ledges, replaced or co-existed with *P. a. amorphognathoides*. The origin of *P. rhodesi* and its relationship to other taxa of *Pterospathodus* are not yet known.

It is possible that also some other species of *Pterospathodus* existed. *Pterospathodus* aff. *P. amorphognathoides* (Nowlan 1981, pl. 7, figs 2–3, 5; later reidentified as *Pterospathodus* n. sp. A by Nowlan 1983), *Pterospathodus* n. sp. B (Nowlan 1983, fig. 4 J, L, Q–R, U) and a conodont identified by Nowlan as *P. pennatus* (Nowlan 1981, pl. 7, figs 1, 4) have been described from eastern Canada (Gaspé Peninsula). *Pterospathodus* n. sp. A has been recognized also on Severnaya Zemlya (Männik, 1983, fig. 5 P) and in the Timan-Pechora region (Melnikov, pers. comm.). It is noteworthy that in all these regions 'real' *Pterospathodus* is extremely rare (Gaspé Peninsula and Timan-Pechora region) or absent (Severnaya Zemlya). So far, only the Pa element of *Pterospathodus* n. sp. A, *Pterospathodus* n. sp. B, and *P. pennatus sensu* Nowlan (1981) are known. It is evident that all these taxa are closely related to each other. However, their relations to the *Pterospathodus* described below are not clear and need further studies.

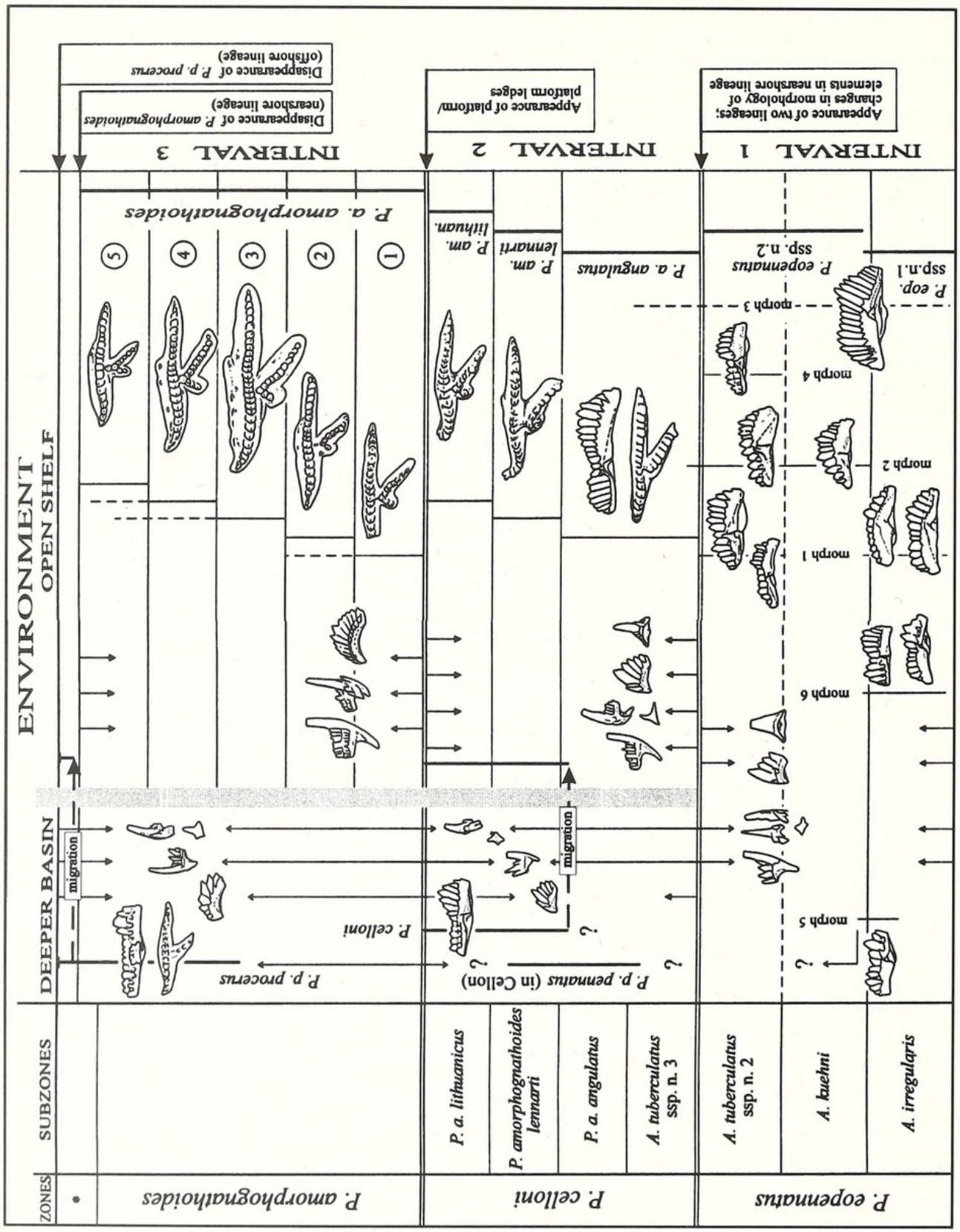


TEXT-FIG. 3. Evolution of *Pterospathodus*. Thick vertical lines – distribution of taxa; '?' at the ends of lines – distribution not known. Thin vertical lines – distribution of selected elements (dotted line = rare occurrence). Thin lines with arrows at the ends – indicate relationships between taxa or similarities between particular elements. Arrows with '?' – relations possible but not proved. Short arrows starting from the boundaries between the zones and pointing to the figures of elements – figured types of elements disappear (arrow points down) or appear (arrow points up) at the indicated boundary. Numbers in circles – populations in *P. a. amorphognathoides*. * – zonation for this interval in Jeppsson (1994, 1997).

Several other taxa, originally also described as species of *Pterospathodus*, appear to belong to some other genera. *P. posteritenuis* (Uyeno and Barnes 1983, pl. 2, figs 1–11, 14–18) is, most probably, identical to *Pranognathus tenuis* (Männik and Aldridge 1989, text-fig. 5). The apparatus of *P. cadiaensis* of Bischoff (1986) was studied in detail by Wang and Aldridge (1996), and reidentified as *Gamachignathus macroexcavatus*. *P. retroramus* of McCracken (1991, pl. 4, figs 24–25; pl. 5, figs 1–5, 8) is most probably related to *Astropentagnathus*, not to *Pterospathodus*.

P. eopennatus *lineage*

*P. eopennatus* sp. nov.

| | |
|---|---|
| 1971 | *Spathognathodus celloni* Walliser, 1964; Schönlaub, p. 44, pl. 2, figs 1–5. |
| p 1971 | *Carniodus carinthiacus* Walliser, 1964; Schönlaub, p. 46, pl. 3, fig. 6 (*non* figs 7–8 [= *P. a. amorphognathoides*]). |
| vp .1972 | *Neoprioniodus costatus paucidentatus* Walliser, 1964; Aldridge, p. 193, pl. 5, fig. 21 (*non* fig. 20 [indet.]). |
| v. 1972 | *Ozarkodina adiutricis* Walliser, 1964; Aldridge, p. 198, pl. 5, figs 2–3. |
| .1975 | *Llandoverygnathus celloni* (Walliser, 1964); Aldridge, pl. 1, figs 20–21. |
| *non* 1975 | *Llandoverygnathus celloni* (Walliser, 1964); Schönlaub, p. 53, pl. 1, figs 18–19 ([= *Aulacognathus*? sp.]). |
| 1978 | *Neoprioniodus costatus paucidentatus* Walliser, 1964; Miller, pl. 2, fig. 12. |
| 1978 | *Exochognathus brevialatus* (Walliser, 1964); Miller, pl. 3, figs 7–8. |
| 1978 | *Ozarkodina adiutricis* Walliser, 1964; Pickett, pl. 1. fig. 27. |
| 1978 | *Neospathognathodus pennatus* (Walliser, 1964); Pickett, pl. 1, figs 24–25. |
| .1979 | *Carniodus* sp. Aldridge, p. 12, pl. 1, fig. 8. |
| .1979 | *Llandoverygnathus celloni* (Walliser, 1964); Aldridge, pl. 1, figs 9–10. |
| .1979 | *Llandoverygnathus pennatus* (Walliser, 1964); Aldridge, pl. 1, fig. 11. |
| .1979 | *Llandoverygnathus* sp. 12 Aldridge, pl. 1, figs 12–15. |
| 1980 | *Pterospathodus celloni* (Walliser, 1964); Aldridge, fig. 1. |
| p? 1983 | simple cone element, group 'c' Uyeno and Barnes, p. 26, pl. 8, figs 6–7, 9–12, 18? (*non* fig. 19 [indet.]). |
| .1985 | *Pterospathodus celloni* (Walliser, 1964); Aldridge, p. 80, pl. 3.1, figs 25–26. |
| 1985 | *Pterospathodus celloni* (Walliser, 1964); Qiu, pl. 1, figs 1–2. |
| v. 1986 | *Pterospathodus celloni* (Walliser, 1964); Bischoff, p. 194, pl. 28, figs 34–39; pl. 29, figs 1–8. |
| v. 1986 | *Pterospathodus pennatus* (Walliser, 1964); Bischoff, p. 200, pl. 30, figs 12–14, 23–30. |
| ? 1986 | *Pterospathodus pennatus* (Walliser, 1964); Jiang *et al.*, pl. 4, fig. 3. |
| p? 1986 | *Spathognathodus celloni* Walliser, 1964; Jiang *et al.*, pl. 4, figs 5, 17 (*non* fig. 6 [indet.]). |
| ? 1987 | *Pterospathodus celloni* (Walliser, 1964); Over and Chatterton, p. 2, fig. 1. |
| 1988 | *Pterospathodus celloni* (Walliser, 1964); Qiu, pl. 1, fig. 3 [cop. Qiu 1985, pl. 1, fig. 1]. |
| v. 1989 | *Pterospathodus*, celloni-morph Männik and Aldridge, text-fig. 3*A*. |
| 1990 | *Carniodus* sp. Armstrong, pl. 8, fig. 5. |
| 1990 | *Pterospathodus celloni* (Walliser, 1964); Armstrong, p. 118, pl. 19, figs 6–14. |
| 1990 | *Pterospathodus pennatus pennatus* (Walliser, 1964); Armstrong, p. 119, pl. 19, figs 15–17. |
| 1990 | *Pterospathodus celloni* (Walliser, 1964); Uyeno, p. 65, pl. 3, figs 1–7, 13–14; pl. 11, figs 25–30. |
| p 1990 | *Pterospathodus* cf. *P. celloni* (Walliser, 1964); Uyeno, pl. 11, figs 18–20 (*non* pl. 3, figs 8–10 [= *Astropentagnathus*? sp.]). |
| v. 1990 | *Pterospathodus celloni* (Walliser, 1964); Männik and Viira, pl. 17, figs 18, 21. |
| ? 1991 | *Pterospathodus celloni* (Walliser, 1964); McCracken, p. 109, pl. 4, figs 4–11. |
| ? 1996 | *Carniodus carnulus* Walliser, 1964; Wang and Aldridge, pl. 4, fig. 12. |
| ? 1996 | *Pterospathodus celloni* (Walliser, 1964); Wang and Aldridge, pl. 5, figs 2–3. |

*Derivation of name*. In reference to the morphological similarity and postulated direct evolutionary relationship to *P. pennatus*.

*Holotype*. Pa element Cn 7879, Nurme core, sample M-889, int. 30·20–30·30 m; Plate 1, figure 19.

*Type horizon and locality*. Lower part of the Velise Formation, Adavere Regional Stage, Telychian; Nurme core, interval 14·00–30·30 m.

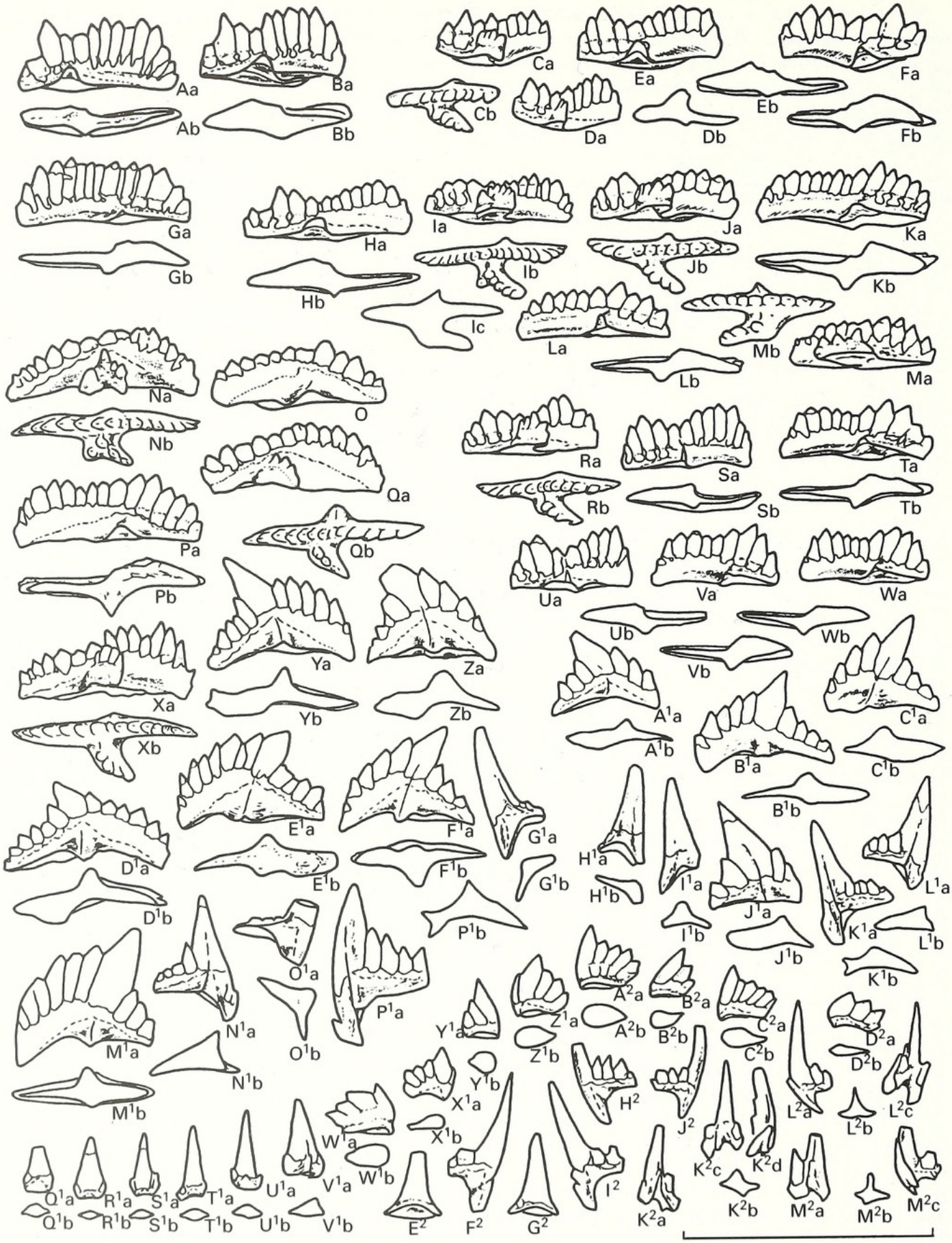


TEXT-FIG. 4. For caption see opposite.

*Diagnosis*. Pa element morphologically highly variable, with a pennate inner lateral process. $Pb_2$ element without anterior process. Posterior processes of S elements evenly denticulated. Processes of carniciform element undenticulated.

*Description*. Pa element is represented by eight main morphs.

*Morph 1a* – elements relatively long (up to 16–18 denticles). Sinistral elements (Pl. 1, figs 18–19; Pl. 2, fig. 35; Text-figs 4P, 5M, R–S), as a rule, without lateral process. The denticles are lower in the middle of the blade and relatively higher at each end. Dextral elements (Pl. 1, figs 10, 20, 22; Pl. 2, figs 34, 40; Text-figs 4X, 6A) differ by having a pennate lateral process and have higher denticles only at the anterior end of the blade. Both sinistral and dextral elements possess a short, triangular, generally undenticulated outer lateral lobe or process (a few specimens have a single denticle on it). Basal cavity deep and wide under posterior part of element. The lower line of the denticle roots turns steeply down in the posterior part of the blade.

*Occurrence*. Appears in the *A. irregularis* Subzone, is quite rare in the *A. kuehni* Subzone, but becomes common in the *A. tuberculatus* ssp. nov. 2 Subzone.

*Morph 1b* (Pl. 1, fig. 21; Text-figs 4N–O, Q, 6E–F, J–K) – similar to morph 1a but differs from it by having considerably shorter denticles and a higher base. Rare dextral specimens may possess a bifurcated lateral process (Text-fig. 4N).

*Occurrence*. The same as for morph 1a.

*Morph 2a* – short elements with distinctly higher denticles on the posterior part (sinistral element – Pl. 2, figs 32, 37, 39; Text-figs 5L, 6I, N, T) or anterior part (dextral element – Pl. 2, figs 23, 36; Text-figs 5J–K, 6G–H, M) of the blade. Lateral process better developed on the dextral element. Short triangular undenticulated lateral process is common on the outer side on both elements. Denticles are relatively tall.

*Occurrence*. Appears in the uppermost part of the *A. irregularis* Subzone and reaches the *A. tuberculatus* ssp. nov. 3 Subzone. Dominates in the *A. kuehni* Subzone but is less common below and above that interval.

*Morph 2b* (Text-fig. 5O–P) – similar to morph 2a; differs from it by having shorter denticles and higher base.

*Occurrence*. The same as for morph 2a, but morph 2b is less common.

*Morph 3* (Pl. 1, figs 16–17; Text-figs 4A–B, G, 5D, G–I, 7H–I, Q) – dextral and sinistral forms almost identical. Elements relatively long with narrow, tall denticles. Denticle roots (white matter) almost reaches the base line on the distal parts of the blade. The denticles are somewhat lower near the cusp but higher on the distal parts of the blade. A denticulated lateral process is common on dextral, but rare on sinistral elements. Basal cavity shallow and narrow.

*Occurrence*. Relatively rare but occasionally present from the *A. irregularis* Subzone to *A. tuberculatus* ssp. nov. 3 Subzone.

*Morph 4* (Pl. 2, figs 33, 38, 41; Text-fig. 6L, O–P, U) – relatively short, anterior denticles highest proximally, decreasing gradually in height in the distal direction. Posterior denticles are considerably shorter. The sharp decrease in the height of denticles just behind the cusp is the most characteristic feature of this morph. Intermediates between morphs 4 and 2 have been found.

*Occurrence*. *A. tuberculatus* ssp. nov. 2 Subzone.

---

TEXT-FIG. 4. *Pterospathodus eopennatus* ssp. nov. 1; *Astropentagnathus irregularis* Subzone. A–B, G, Pa element, morph 3. C–F, H–M, Pa element, morph 5. N–O, Q, Pa element, morph 1b. P, X, Pa element, morph 1a. R–W, Pa element, morph 6. Y–Z, $A^1$–$F^1$, $J^1$, $M^1$, $Pb_1$ element. $W^1$–$D^2$, $Pb_2$ element. $G^1$–$I^1$, $O^1$, $M_1$ element; $K^1$–$L^1$, $N^1$, $P^1$, Pc element. $Q^1$–$U^1$, carnuliform element, morph a. $V^1$, modified carnuliform element. $E^2$, $G^2$, carniciform element. $F^2$, $I^2$, $Sc_1$ element. $H^2$, $J^2$, $Sc_2$ element. $K^2$, $Sb_2$ element. $L^2$, Sa element. $M^2$, $Sb_1$ element. Scale bar represents 1 mm.

*Morph 5* – both sinistral (Pl. 1, figs 25–27, 33; Text-figs 4F, K–M, 5B–C, F) and dextral (Pl. 1, figs 28(?), 30, 35–36; Text-figs 4C–E, H–J, 5A, E) forms relatively short with higher denticles close to the ends of the blade. Those on the anterior blade are slightly higher than on the posterior. Basal margin almost straight in lateral view (Pl. 1, figs 26, 30; Text-fig. 4H–M) or slightly convex (Pl. 1, fig. 28(?); Text-fig. 4C–F). Inner denticulated lateral process well developed on both forms. Shorter outer lateral process better developed (often bearing one or two denticles) on the sinistral forms.

*Occurrence*. Upper part of the *A. irregularis* Subzone and the lowermost part of the *A. kuehni* Subzone.

*Morph 6* (Pl. 1, figs 23(?), 24, 29, 34; Text-fig. 4R–W) – similar to morph 5 but differs by being relatively shorter, possessing higher denticles (particularly on dextral elements – Pl. 1, figs 29, 34; Text-fig. 4R–S, U) and having poorly developed lateral process(es).

*Occurrence*. *A. irregularis* Subzone.

---

EXPLANATION OF PLATE 1

Figs 1–9, 11–15. *Pterospathodus eopennatus* ssp. nov. 2. 1, Cn 7861; outer lateral view of sinistral $Pb_1$ element. 2, Cn 7862; outer lateral view of dextral $Pb_2$ element. 3, Cn 7863; posterior view of dextral $Sb_2$ element. 4, Cn 7864; outer lateral view of sinistral modified carnuliform element. 5, Cn 7865; outer lateral view of dextral curved element, morph a. 6, Cn 7866; inner lateral view of dextral $Sc_2$ element. 7, Cn 7867; outer lateral view of sinistral carnuliform element, morph a. 8, Cn 7868; posterior view of sinistral $Sb_1$ element. 9, Cn 7869; inner lateral view of dextral carniciform element. 11, Cn 7870; outer lateral view of dextral $Pb_1$ element. 12, Cn 7871; inner lateral view of dextral $Sc_3$ element. 13, Cn 7872; inner lateral view of dextral $Sc_1$ element. 14, Cn 7873; outer lateral view of dextral Pc element. 15, Cn 7874; outer lateral view of dextral $Pb_1$ element. Figs 1 and 11 from Nurme core, sample M-900, int. 22·65–22·80 m; figs 2–3, 5, 8 and 14 from Nurme core, sample M-907, int. 17·50–17·60 m; figs 4, 6–7, 9, 12–13 and 15 from Viki core, sample M-8, int. 168·60–168·80 m.

Figs 10, 16–46. *Pterospathodus eopennatus* ssp. nov. 1. 10, Cn 7875; inner lateral view of dextral Pa element, morph 1a. 16, Cn 7876; inner lateral view of sinistral Pa element, morph 3. 17, Cn 7877; inner lateral view of dextral Pa element, morph 3. 18, Cn 7878; inner lateral view of sinistral Pa element, morph 1a. 19, Cn 7879; inner lateral view of sinistral Pa element, morph 1a. 20, Cn 7880; upper view of dextral Pa element, morph 1a. 21, Cn 7881; inner lateral view of sinistral Pa element, morph 1b. 22, Cn 7882; inner lateral view of dextral Pa element, morph 1a. 23, Cn 7883; inner lateral view of sinistral Pa element, morph 6(?). 24, Cn 7884; inner lateral view of sinistral Pa element, morph 6. 25, Cn 7885; inner lateral view of sinistral Pa element, morph 5. 26, Cn 7886; inner lateral view of sinistral Pa element, morph 5. 27, Cn 7887; upper view of sinistral Pa element, morph 5. 28, Cn 7888; inner lateral view of dextral Pa element, morph 5(?). 29, Cn 7889; inner lateral view of dextral Pa element, morph 6. 30, Cn 7890; inner lateral view of dextral Pa element, morph 5. 31, Cn 7891; outer lateral view of dextral Pc element. 32, Cn 7892; outer lateral view of dextral Pc element. 33, Cn 7893; upper view of sinistral Pa element, morph 5. 34, Cn 7894; inner lateral view of dextral Pa element, morph 6. 35, Cn 7895; upper view of dextral Pa element, morph 5. 36, Cn 7896; upper view of dextral Pa element, morph 5. 37, Cn 7897; outer lateral view of sinistral Pc element. 38, Cn 7900; lateral view of symmetrical $Pb_2$ element. 39, Cn 7899; outer lateral view of dextral $Pb_2$ element. 40, Cn 7898; outer lateral view of sinistral $Pb_2$ element. 41, Cn 7901; outer lateral view of sinistral $Pb_1$ element. 42, Cn 7902; outer lateral view of sinistral $Pb_1$ element. 43, Cn 7903; outer lateral view of dextral $Pb_1$ element. 44, Cn 7904; inner lateral view of sinistral $Sc_2$ element. 45, Cn 7905; inner lateral view of dextral $Sc_2$ element. 46, Cn 7906; inner lateral view of sinistral carniciform element. Figs 10, 18, 20 and 21 from Valgu section, sample M-882; figs 16–17 from Nurme core, sample M-891, int. 29·10–29·20 m; figs 19, 22 and 32 from Nurme core, sample M-889, int. 30·20–30·30 m; figs 23–24, 34 and 41–43 from Viki core, sample M-954, int. 183·17–183·32 m; figs 25, 28 and 35 from Viki core, sample M-960, int. 181·81–181·91 m; fig. 26 from Viki core, sample M-956, int. 182·90–183·04 m; figs 27, 31 and 37 from Viki core, sample M-962, int. 181·29–181·40 m; fig. 29 from Viki core, sample M-958, int. 182·22–182·30 m; figs 30, 33 and 36 from Nurme core, sample M-890, int. 29·50–29·60 m; figs 38–40, 44–46 from Nurme core, sample M-903, int. 20·40–20·50 m.

All × 50.

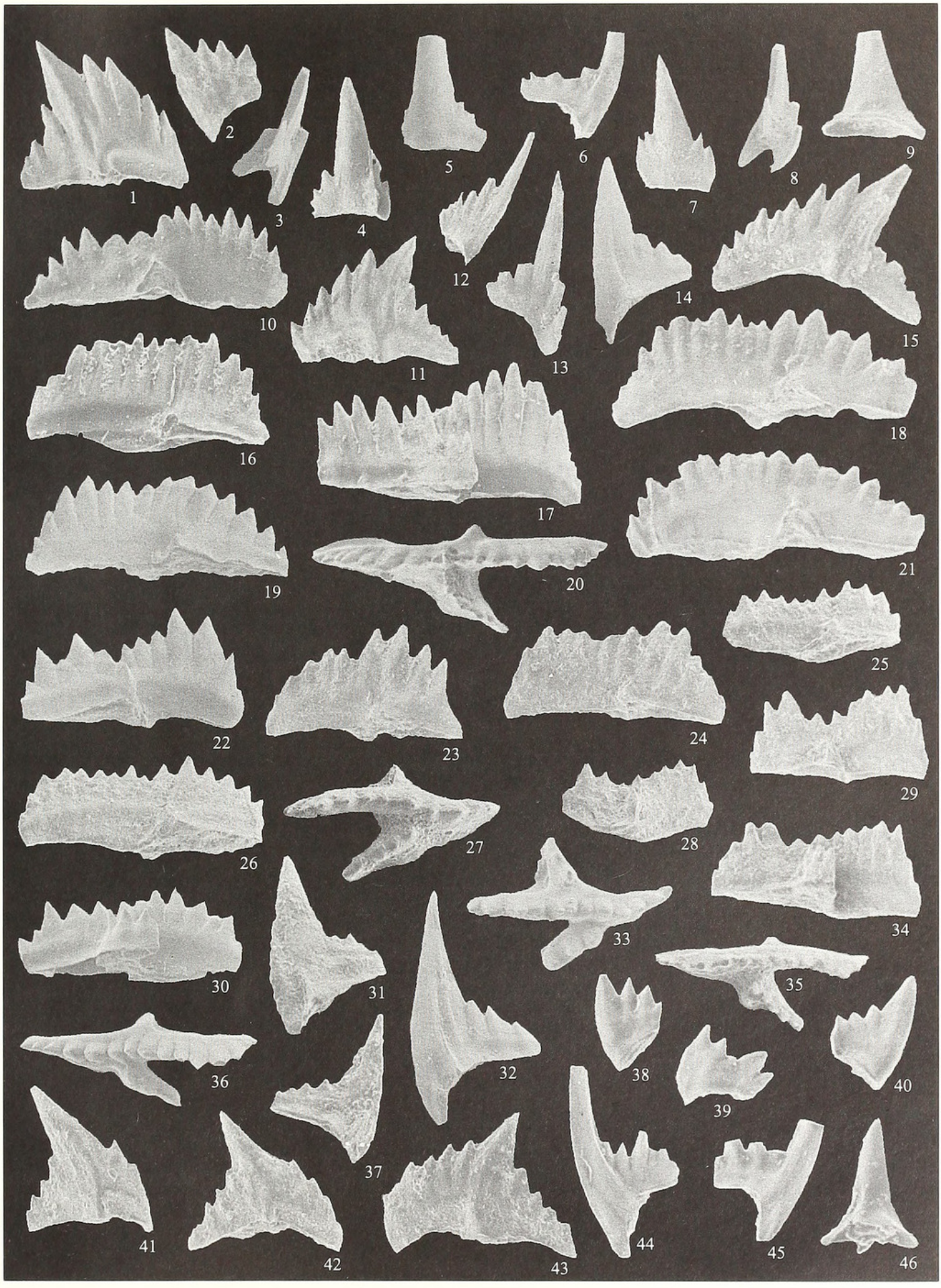


MÄNNIK, *Pterospathodus*

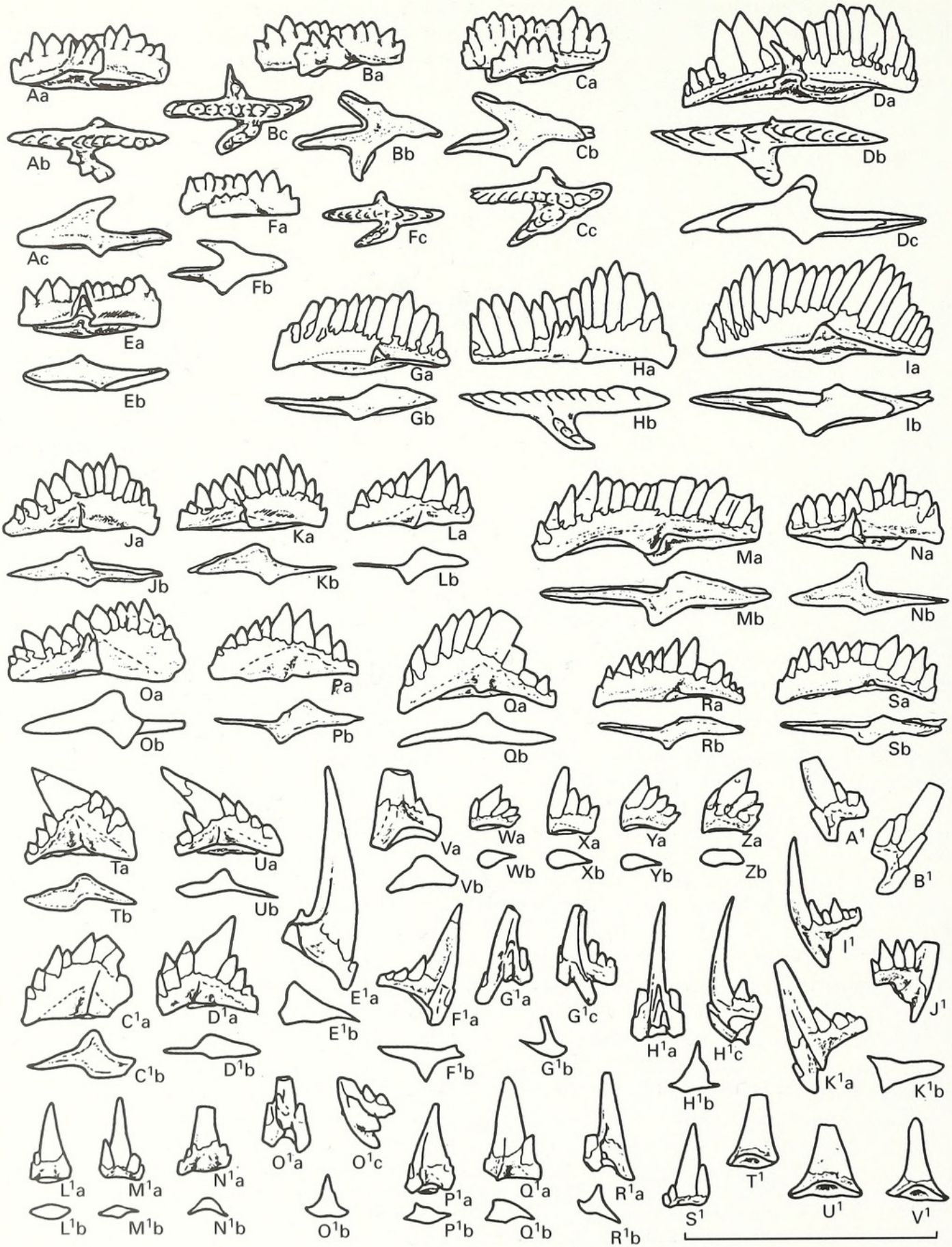


TEXT-FIG. 5. For caption see opposite.

*Remarks.* In all morphs the sinistral and dextral forms of the Pa element are morphologically different from each other. The pennate inner lateral process tends to be more common on the dextral element. In this paper two populations, evolutionarily connected and stratigraphically following each other, are described as subspecies of *P. eopennatus*: *P. eopennatus* ssp. nov. 1 and *P. eopennatus* ssp. nov. 2.

*P. eopennatus* can be recognized world-wide (see synonymy). However, a revision of collections is needed to identify subspecies.

### *Pterospathodus eopennatus* ssp. nov. 1

Plate 1, figures 10, 16–46; Text-figures 4, 5A–C, E–F

*Material.* Several hundred to over a thousand of each of Pa, $Pb_1$ and Pc elements; tens to hundreds of $Pb_2$, M, $Sc_1$, $Sc_2$, Sb, Sa and carnuliform elements; few tens of carniciform elements.

*Diagnosis. P. eopennatus* with Pa element represented by morphs 1a, 1b, 3, 5 and 6; the last two are found only in this taxon. $Pb_1$ element relatively long, arched in lateral view.

*Remarks.* The relative abundance of morphs varies in different parts of the studied area. Morphs 1a and 1b dominate faunas in the continental part of Estonia whereas morph 6 is the most abundant in the Viki core from the western part of the island of Saaremaa (Text-fig. 1). However, all morphs described above have been found in all studied sections from this interval.

*Occurrence. A. irregularis* Subzone and the lowermost part of the *A. kuehni* Subzone.

### *Pterospathodus eopennatus* ssp. nov. 2

Plate 1, figures 1–9, 11–15; Plate 2, figures 23, 32–41; Text-figures 5D, G–V¹, 6

v. 1998 *Pterospathodus* sp. nov. e Männik and Małkowski, pl. 1, figs 19, 23–25, 27.

*Material.* Several hundred Pa and $Pb_1$ elements; tens to hundreds of $Pb_2$, Pc, M, $Sc_1$ and $Sc_2$ elements; a few tens of $Sc_3$, Sb, Sa, carnuliform and carniciform elements.

*Diagnosis. P. eopennatus* with the Pa element represented by morphs 1a, 1b, 2a, 2b, 3 and 4. $Pb_1$ element short and triangular in lateral view.

*Remarks.* $Pb_1$ element dominated by forms which are relatively short and almost triangular in lateral view (Pl. 1, figs 1, 11; Text-figs 5T–U, C¹–D¹, 6Q–R). Rare specimens with a longer anterior process (Pl. 1, fig. 15; Text-fig. 5Q) may be found in the lower part of the *P. eopennatus* ssp. nov. 2 range but become dominant in the upper part (in the *A. tuberculatus* ssp. nov. 2 Subzone). Other elements are morphologically identical in both subspecies.

Two chronological populations are recognized in the range of *P. eopennatus* ssp. nov. 2.

1. The population in the *A. kuehni* Subzone (Text-fig. 5D, G–V¹) is dominated by morph 2a; morphs 1a and 1b are rare and morph 3 can be found occasionally.
2. The population in the *A. tuberculatus* ssp. nov. 2 Subzone (Text-fig. 6) is dominated by morphs 1a and 1b; morphs 2a and 2b occur but are rare. Morph 4 is restricted to this subzone. Also, the oldest $Sc_3$ elements (Pl. 1, fig. 12; Text-fig. 6I¹–K¹) found so far come from this population.

*Occurrence. A. kuehni* and *A. tuberculatus* ssp. nov. 2 subzones.

---

TEXT-FIG. 5. *Pterospathodus eopennatus* ssp. nov.; *Aulacognathus kuehni* Subzone. A–C, E–F. *Pterospathodus eopennatus* ssp. nov. 1, Pa element, morph 5. D, G–V¹, *Pterospathodus eopennatus* ssp. nov. 2. D, G–I, Pa element, morph 3. J–L, Pa element, morph 2a. M–N, R–S, Pa element, morph 1a. O–P, Pa element, morph 2b. Q, T–U, C¹–D¹, $Pb_1$ element. V, E¹, $M_1$ element. W–Z, $Pb_2$ element. A¹–B¹, $Sc_1$ element. F¹, K¹, Pc element. H¹, $Sb_2$ element. G¹, R¹, $Sb_1$ element. I¹–J¹, $Sc_2$ element. L¹–M¹, S¹, carnuliform element, morph a. N¹, curved element, morph a. O¹, Sa element. P¹–Q¹, modified carnuliform element. T¹–V¹, carniciform element. Scale bar represents 1 mm.

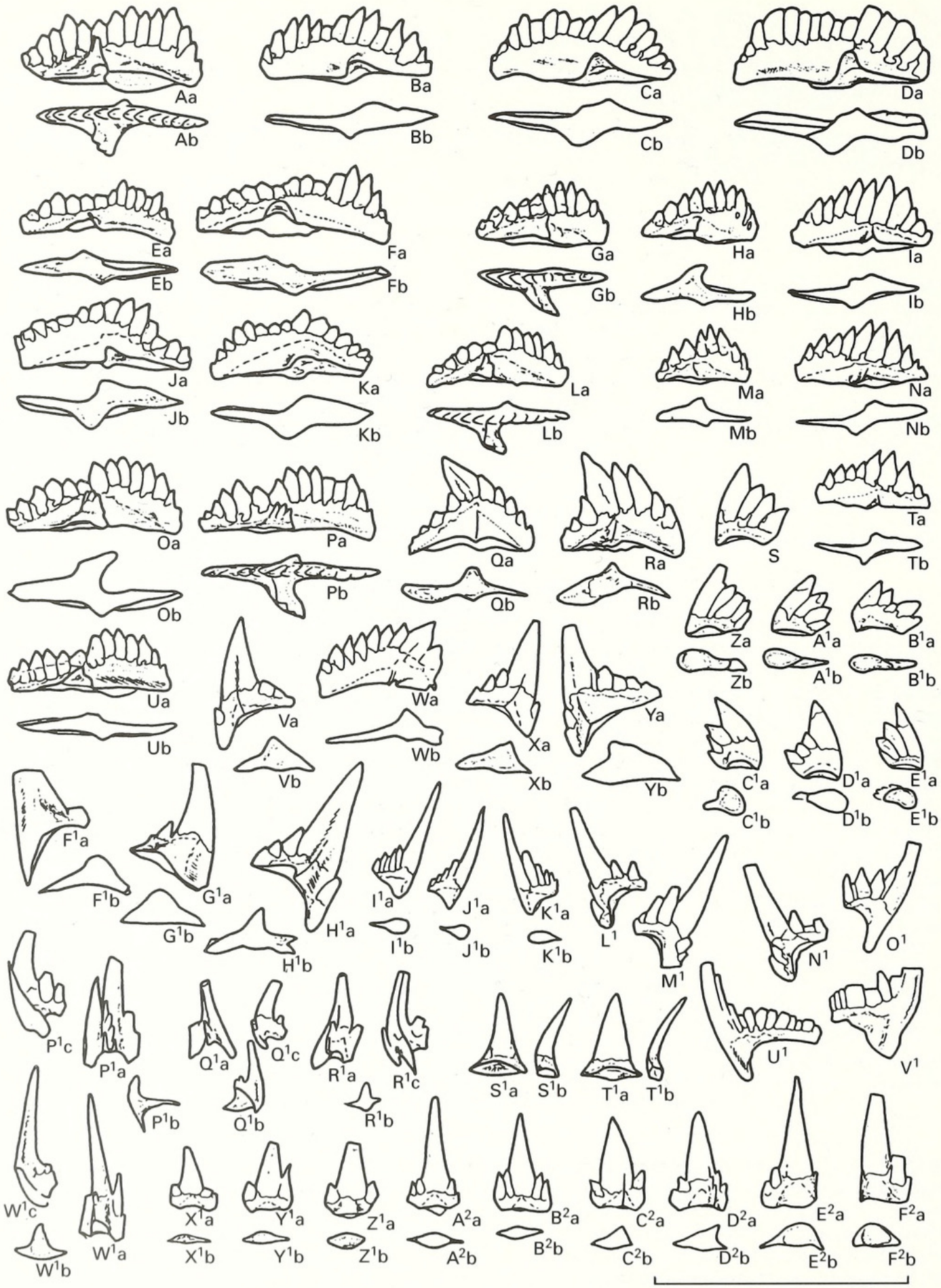


TEXT-FIG. 6. For caption see opposite.

P. amorphognathoides *lineage*

*Pterospathodus amorphognathoides* Walliser, 1964 *sensu nov.*

*Diagnosis.* The Pa element of *P. amorphognathoides* is characterized by an inner lateral process, pennate in the older and bifurcated in the younger forms; with (in younger populations) or without (in older ones) a basal platform; may or may not possess a triangular to semiquadrate lateral lobe or short, usually undenticulated process on the outer side of element. $Pb_2$ element with anterior and posterior processes. Posterior processes of the S elements unevenly denticulated; within the row of short narrow denticles a few larger ones are randomly situated. Processes of the carniciform element bear up to four or five tiny denticles.

*Remarks. P. amorphognathoides* is represented by a morphologically variable sequence of closely related populations including several evolutionarily connected successive subspecies: *P. a. angulatus*, *P. a. lennarti* ssp. nov., *P. a. lithuanicus* and *P. a. amorphognathoides* (see below). The changes in the morphology of the elements in the apparatus at the boundary between the *P. eopennatus* and *P. amorphognathoides* lineages are relatively sharp and took place at the level corresponding to one of the main events in the evolution of Telychian conodont faunas (Männik 1995).

*Pterospathodus amorphognathoides angulatus* (Walliser, 1964)

Plate 2, figures 1–22, 24–31; Text-figures 7–8

v.* 1964 *Spathognathodus pennatus angulatus* Walliser, p. 79, pl. 14, figs 19–22.
1975 *Llandoverygnathus pennatus* (Walliser, 1964); Aldridge, pl. 1, figs 24–25.
1981 *Pterospathodus pennatus procerus* (Walliser, 1964); Uyeno and Barnes, pl. 1, fig. 23.
? 1981 *Pterospathodus celloni* (Walliser, 1964); Uyeno and Barnes, pl. 1, figs 20–21.
? 1981 *Carniodus carnulus* Walliser, 1964; Uyeno and Barnes, pl. 1, figs 18–19.
.1982 *Pterospathodus pennatus angulatus* (Walliser, 1964); Aldridge and Mohamed, pl. 2, figs 8–11.
.1982 *Pterospathodus pennatus pennatus* (Walliser, 1964); Aldridge and Mohamed, pl. 2, fig. 12.
1982 *Pterospathodus celloni* (Walliser, 1964); Aldridge and Mohamed, pl. 2, fig. 7.
? 1983 *Carniodus carnulus* Walliser, 1964; Uyeno and Barnes, p. 16, pl. 5, figs 1–10 (figs 2–3 [= cop. Uyeno and Barnes 1981, pl. 1, figs 18–19]).
p? 1983 *Pterospathodus celloni* (Walliser, 1964); Uyeno and Barnes, p. 24, pl. 5, figs 17–18, 20–24 (*non* fig. 18 [indet.]; figs 20–22 [= cop. Uyeno and Barnes 1981, pl. 1, figs 20–21]).
p 1983 *Ozarkodina polinclinata* (Nicoll and Rexroad, 1968); Uyeno and Barnes, p. 22, pl. 5, fig. 19 (*non* figs 11–16 [= *O. polinclinata*]).
1983 *Pterospathodus pennatus procerus* (Walliser, 1964); Uyeno and Barnes, p. 24, pl. 8, figs 1–3 [fig. 1 [= cop. Uyeno and Barnes 1981, pl. 1, fig. 23]).
? 1985 *Pterospathodus pennatus pennatus* (Walliser, 1964); Aldridge, p. 80, pl. 3.1, fig. 27.
1987 *Pterospathodus celloni* (Walliser, 1964); An, p. 202, pl. 33, figs 8–10.
1987 *Neoprioniodus triangularis paucidentatus* Walliser, 1964; An, pl. 35, figs 21–22.
1987 *Pterospathodus pennatus* (Walliser, 1964); Dumoulin and Harris, fig. 4*N*.
? 1988 *Pterospathodus pennatus procerus* (Walliser, 1964); Qiu, pl. 1, figs 5–7 [cop. Qiu 1985, pl. 1, figs 5, 8–9]).
v. 1989 *Pterospathodus*, angulatus-morph Männik and Aldridge, text-fig. 3*B*.
v. 1989 *Pterospathodus*, pennatus-morph Männik and Aldridge, text-fig. 3*C*.

---

TEXT-FIG. 6. *Pterospathodus eopennatus* ssp. nov. 2; *Apsidognathus tuberculatus* ssp. nov. 2 Subzone. A–D, Pa element, morph 1a. E–F, J–K, Pa element, morph 1b. G–I, M–N, T, Pa element, morph 2a. L, O–P, U, Pa element, morph 4. Q–R, W, $Pb_1$ element. S, Z–$E^1$, $Pb_2$ element. V, X–Y, $H^1$, Pc element. $F^1$–$G^1$, $M_1$ element. $L^1$–$N^1$, $Sc_1$ element. $I^1$–$K^1$, $Sc_3$ element. $O^1$, $U^1$–$V^1$, $Sc_2$ element. $P^1$, $Sb_2$ element. $Q^1$–$R^1$, $Sb_1$ element. $S^1$–$T^1$, carniciform element. $W^1$, Sa element. $X^1$–$Z^1$, carnuliform element, morph a. $A^2$–$B^2$, carnuliform element, morph b(?). $C^2$–$D^2$, modified carnuliform element. $E^2$–$F^2$, curved element, morph a. Scale bar represents 1 mm.

v. 1998 *Pterospathodus* cf. *amorphognathoides angulatus* (Walliser, 1964); Männik and Małkowski, pl. 1, figs 20–22.

*Material.* Several hundred of each of the P, M, Sc and carnuliform elements; tens to hundreds of Sb, Sa and carniciform elements.

*Diagnosis. P. amorphognathoides* with elements without platform. Pa element long, with pennate inner lateral process and lower denticles in the middle part of the blade.

*Remarks.* Pa element of *P. a. angulatus* is similar to the morphs 1a and 1b of the Pa element of *P. eopennatus* ssp. nov. 2 (Pl. 2, figs 34–35; Text-fig. 6A–F, J–K) but differs by having a very long blade with at least 20, usually even more denticles on mature specimens. The Pa element of *P. a. angulatus* is represented by two morphs, one of them with tall denticles (Pl. 2, figs 1, 3–4, 9; Text-figs 7A–B, D, 8B–C, F–H) and the other with short denticles (Pl. 2, fig. 12; Text-figs 7C, G, K, 8A). The ends of lateral processes on Sb elements lack bifurcation.

In the lower part of the range of *P. a. angulatus* morphs 2 and 3 of the Pa, but also extremely rare specimens of the $Pb_2$ and the carniciform elements typical of *P. eopennatus* ssp. nov. 2 occur occasionally.

*P. a. angulatus* is the oldest representative of the *P. amorphognathoides* lineage and was evolutionarily followed by *P. amorphognathoides lennarti* ssp. nov.

---

EXPLANATION OF PLATE 2

Figs 1–22, 24–31. *Pterospathodus amorphognathoides angulatus* (Walliser, 1964). 1, Cn 7907; inner lateral view of dextral Pa element, morph a. 2, Cn 7908; outer lateral view of dextral $Pb_2$ element. 3, Cn 7909; inner lateral view of sinistral Pa element, morph a. 4, Cn 7910; upper view of dextral Pa element, morph a. 5, Cn 7911; outer lateral view of sinistral $Pb_2$ element. 6, Cn 7912; outer lateral view of sinistral $Pb_1$ element. 7, Cn 7913; outer lateral view of sinistral Pc element. 8, Cn 7914; outer lateral view of sinistral $Pb_2$ element. 9, Cn 7915; inner lateral view of sinistral Pa element, morph a. 10, Cn 7916; outer lateral view of dextral $Pb_1$ element. 11, Cn 7917; outer lateral view of dextral $Pb_1$ element. 12, Cn 7918; inner lateral view of sinistral Pa element, morph b. 13, Cn 7919; outer lateral view of sinistral carnuliform element, morph a. 14, Cn 7920; outer lateral view of sinistral carnuliform element, morph a(?). 15, Cn 7921; outer lateral view of sinistral modified carnuliform element. 16, Cn 7922; inner lateral view of sinistral $Sc_3$ element. 17, Cn 7923; inner lateral view of sinistral $Sc_1$ element. 18, Cn 7924; inner lateral view of dextral $M_1$ element. 19, Cn 7925; inner lateral view of sinistral $M_1$ element. 20, Cn 7926; inner lateral view of sinistral $Sc_2$ element. 21, Cn 7927; inner lateral view of dextral $Sb_1$ element. 22, Cn 7928; inner lateral view of dextral $Sc_2$ element. 24, Cn 7929; inner lateral view of dextral carniciform element. 25, Cn 7930; outer lateral view of sinistral curved element, morph a. 26, Cn 7931; outer lateral view of sinistral curved element, morph b. 27, Cn 7932; posterior view of dextral $Sb_1$ element. 28, Cn 7933; posterior view of dextral $Sb_2$ element. 29, Cn 7934; lateral view of Sa element. 30, Cn 7935; outer lateral view of dextral $Sb_2$ element. 31, Cn 7936; posterior view of Sa element. Figs 1, 3–4, 6–7, 9, 11, 15 and 24 from Nurme core, sample M-1051, int. 12·70–12·85 m; figs 2, 5 and 10 from Uulu-330 core, sample M-1298, int. 139·84–139·92 m; figs 8 and 12 from Nurme core, sample M-1050, int. 13·30–13·40 m; figs 13–14, 16–22 and 25–31 from Velise-Kõrgekalda section, sample VE-2.

Figs 23, 32–41. *Pterospathodus eopennatus* ssp. nov. 2. 23, Cn 7937; inner lateral view of dextral Pa element, morph 2a. 32, Cn 7938; inner lateral view of sinistral Pa element, morph 2a. 33, Cn 7939; upper view of dextral Pa element, morph 4. 34, Cn 7940; inner lateral view of dextral Pa element, morph 1a. 35, Cn 7941; inner lateral view of sinistral Pa element, morph 1a. 36, Cn 7942; inner lateral view of dextral Pa element, morph 2a. 37, Cn 7943; inner lateral view of sinistral Pa element, morph 2a. 38, Cn 7944; upper view of dextral Pa element, morph 4(?). 39, Cn 7945; inner lateral view of sinistral Pa element, morph 2a. 40, Cn 7946; inner lateral view of dextral Pa element, morph 1a. 41, Cn 7947; inner lateral view of dextral Pa element, morph 4. Figs 23, 34–35 and 37–38 from Nurme core, sample M-907, int. 17·50–17·60 m; figs 32 and 36 from Viki core, sample M-11, int. 175·60–175·80 m; figs 33, 39 and 41 from Nurme core, sample M-900, int. 22·65–22·80 m; fig. 40 from Viki core, sample M-8, int. 168·60–168·80 m.

All × 50.

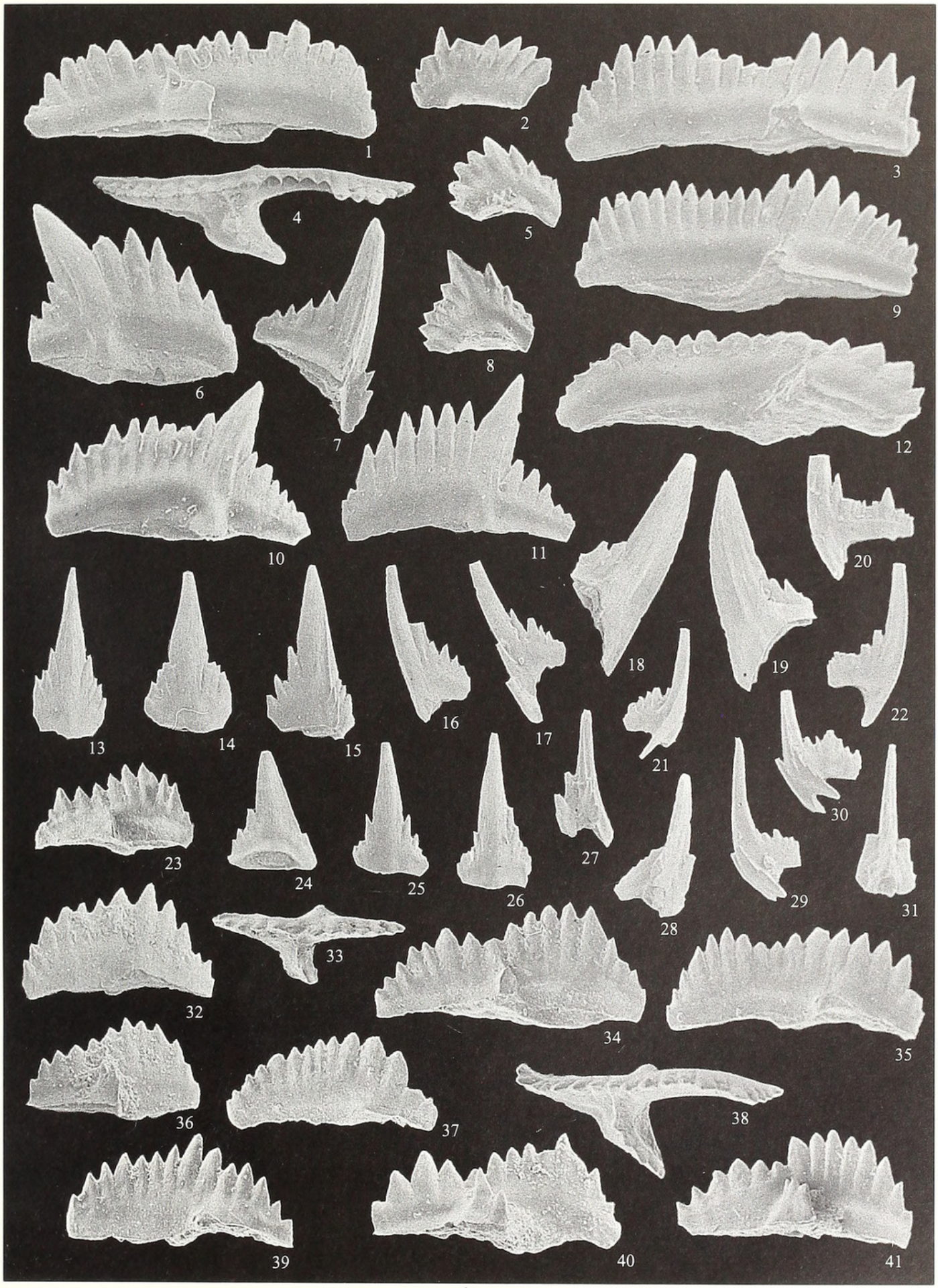


MÄNNIK, *Pterospathodus*

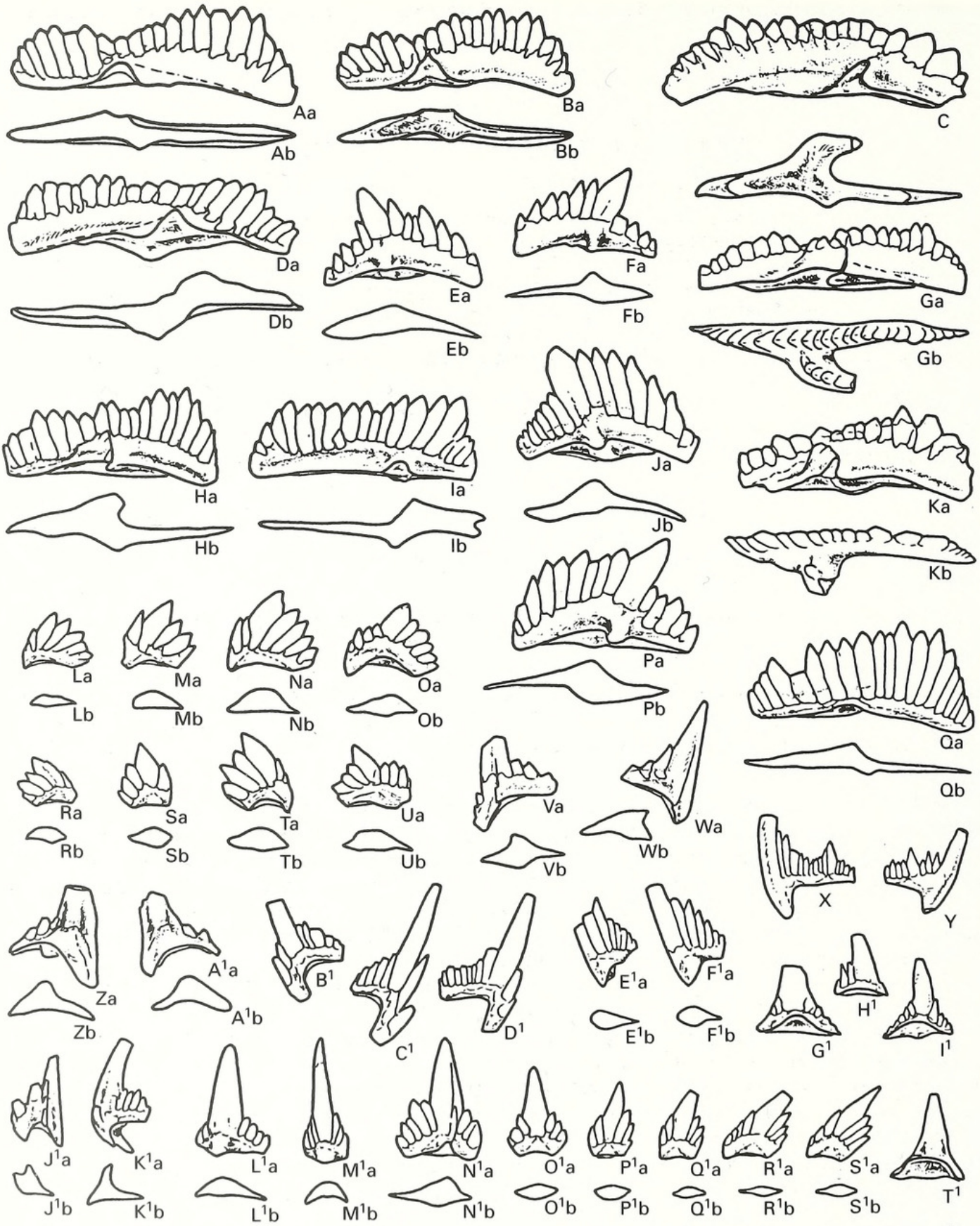


TEXT-FIG. 7. *Pterospathodus amorphognathoides angulatus* (Walliser, 1964); *Apsidognathus tuberculatus* ssp. nov. 3 Subzone. A–B, D, Pa element, morph a. C, G, K, Pa element, morph b. H–I, Q, Pa element, morph 3. E–F, J, P, $Pb_1$ element. L–O, R–U, $Pb_2$ element. V–W, Pc element. X–Y, $Sc_2$ element. Z, $A^1$, $M_1$ element. $B^1$–$D^1$, $Sc_1$

*Occurrence. A. tuberculatus* ssp. nov. 3 and *P. a. angulatus* subzones. *P. a. angulatus* can be recognized worldwide (see synonymy).

### *Pterospathodus amorphognathoides lennarti* ssp. nov.

Plate 3, figures 21–46; Text-figure 9

p. 1972 *Pterospathodus amorphognathoides* Walliser, 1964; Aldridge, p. 208, pl. 3, fig. 18 (*non* figs 17, 19 [= *P. a. amorphognathoides*]).
? 1972 *Neoprioniodus costatus costatus* Walliser, 1964; Aldridge, p. 193, pl. 5, fig. 22.
? 1972 *Ozarkodina gaertneri* Walliser, 1964; Aldridge, p. 200, pl. 5, fig. 7.
.1985 *Pterospathodus pennatus* subsp. nov. Aldridge, p. 81, pl. 3.1, fig. 28.
v. 1986 *P. celloni* (Walliser); Nakrem, fig. 6*a*.
vp. 1986 *Carniodus carnulus* Walliser, 1964; Nakrem, fig. 6*l* (*non* fig. 7*c*, *f* [= *P. a. lithuanicus*]).

*Derivation of name.* In honour of Dr Lennart Jeppsson, an expert on Silurian conodonts.

*Material.* Several hundred to a thousand carnuliform elements; several hundred P, M, Sc, carniciform and curved elements; many tens to hundreds of Sb and Sa elements.

*Holotype.* Dextral Pa element Cn 7968, Pahapilli core, sample M-1520, int. 47·30–47·20 m (Velise Formation, northern Saaremaa, Estonia); Plate 3, figure 21.

*Type horizon and locality.* Middle part of the Velise Formation, Adavere Regional Stage; Pahapilli core, interval 46·60–50·30 m.

*Diagnosis. P. amorphognathoides* with elements without platform. The first denticle on the bifurcated lateral process of the Pa element is situated away from the main row of denticles and is connected with the last one by a narrow high ridge.

*Remarks.* The most characteristic feature separating the Pa element of *P. amorphognathoides lennarti* ssp. nov. from that of younger subspecies (e.g. *P. a. lithuanicus*; Pl. 4, figs 29–32, 34–35; Text-fig. 10A–B, D–E) is the deep groove between the main row of denticles and the first one on the inner lateral process (Text-fig. 9A, D–E). As a rule, that denticle is connected with the main row by a narrow high ridge (Pl. 3, figs 21–22, 25, 27; Text-fig. 9A, D–E). The configuration (the direction of the branches) of the lateral process is highly variable. The distal part of the posterior branch is usually turned parallel to the anterior one (Pl. 3, fig. 27).

The Pa element of *P. amorphognathoides lennarti* ssp. nov. is represented by two morphs. Morph 1 has tall denticles and a relatively low base (Text-fig. 9A, C, G) whereas morph 2 is characterized by short denticles and a higher base (Text-fig. 9E). The denticulation of morph 1 tends to be more irregular and includes overgrown denticles (Text-fig. 9G). A sub-triangular outer lateral lobe/short process is also characteristic, better developed on the sinistral element.

*P. amorphognathoides lennarti* ssp. nov. is a direct descendant of *P. a. angulatus*. These two taxa differ mainly in the lack (or extremely rare occurrence) of bifurcation on the inner lateral process in *P. a. angulatus* and in the development of an outer lateral lobe on the Pa elements of *P. a. lennarti* ssp. nov. The apparatus of *P. a. lennarti* ssp. nov. differs from earlier taxa in the presence of short

---

element. $E^1$–$F^1$, $Sc_3$ element. $G^1$–$I^1$, $T^1$, carniciform element. $J^1$, $Sb_1$ element. $K^1$, $Sb_2$ element. $L^1$, curved element, morph a. $M^1$, curved element, morph b. $N^1$, modified carnuliform element. $O^1$–$S^1$, carnuliform element, morph a. Scale bar represents 1 mm.

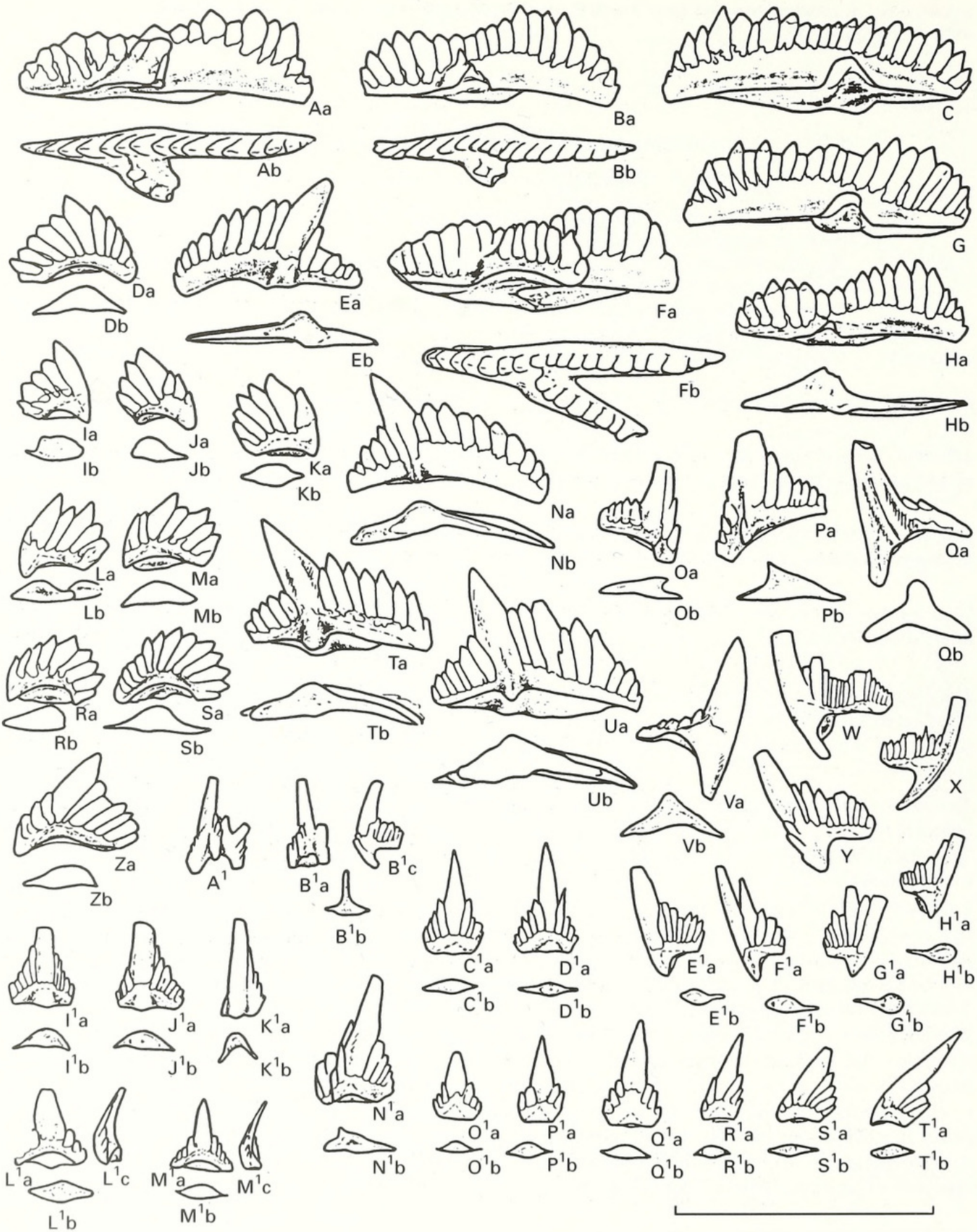


TEXT-FIG. 8. *Pterospathodus amorphognathoides angulatus* (Walliser, 1964); *P. a. angulatus* Subzone. A, Pa element, morph b. B–C, F–H, Pa element, morph a. E, N, T–U, $Pb_1$ element. D, I–M, R–S, Z, $Pb_2$ element. O–P, Pc element. Q, V, $M_1$ element. W–X, $Sc_2$ element. Y, $Sc_1$ element. $A^1$, $Sb_1$ element. $B^1$, $Sb_2$ element. $C^1$–$D^1$, carnuliform

and modified short morphs of the carnuliform element (Pl. 3, figs 24, 33; Text-fig. 9V–W, L$^1$–M$^1$, V$^1$–W$^1$).

*Occurrence*. The *P. amorphognathoides lennarti* Subzone. On Gotland *P. a. lennarti* ssp. nov. has been found in loose pebbles from Själsö (collection of L. Jeppsson – sample G88-637LJ). *P. a. lennarti* ssp. nov. has also been found in Carnic Alps (Seewarte section – collection of H. P. Schönlaub, sample 195/1–2, and probably in the Cellon section – collection of O. H. Walliser, one fragment in sample 10 H/J), in Great Britain (Aldridge 1972, pl. 3, fig. 18, Ticklerton 2 section; 1985, pl. 3.1, fig. 28, loc. 23 – uppermost Purple Shales of small stream 850 m south-west of Ticklerton, Shropshire) and Norway (Nakrem 1986, fig. 6*a*, Malmøyakalven section, Vik Fm., 42·5 m).

## *Pterospathodus amorphognathoides lithuanicus* Brazauskas, 1983 *sensu novo*

Plate 3, figures 1–20, Plate 4, figures 21, 28–35; Text-figure 10

v.* 1983 *Pterospathodus amorphognathoides lithuanicus* Brazauskas, p. 60, figs 1–7.
v. 1986 *Pterospathodus amorphognathoides* Walliser, 1964; Nakrem, fig. 6*b–d, e*(?), *f–g, i*.
v.? 1986 *Pterospathodus pennatus pennatus* (Walliser, 1964); Nakrem, fig. 6*h*.

*Material*. Several hundreds to a thousand of each of the Pa, Pb and carnuliform elements; many hundreds of the Pc, M, S, carniciform and curved elements.

*Emended diagnosis*. *P. amorphognathoides* without basal platform. The first denticle on the bifurcated inner lateral process is situated close to the main row of denticles.

*Remarks*. Brazauskas (1983) described only the Pa element of the apparatus. Here *P. a. lithuanicus* is considered to include the complete set of elements of the *Pterospathodus* apparatus. Morphologically the most distinct element in this apparatus is the Pa element (Pl. 4, figs 21, 29–32, 34, 45; Text-fig. 10A–B, D–E). The $Pb_1$ (Pl. 3, figs 15, 17; Text-fig. 10C, F, O, U) and $Pb_2$ (Pl. 3, fig. 1; Pl. 4, fig. 28; Text-fig. 10G–L, P) elements can also be quite easily separated from those of the older subspecies, as they possess a weak lateral basal thickening lacking on the corresponding elements of *P. a. lennarti* ssp. nov.

As a rule, the sinistral Pa element (Pl. 4, figs 31–32; Text-fig. 10B, E) possesses a distinct rounded or triangular lateral lobe on the outer side of the element. This structure is almost absent on the dextral element (Pl. 4, figs 29–30; Text-fig. 10A, D). In the apparatus of *P. a. lithuanicus* a new modification of curved element, morph c, appears (Pl. 3, fig. 16; Text-fig. 10Y$^1$–Z$^1$).

*Occurrence*. In the *P. a. lithuanicus* Subzone. Outside the Baltic (Estonia, Lithuania) *P. a. lithuanicus* has so far been illustrated only from Norway (Nakrem 1986, fig. 6*d, e*(?), *g–i*, Malmøyakalven section, Vik Fm.). However, it is most probable, that after revision of collections from other regions of the world this taxon will be recognized to have a much wider distribution.

## *Pterospathodus amorphognathoides amorphognathoides* Walliser, 1964

Plate 4, figures 1–20, 22–27; Plate 5; Text-figures 11–15

v.* 1964 *Pterospathodus amorphognathoides* Walliser, p. 67, pl. 15, figs 9–15.
v. 1964 *Ozarkodina gaertneri* Walliser, p. 57, pl. 27, figs 12–19.
v. 1964 ?*Carniodus carinthiacus* Walliser, p. 31, pl. 27, figs 20–26.
v. 1964 *Carniodus carnulus* Walliser, p. 32, pl. 27, figs 27–38; pl. 28, fig. 1.

---

element, morph b. E$^1$–H$^1$, $Sc_3$ element. I$^1$–J$^1$, curved element, morph a. K$^1$, curved element, morph b. L$^1$–M$^1$, carniciform element. N$^1$, modified carnuliform element. O$^1$–T$^1$, carnuliform element, morph a. Scale bar represents 1 mm.

v. 1964 *Carniodus carnus* Walliser, p. 34, pl. 28, figs 2–7.
v. 1964 *Carniodus carnicus* Walliser, p. 32, pl. 28, figs. 8–11.
vp. 1964 *Neoprioniodus subcarnus* Walliser, p. 51, pl. 28, figs 13–18 (*non* fig. 12 [= *P. celloni*]).
v. 1964 *Neoprioniodus triangularis triangularis* Walliser, p. 52, pl. 28, figs 25–30.
v. 1964 *Neoprioniodus costatus costatus* Walliser, p. 48, pl. 28, figs 36–41.
v. 1964 *Roundya latialata* Walliser, p. 71, pl. 31, figs 11–14.
.1966 *Ozarkodina gaertneri* Walliser, 1964; Spasov and Filipović, p. 44, pl. 1, figs 1–2.
.1966 *Carniodus carinthiacus* Walliser, 1964; Spasov and Filipović, p. 38, pl. 1, fig. 3.
.1966 *Pterospathodus amorphognathoides* Walliser, 1964; Spasov and Filipović, p. 48, pl. 1, figs 4–5.
.1966 *Neoprioniodus subcarnus* Walliser, 1964; Spasov and Filipović, p. 42, pl. 1, figs 8–9.
.1966 *Neoprioniodus costatus costatus* Walliser, 1964; Spasov and Filipović, p. 42, pl. 1, figs 10–11.
.1966 *Carniodus carnus* Walliser, 1964; Sapsov and Filipović, p. 40, pl. 1, figs 12–13.
1966 *Roundya brevialata* Walliser, 1964; Spasov and Filipović, p. 49, pl. 1, fig. 14.
.1966 *Carniodus carnulus* Walliser, 1964; Spasov and Filipović, p. 39, pl. 1, fig. 15.
.1966 *Carniodus carnicus* Walliser, 1964; Spasov and Filipović, p. 38, pl. 1, fig. 16.

---

EXPLANATION OF PLATE 3

Figs 1–20. *Pterospathodus amorphognathoides lithuanicus* Brazauskas, 1983. 1, Cn 7948; outer lateral view of dextral $Pb_2$ element. 2, Cn 7949; outer lateral view of sinistral $Sb_1$ element. 3, Cn 7950; inner lateral view of dextral $Sc_2$ element. 4, Cn 7951; inner lateral view of sinistral $Sc_2$ element. 5, Cn 7952; outer lateral view of sinistral curved element, morph a. 6, Cn 7953; inner(?) lateral view of dextral(?) modified carnuliform element, short morph. 7, Cn 7954; outer lateral view of sinistral curved element, morph b. 8, Cn 7955; posterior view of dextral $Sb_1$ element. 9, Cn 7956; inner lateral view of sinistral $M_1$ element. 10, Cn 7957; inner lateral view of dextral $Sc_2$ element. 11, Cn 7958; posterior view of sinistral $Sb_1$ element. 12, Cn 7959; inner lateral view of dextral $Sc_3$ element. 13, Cn 7960; posterior view of sinistral $Sb_2$ element. 14, Cn 7961; outer lateral view of sinistral Pc element. 15, Cn 7962; outer lateral view of dextral $Pb_1$ element. 16, Cn 7963; outer lateral view of dextral curved element, morph c. 17, Cn 7964; outer lateral view of dextral $Pb_1$ element. 18, Cn 7965; inner lateral view of sinistral $Sc_3$ element. 19, Cn 7966; outer lateral view of dextral carnuliform element, short morph. 20, Cn 7967; inner lateral view of dextral carniciform element. Figs 1, 5–8, 10, 13 and 18–20 from Viki core, sample M-976, int. 149·95–150·08 m; figs 2 and 11 from Viki core, sample M-362, int. 151·87–152·00 m; figs 3–4, 9 and 14–15 from Viki core, sample M-979, int. 148·75–148·85 m; fig. 12 from Viki core, sample M-972, int. 151·25–151·40 m; fig. 16 from Viki core, sample M-971, int. 151·54–151·64 m; fig. 17 from Viki core, sample M-367, int. 146·70–146·80 m.

Figs 21–46. *Pterospathodus amorphognathoides lennarti* ssp. nov. 21, Cn 7968; upper view of dextral Pa element. 22, Cn 7969; upper view of sinistral Pa element. 23, Cn 7970; outer lateral view of dextral curved element, morph b. 24, Cn 7971; inner lateral view of sinistral modified carnuliform element, short morph. 25, Cn 7972; upper view of dextral Pa element. 26, Cn 7973; outer lateral view of sinistral $Pb_2$ element. 27, Cn 7974; upper view of dextral Pa element. 28, Cn 7975; inner lateral view of dextral $Sc_3$ element. 29, Cn 7976; outer lateral view of sinistral Pc element. 30, Cn 7977; inner lateral view of sinistral $Sc_2$ element. 31, Cn 7978; inner lateral view of dextral $M_1$ element. 32, Cn 7979; inner lateral view of dextral $Sc_3$ element. 33, Cn 7980; outer(?) lateral view of dextral(?) modified carnuliform element, short morph. 34, Cn 7981; outer lateral view of dextral $Sb_2$ element. 35, Cn 7982; outer lateral view of dextral $Pb_1$ element. 36, Cn 7983; outer lateral view of sinistral $Pb_1$ element. 37, Cn 7984; inner lateral view of sinistral $Sc_3$ element. 38, Cn 7985; inner lateral view of sinistral $Sc_3$ element. 39, Cn 7986; inner lateral view of sinistral $M_1$ element. 40, Cn 8080; outer lateral view of sinistral curved element, morph a. 41, Cn 7987; posterior view of Sa element. 42, Cn 7988; outer lateral view of dextral $Pb_1$ element. 43, Cn 7989; inner lateral view of dextral $Sc_2$ element. 44, Cn 7990; posterior view of dextral $Sb_1$ element. 45, Cn 7991; lateral view of symmetrical(?) carnuliform element, morph b. 46, Cn 7992; outer lateral view of dextral modified carnuliform element. Fig. 21 from Pahapilli core, sample M-1520, int. 47·20–47·30 m; figs 22–25, 33, 35, 42–43 and 45–46 from Viki core, sample M-966, int. 153·88–154·05 m; figs 26–27 from Uulu-330 core, sample M-1070, int. 137·70–137·85 m; figs 28, 34, 40–41 and 44 from Uulu-330 core, sample M-1301, int. 138·05–138·15 m; figs 29–31 and 39 from Viki core, sample M-967, int. 153·60–153·72 m, figs 32 and 37–38 from Viki core, sample M-360, int. 153·35–153·50 m; fig. 36 from Viki core, sample M-968, int. 153·05–153·20 m.

All × 50.

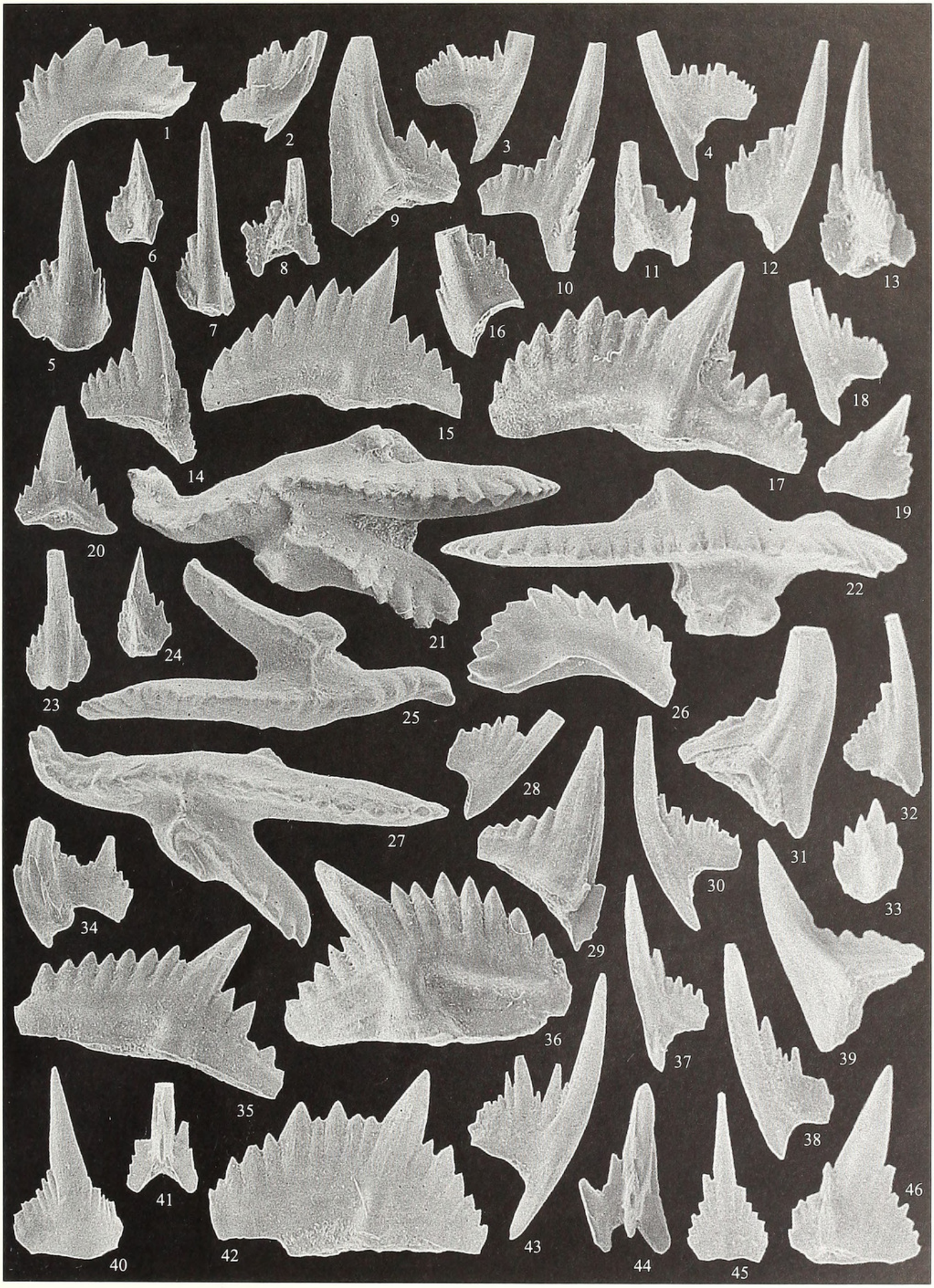


MÄNNIK, *Pterospathodus*

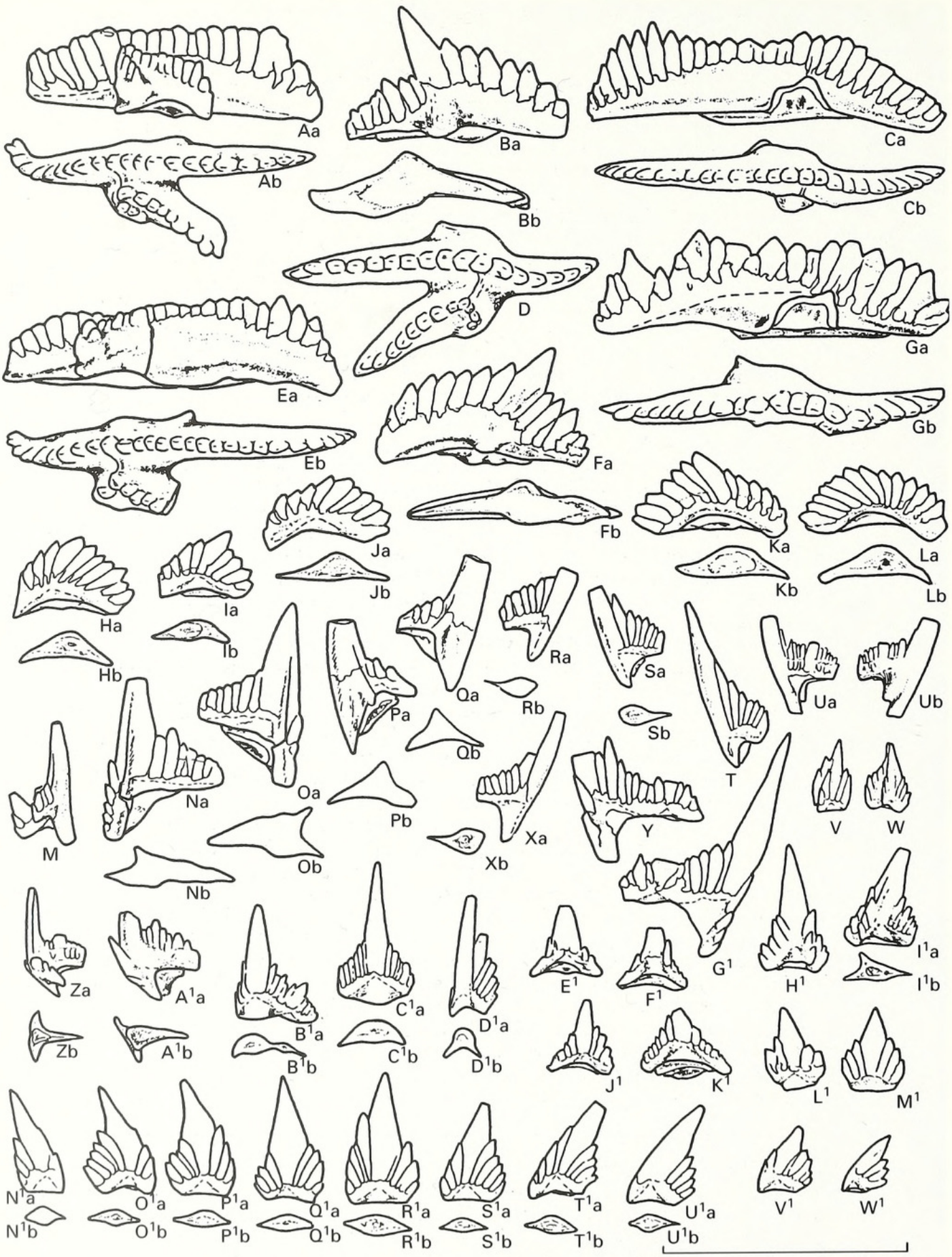


TEXT-FIG. 9. For caption see opposite.

p. 1968 *Ozarkodina gaertneri* Walliser, 1964; Igo and Koike, p. 14, pl. 1, figs 5–6 (*non* figs 7–9 [= *P. pennatus procerus*]).
1968 *Pterospathodus amorphognathoides* Walliser, 1964; Igo and Koike, p. 16, pl. 2, figs 12–13.
p. 1968 *Carniodus* sp. A Igo and Koike, p. 8, pl. 3, fig. 3 (*non* fig. 2 [= *P. p. procerus*?]).
p. 1968 *Neoprioniodus* spp. Igo and Koike, p. 14, pl. 3, fig. 4 (*non* fig. 24 [= *P. p. procerus*?]).
.1968 *Ozarkodina gaertneri* Walliser, 1964; Nicoll and Rexroad, p. 49, pl. 2, figs 12–14.
.1968 *Ozarkodina neogaertneri* Nicoll and Rexroad, p. 50, pl. 2, figs 15–16.
1968 *Pterospathodus amorphognathoides* Walliser, 1964; Nicoll and Rexroad, p. 56, pl. 3, figs 1–5, 6?, 7.
.1968 *Carniodus carinthiacus* Walliser, 1964; Nicoll and Rexroad, p. 24, pl. 5, figs 1–2.
1968 *Carniodus carnicus* Walliser, 1964; Nicoll and Rexroad, p. 25, pl. 5, fig. 3.
.1968 *Carniodus carnulus* Walliser, 1964; Nicoll and Rexroad, p. 25, pl. 5, figs 4–5.
p. 1968 *Carniodus carnus* Walliser, 1964; Nicoll and Rexroad, p. 26, pl. 5, figs 6, 8 (*non* fig. 7 [indet.]).
.1968 *Neoprioniodus subcarnus* Walliser, 1964; Nicoll and Rexroad, p. 41, pl. 5, fig. 10.
.1968 *Neoprioniodus costatus* Walliser, 1964; Nicoll and Rexroad, p. 40, pl. 5, figs 15–16.
.1968 *Neoprioniodus triangularis* Walliser, 1964; Nicoll and Rexroad, p. 42, pl. 5, fig. 17.
1969 *Carniodus carnulus* Walliser, 1964; Schönlaub, pl. 1, fig. 5.
.1969 *Pterospathodus amorphognathoides* Walliser, 1964; Schönlaub, pl. 1, fig. 8.
.1969 ?*Carniodus carinthiacus* Walliser, 1964; Schönlaub, pl. 1, fig. 12.
.1969 *Ozarkodina gaertneri* Walliser, 1964; Schönlaub, pl. 1, fig. 15.
1969 *Pterospathodus amorphognathoides* Walliser, 1964; Drygant, p. 49, pl., fig. 6.
.1969 *Carniodus*? *carinthiacus* Walliser, 1964; Drygant, p. 54, pl., fig. 5.
? 1969 *Neoprioniodus subcarnus* Walliser, 1964; Drygant, p. 53, pl., figs 12–14.
.1970 *Pterospathodus amorphognathoides* Walliser, 1964; Manara and Vai, p. 494, pl. 62, fig. 15.
.1970 *Ozarkodina gaertneri* Walliser, 1964; Manara and Vai, p. 487, pl. 62, fig. 17.
.1971 *Pterospathodus amorphognathoides* Walliser, 1964; Schönlaub, p. 45, pl. 2, figs 6–12.
p. 1971 *Carniodus carinthiacus* Walliser, 1964; Schönlaub, p. 46, pl. 3, figs 7–8 (*non* fig. 6 [= *P. eopennatus*]).
.1971 *Neoprioniodus subcarnus* Walliser, 1964; Rexroad and Nicoll, pl. 1, fig. 11.
.1971 *Pterospathodus amorphognathoides* Walliser, 1964; Rexroad and Nicoll, pl. 2, figs 20–21.
.1971 *Ozarkodina gaertneri* Walliser, 1964; Rexroad and Nicoll, pl. 2, fig. 22.
.1971 *Ozarkodina neogaertneri* Nicoll and Rexroad, 1968; Rexroad and Nicoll, pl. 2, fig. 23.
.1972 *Ozarkodina gaertneri* Walliser, 1964; Rexroad and Nicoll, pl. 1, figs 1–3.
.1972 *Pterospathodus amorphognathoides* Walliser, 1964; Rexroad and Nicoll, pl. 1, figs 4–7.
.1972 *Carniodus carnulus* Walliser, 1964; Rexroad and Nicoll, pl. 1, figs 8–11.
.1972 *Carniodus carnus* Walliser, 1964; Rexroad and Nicoll, pl. 1, figs 12–13.
.1972 *Carniodus carinthiacus* Walliser, 1964; Rexroad and Nicoll, pl. 2, figs 1–3.
1972 *Carniodus carnicus* Walliser, 1964; Rexroad and Nicoll, pl. 2, figs 4, 5?.
.1972 *Neoprioniodus subcarnus* Walliser, 1964; Rexroad and Nicoll, pl. 2, figs 6–7.
.1972 *Neoprioniodus costatus* Walliser, 1964; Rexroad and Nicoll, pl. 2, figs 8–11.
.1972 *Neoprioniodus triangularis* Walliser, 1964; Rexroad and Nicoll, pl. 2, figs 12–13.
1972 *Exochognathus brevialatus* (Walliser, 1964); Rexroad and Nicoll, pl. 2, figs 21?, 22.
.1972 *Ozarkodina neogaertneri* Nicoll and Rexroad, 1968; Rexroad and Nicoll, pl. 2, fig. 34.
p. 1972 *Ozarkodina gaertneri* Walliser, 1964; Aldridge, p. 200, pl. 5, fig. 5 (*non* fig. 7 [= *P. amorphognathoides lennarti* ssp. nov or *P. a. lithuanicus*]).
.1972 *Carniodus carinthiacus* Walliser, 1964; Aldridge, p. 168, pl. 5, figs 8–10.
.1972 *Carniodus carnicus* Walliser, 1964; Aldridge, p. 168, pl. 5, fig. 11.
.1972 *Carniodus carnulus* Walliser, 1964; Aldridge, p. 169, pl. 5, figs 12–14.
.1972 *Carniodus carnus* Walliser, 1964; Aldridge, p. 169, pl. 5, figs 15–16.

---

TEXT-FIG. 9. *Pterospathodus amorphognathoides lennarti* ssp. nov. A, C–D, G?, Pa element, morph a. E, Pa element, morph b. B, F, $Pb_1$ element. H–L, $Pb_2$ element. N–O, Pc element. P–Q, $M_1$ element. R–T, X, $Sc_3$ element. U, $Sc_2$ element. V–W, modified carnuliform element, short morph. Y, $G^1$, $Sc_1$ element. Z, Sa element. $A^1$, $Sb_2$ element. $B^1$–$C^1$, curved element, morph a. $D^1$, curved element, morph b. $E^1$–$F^1$, $J^1$–$K^1$, carniciform element. $H^1$–$I^1$, modified carnuliform element. $L^1$–$M^1$, $V^1$–$W^1$, carnuliform element, short morph. $N^1$–$U^1$, carnuliform element, morph a. Scale bar represents 1 mm.

.1972 *Neoprioniodus subcarnus* Walliser, 1964; Aldridge, p. 195, pl. 5, fig. 17.
p. 1972 *Pterospathodus amorphognathoides* Walliser, 1964; Aldridge, pl. 3, figs 17, 19 (*non* fig. 18 [= *P. a. lennarti* ssp. nov.]).
.1974 *Pterospathodus amorphognathoides* Walliser, 1964; Aldridge, fig. 1*E–F*.
.1975 *Pterospathodus amorphognathoides* Walliser, 1964; Aldridge, pl. 1, figs 22–23.
.1975 *Carniodus carnulus* Walliser, 1964; Aldridge, pl. 1, figs 3–4, 8–9.
.1975 *Exochognathus latialatus* (Walliser, 1964); Aldridge, pl. 3, fig. 15.
1975 *Neoprioniodus costatus costatus* Walliser, 1964; Aldridge, pl. 3, fig. 17.
1975 *Distomodus triangularis* (Walliser, 1964); Aldridge, pl. 3, fig. 19.
1975 *Pterospathodus amorphognathoides* Walliser, 1964; Saladžius, pl. 2, figs 7, 8(?).
1975 *Carniodus carinthiacus* Walliser, 1964; Saladžius, pl. 1, fig. 5.
1975 *Neoprioniodus costatus* Walliser, 1964; Saladžius, pl. 1, fig. 9.
1975 *Neoprioniodus subcarnus* Walliser, 1964; Saladžius, pl. 1, fig. 11.
1975 *Neoprioniodus triangularis* Walliser, 1964; Saladžius, pl. 1, fig. 12.
1975 *Neoprioniodus triangularis triangularis* Walliser, 1964; Saladžius, pl. 1, fig. 13.
.1976 *Carniodus carnulus* Walliser, 1964; Barrick and Klapper, p. 68, pl. 1, figs 1–2, 6–8, 12–14.
.1976 *Pterospathodus amorphognathoides* Walliser, 1964; Barrick and Klapper, p. 82, pl. 1, figs 4, 9–11, 16.
.1976 *Pterospathodus amorphognathoides* Walliser, 1964; Kuwano, pl. 2, fig. 2.
.1976 *Pterospathodus amorphognathoides* Walliser, 1964; Miller, fig. 822.
1976 *Ozarkodina gaertneri* Walliser, 1964; Miller, fig. 820.
.1977 *Pterospathodus amorphognathoides* Walliser, 1964; Cooper, p. 1065, pl. 2, figs 3, 6.
1977 *Neoprioniodus subcarnus* Walliser, 1964; Liebe and Rexroad, pl. 1, fig. 1.

---

EXPLANATION OF PLATE 4

Figs 1–4. *Pterospathodus amorphognathoides amorphognathoides* Walliser, 1964; Population 2. 1, Cn 7993; upper view of dextral Pa element. 2, Cn 7994; upper view of sinistral Pa element. 3, Cn 7995; outer lateral view of sinistral $Pb_1$ element. 4, Cn 7996; outer lateral view of dextral $Pb_1$ element. Figs 1 and 3–4 from Viki core, sample M-375, int. 137·95–138·10 m; fig. 2 from Viki core, sample M-374, int. 138·95–139·10 m.

Figs 5–20, 22–27. *Pterospathodus amorphognathoides amorphognathoides* Walliser, 1964; Population 1. 5, Cn 7997; outer lateral view of dextral $Pb_1$ element. 6, Cn 7998; upper view of dextral Pa element. 7, Cn 7999; outer lateral view of dextral $Pb_2$ element. 8, Cn 8000; upper view of sinistral Pa element. 9, Cn 8001; outer lateral view of dextral $Pb_1$ element. 10, Cn 8002; outer lateral view of sinistral $Pb_1$ element. 11, Cn 8003; outer lateral view of dextral $Pb_2$ element. 12, Cn 8004; outer lateral view of dextral Pa element. 13, Cn 8005; outer lateral view of dextral carnuliform element, short morph. 14, Cn 8006; outer lateral view of sinistral curved element, morph a. 15, Cn 8007; inner lateral view of sinistral $Sc_3$ element. 16, Cn 8008; inner lateral view of sinistral $Sc_2$ element. 17, Cn 8009; inner lateral view of dextral $Sc_3$ element. 18, Cn 8010; inner lateral view of sinistral $Sc_1$ element. 19, Cn 8011; lateral view of Sa element. 20, Cn 8012; inner lateral view of dextral carniciform element. 22, Cn 8013; outer lateral view of sinistral curved element, morph b. 23, Cn 8014; outer lateral view of dextral carnuliform element, morph a. 24, Cn 8015; inner lateral view of dextral $M_1$ element. 25, Cn 8016; posterior view of dextral $Sb_2$ element. 26, Cn 8017; outer lateral view of dextral Pc element. 27, Cn 8018; posterior view of dextral $Sb_1$ element. Figs 5–6 and 8–10 from Viki core, sample M-367, int. 146·70–146·80 m; figs 7, 11–17, 19–20 and 22–27 from Viki core, sample M-368, int. 145·40–145·55 m; fig. 18 from Viki core, sample M-369, int. 144·45–144·50 m.

Figs 21, 28–35. *Pterospathodus amorphognathoides lithuanicus* Brazauskas, 1983. 21, Cn 8019; inner lateral view of dextral Pa element. 28, Cn 8020; outer lateral view of sinistral $Pb_2$ element. 29, Cn 8021; upper view of dextral Pa element. 30, LO 7736t; upper view of dextral Pa element. 31, LO 7737t; upper view of sinistral Pa element, juvenile specimen. 32, Cn 8022; upper view of sinistral Pa element. 33, Cn 8023; outer lateral view of sinistral carnuliform element, morph a(?). 34, Cn 8024; outer lateral view of dextral Pa element. 35, Cn 8025; outer lateral view of sinistral Pa element. Figs 21 and 34–35 from Viki core, sample M-979, int. 148·75–148·85 m; figs 28 and 33 from Viki core, sample M-976, int. 149·95–150·08 m; figs 29 and 32 from Uulu-330 core, sample M-1302, int. 137·44–137·50 m; figs 30–31 from Själsö section (Gotland), sample G88-637LJ.

All × 50.

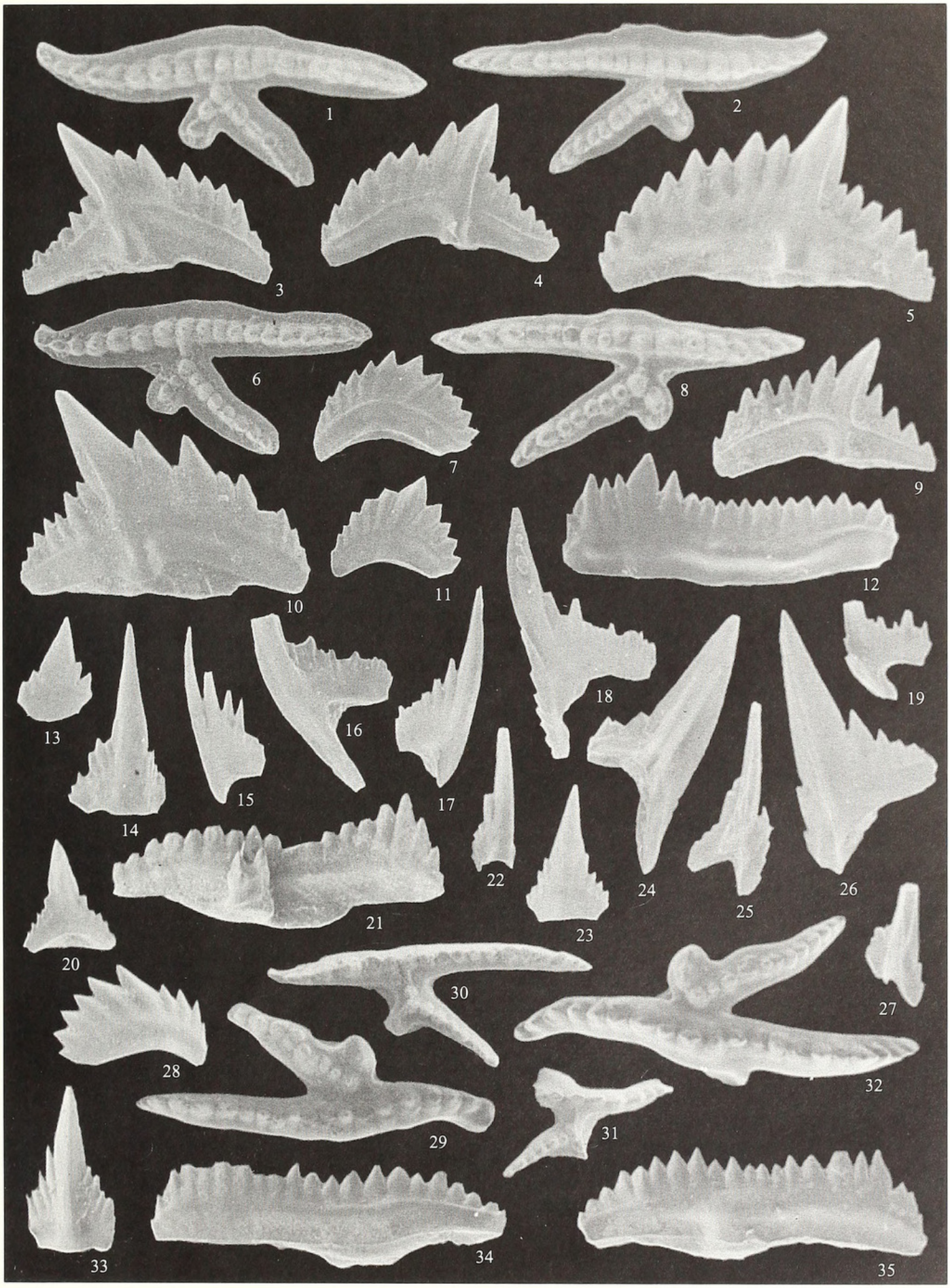


MÄNNIK, *Pterospathodus*

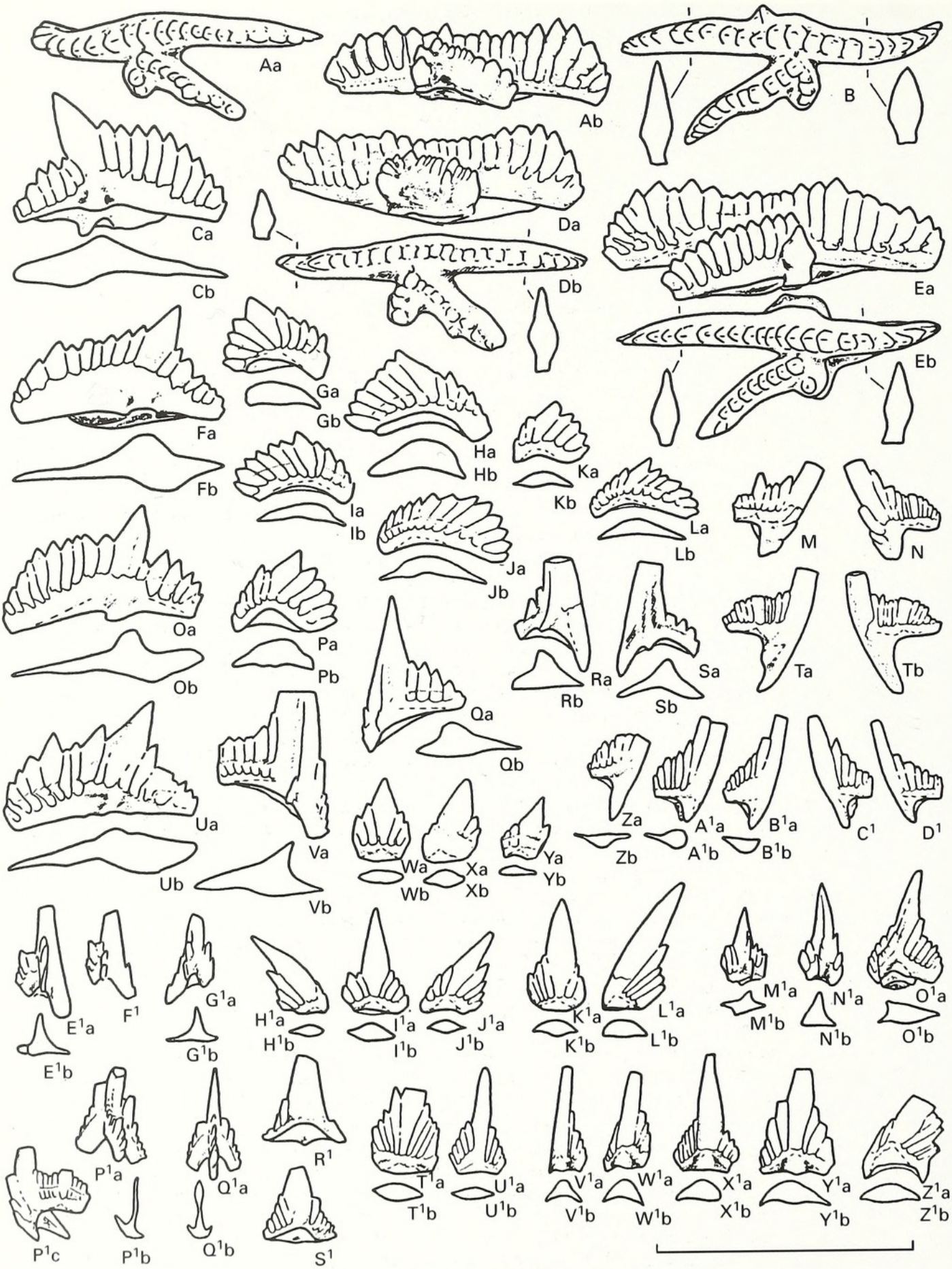


TEXT-FIG. 10. For caption see opposite.

.1977 *Carniodus carinthiacus* Walliser, 1964; Liebe and Rexroad, pl. 1, fig. 2.
.1977 *Carniodus carnulus* Walliser, 1964; Liebe and Rexroad, pl. 1, fig. 3.
.1977 *Carniodus carnicus* Walliser, 1964; Liebe and Rexroad, pl. 1, fig. 4.
.1977 *Pterospathodus amorphognathoides* Walliser, 1964; Liebe and Rexroad, pl. 1, fig. 9.
.1977 *Ozarkodina gaertneri* Walliser, 1964; Liebe and Rexroad, pl. 1, fig. 10.
.1977 *Exochognathus latialatus* (Walliser, 1964); Liebe and Rexroad, pl. 1, fig. 16.
.1977 *Distomodus triangularis* (Walliser, 1964); Liebe and Rexroad, pl. 2, fig. 29.
.1977 *Neoprioniodus costatus* Walliser, 1964; Liebe and Rexroad, pl. 2, figs 30–31.
1977 *Exochognathus brevialatus* (Walliser, 1964); Liebe and Rexroad, pl. 2, fig. 38.
1978 *Neoprioniodus costatus costatus* Walliser, 1964; Miller, pl. 2, figs 10–11.
.1978 *Apparatus 'C' Walliser*, 1964; Miller, pl. 4, figs 8–11.
.1980 *Carniodus carnulus* Walliser, 1964; Helfrich, pl. 1, figs 1–6.
1980 *Pterospathodus amorphognathoides* Walliser, 1964; Helfrich, pl. 2, figs 17–19.
1980 *Pterospathodus celloni* (Walliser, 1964); Helfrich, pl. 2, fig. 30.
.1981 *Pterospathodus amorphognathoides* Walliser, 1964; Nowlan, pl. 7, fig. 6.
.1981 *Pterospathodus amorphognathoides* Walliser, 1964; Uyeno and Barnes, pl. 1, fig. 24.
.1982 *Pterospathodus amorphognathoides* Walliser, 1964; Aldridge and Mohamed, pl. 2, figs 13–16.
.1982 *Carniodus carnulus* Walliser, 1964; Aldridge and Mohamed, pl. 2, figs 17–24.
.1983 *Carniodus carnulus* Walliser, 1964; Mabillard and Aldridge, pl. 2, figs 13–14.
.1983 *Pterospathodus amorphognathoides* Walliser, 1964; Mabillard and Aldridge, pl. 2, figs 25–27.
.1983 *Pterospathodus amorphognathoides* Walliser, 1964; Nowlan, fig. 4*K* [cop. Nowlan 1981, pl. 7, fig. 6].
.1983 *Pterospathodus amorphognathoides* Walliser, 1964; Uyeno and Barnes, p. 24, pl. 8, fig. 24 [cop. Uyeno and Barnes 1981, pl. 1, fig. 24].
.1983 *Pterospathodus amorphognathoides* Walliser, 1964; Barrick, fig. 18*M*.
.1984 *Carniodus? carinthiacus* Walliser, 1964; Drygant, p. 83, pl. 3, figs 8–11.
1984 *Neoprioniodus subcarnus* Walliser, 1964; Drygant, p. 84, pl. 3, figs 14–17.
.1984 *Pterospathodus amorphognathoides* Walliser, 1964; Drygant, p. 109, pl. 7, figs 13–16.
1984 *Ozarkodina gaertneri* Walliser, 1964; Drygant, p. 110, pl. 7, figs 22–27.
(?) 1984 *Carniodus carnicus* Walliser, 1964; Drygant, p. 82, pl. 3, figs 12–13.
v. 1985 *Pterospathodus amorphognathoides* Walliser, 1964; Nehring-Lefeld, p. 635, pl. 1, figs 3–8.
1985 *Carniodus carnulus* Walliser, 1964; Kleffner, pl. 2, figs 26–28.
1985 *Pterospathodus amorphognathoides* Walliser, 1964; Kleffner, pl. 1, fig. 3; pl. 2, figs 29–31.
v. 1985 *Carniodus carnulus* Walliser, 1964; Nehring-Lefeld, p. 632, pl. 2, figs 1–10.
(?) 1985 *Pterospathodus amorphognathoides* Walliser, 1964; Yu, p. 24, pl. 2, fig. 9.
1986 *Pterospathodus amorphognathoides* Walliser, 1964; Jiang *et al.*, pl. 4, figs 1–2.
p. 1987 *Pterospathodus amorphognathoides* Walliser, 1964; Over and Chatterton, pl. 4, figs 1–2 (*non* fig. 3 [= *P. rhodesi*?]).
.1987 *Carniodus carnulus* Walliser, 1964; Kleffner, fig. 5*1–7*.
.1987 *Pterospathodus amorphognathoides* Walliser, 1964; Kleffner, fig. 5*8–9, 11*.
.1987 *Pterospathodus pennatus procerus* (Walliser, 1964); Kleffner, fig. 5*10*.
.1987 *Pterospathodus amorphognathoides* Walliser, 1964; An, p. 201, pl. 33, figs 1–3.
p. 1987 *Pterospathodus pennatus procerus* (Walliser, 1964); An, p. 202, pl. 33, figs 4, 7 (*non* figs 5–6 [= *P. p. procerus*]).
p. 1987 *Exochognathus brassfieldensis* (Branson and Branson, 1947); An, pl. 35, fig. 18 (*non* fig. 17 [indet.]).
1988 *Pterospathodus amorphognathoides* Walliser, 1964; Qiu, pl. 1, fig. 8 [cop. Qiu 1985, pl. 1, fig. 3].
.1989 *Pterospathodus amorphognathoides* Walliser, 1964; Männik and Aldridge, text-fig. 1*G–L*.
v. 1989 *Pterospathodus amorphognathoides* Walliser, 1964; Männik and Aldridge, text-fig. 3*D–E*.

---

TEXT-FIG. 10. *Pterospathodus amorphognathoides lithuanicus* Brazauskas, 1983. A–B, D–E, Pa element. C, F, O, U, $Pb_1$ element. G–L, P, $Pb_2$ element. M–N, $Sc_1$ element. Q, V, Pc element. R–S, $M_1$ element. T, $Sc_2$ element. W–Y, carnuliform element, short morph. Z–$D^1$, $Sc_3$ element. $E^1$–$G^1$, $Sb_1$ element. $H^1$–$L^1$, carnuliform element, morph a. $M^1$, modified carnuliform element, short morph. $N^1$, modified carnuliform element(?). $O^1$, modified carnuliform element. $P^1$, $Sb_2$ element. $Q^1$, Sa element. $R^1$–$S^1$, carniciform element. $T^1$–$U^1$, carnuliform element, morph b. $V^1$–$W^1$, curved element, morph b. $X^1$, curved element, morph a. $Y^1$–$Z^1$, curved element, morph c. Scale bar represents 1 mm.

p. 1990 *Pterospathodus pennatus procerus* (Walliser, 1964); Uyeno, p. 66, pl. 3, fig. 18 (*non* figs 19–20 [= *P. p. procerus*]).
v. 1990 *Pterospathodus amorphognathoides* Walliser, 1964; Männik and Viira, pl. 17, figs 28, 32.
.1991 *Carniodus carnulus* Walliser, 1964; Kleffner, fig. 5*27–28*.
.1991 *Pterospathodus amorphognathoides* Walliser, 1964; Kleffner, fig. 6*21, 26–27*.
.1992 *Pterospathodus amorphognathoides* Walliser, 1964; Barca *et al.*, pl. 10, figs 7–10.
.1992 *Carniodus carnulus* Walliser, 1964; Barca *et al.*, pl. 10, figs 11–12.
.1996 *Pterospathodus amorphognathoides* Walliser, 1964; Wang and Aldridge, pl. 5, fig. 9.
v. 1998 *Pterospathodus amorphognathoides amorphognathoides* Walliser, 1964; Männik and Małkowski, pl. 1, figs 10, 14–17.

*Material.* Several hundreds to thousands of all elements.

*Emended diagnosis. P. amorphognathoides* with distinct basal platform/platform ledges of various configurations and dimensions on all elements.

*Remarks.* The size and shape of the basal platform of the Pa element is highly variable, evidently due to evolutionary changes (see below). The Pa element may or may not possess a triangular lateral lobe/short usually undenticulated process on the outer side of the element. Occasionally, additional

---

EXPLANATION OF PLATE 5

Figs 1–4, 10, 16. *Pterospathodus amorphognathoides amorphognathoides* Walliser, 1964; Population 5. 1, Cn 8026; upper view of dextral Pa element. 2, Cn 8027; upper view of dextral Pa element. 3, LO 7738t; upper view of sinistral Pa element. 4, Cn 8028; outer lateral view of dextral carnuliform element, short morph. 10, Cn 8029; outer lateral view of dextral modified carnuliform element. 16, Cn 8040; inner lateral view of sinistral $Sc_3$ element. Figs 1–2 from Viki core, sample M-391, int. 115·45–115·60 m; fig. 3 from Överstekvarn 2 section (Gotland), sample G88-635LJ; figs 4 and 10 from Viki core, sample M-995, int. 113·80–113·95 m; fig. 16 from Viki core, sample M-390, int. 118·40–118·50 m.

Figs 5–9, 11–15, 17–23, 35. *Pterospathodus amorphognathoides amorphognathoides* Walliser, 1964; Population 4. 5, Cn 8030; outer lateral view of sinistral $Pb_2$ element. 6, Cn 8031; inner lateral view of sinistral $Sc_2$ element. 7, Cn 8032; outer lateral view of dextral $Pb_1$ element. 8, Cn 8033; inner lateral view of dextral carniciform element. 9, Cn 8034; outer lateral view of dextral modified carnuliform element, short morph. 11, Cn 8035; inner lateral view of sinistral $Sc_1$ element. 12, Cn 8036; upper view of dextral Pa element. 13, Cn 8037; upper view of sinistral Pa element. 14, Cn 8038; inner lateral view of dextral $Sc_3$ element. 15, Cn 8039; outer lateral view of sinistral carnuliform element, morph a. 17, Cn 8041; outer lateral view of sinistral modified carnuliform element. 18, Cn 8042; lateral view of symmetrical carnuliform element, morph a. 19, Cn 8043; posterior view of sinistral $Sb_2$ element. 20, Cn 8044; posterior view of dextral $Sb_2$ element. 21, Cn 8045; outer lateral view of dextral curved element, morph b. 22, Cn 8046; posterior view of dextral $Sb_1$ element. 23, Cn 8047; outer lateral view of sinistral Pc element. 35, Cn 8048; outer lateral view of sinistral modified carnuliform element, short morph. Figs 5, 8–9, 11, 14–15, 17–20 and 22 from Viki core, sample M-386, int. 123·25–123·45 m; fig. 6 from Viki core, sample M-385, int. 124·60–124·75 m; figs 7, 12–13, 21, 23 and 35 from Viki core, sample M-384, int. 125·60–125·75 m.

Figs 24–34, 36–40. *Pterospathodus amorphognathoides amorphognathoides* Walliser, 1964; Population 3. 24, Cn 8049; upper view of sinistral Pa element. 25, Cn 8050; inner lateral view of sinistral $Sc_1$ element. 26, Cn 8051; outer lateral view of sinistral $Pb_1$ element. 27, Cn 8052; upper view of sinistral Pa element. 28, Cn 8053; outer lateral view of dextral curved element, morph a. 29, Cn 8054; inner lateral view of dextral $Sc_1$ element. 30, Cn 8055; inner lateral view of sinistral $M_1$ element. 31, Cn 8056; outer lateral view of sinistral $Pb_2$ element. 32, Cn 8057; upper view of dextral Pa element. 33, Cn 8058; inner lateral view of dextral $Sc_2$ element. 34, Cn 8059; outer lateral view of dextral carnuliform element, morph a. 36, Cn 8060; outer lateral view of sinistral modified carnuliform element. 37, Cn 8061; outer lateral view of dextral $Pb_2$ element. 38, Cn 8062; inner lateral view of sinistral $Sc_3$ element. 39, Cn 8063; outer lateral view of sinistral carnuliform element, short morph. 40, Cn 8064; outer lateral view of dextral $Sb_2$ element. Figs 24, 26, 28, 31–33, 36 and 38–39 from Viki core, sample M-378, int. 134·80–134·90 m; figs 25 and 29 from Viki core, sample M-380, int. 131·85–132·00 m; figs 27, 30, 34, 37 and 40 from Viki core, sample M-381, int. 130·45–130·55 m.

All × 50.

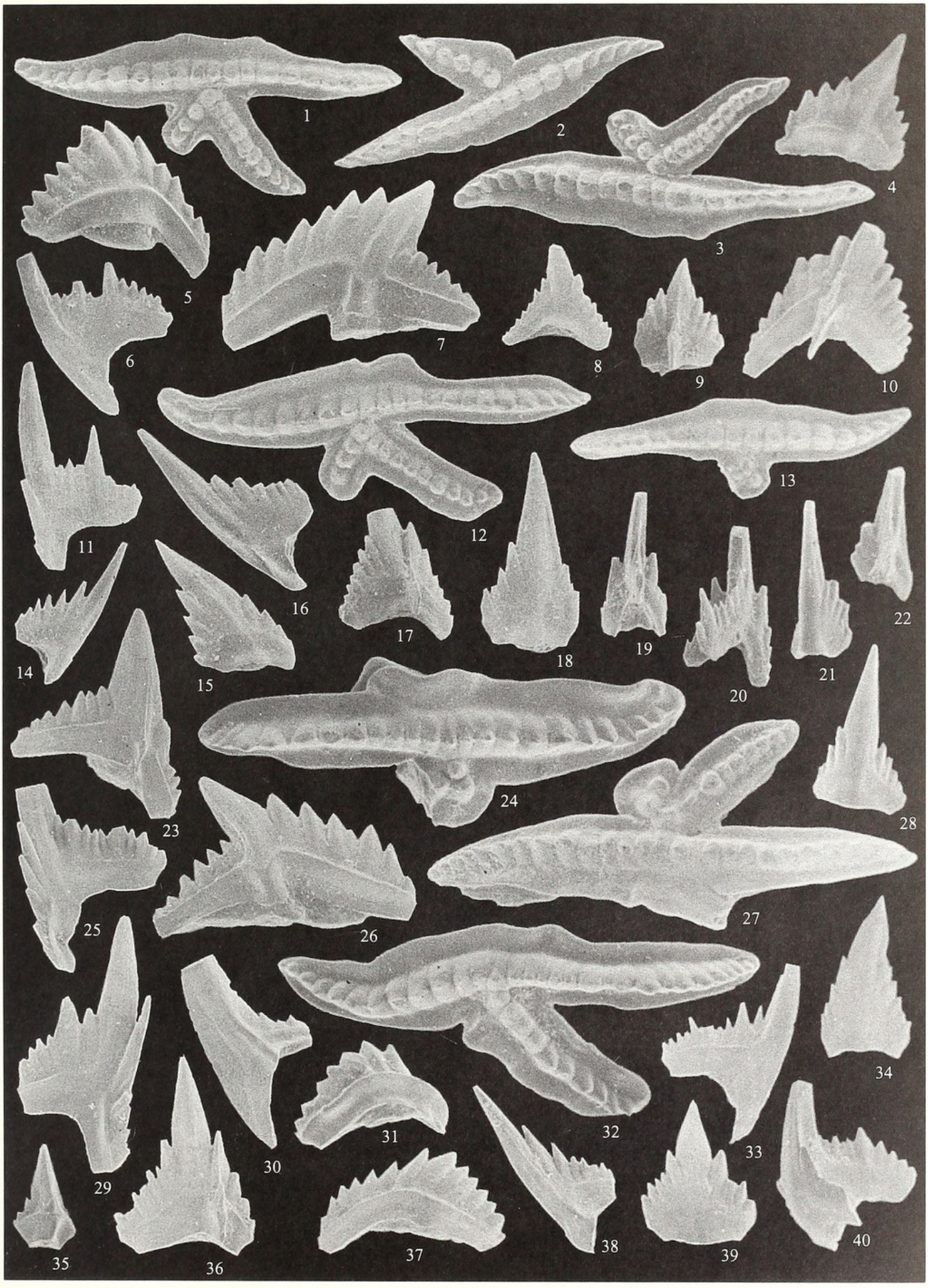


MÄNNIK, *Pterospathodus*

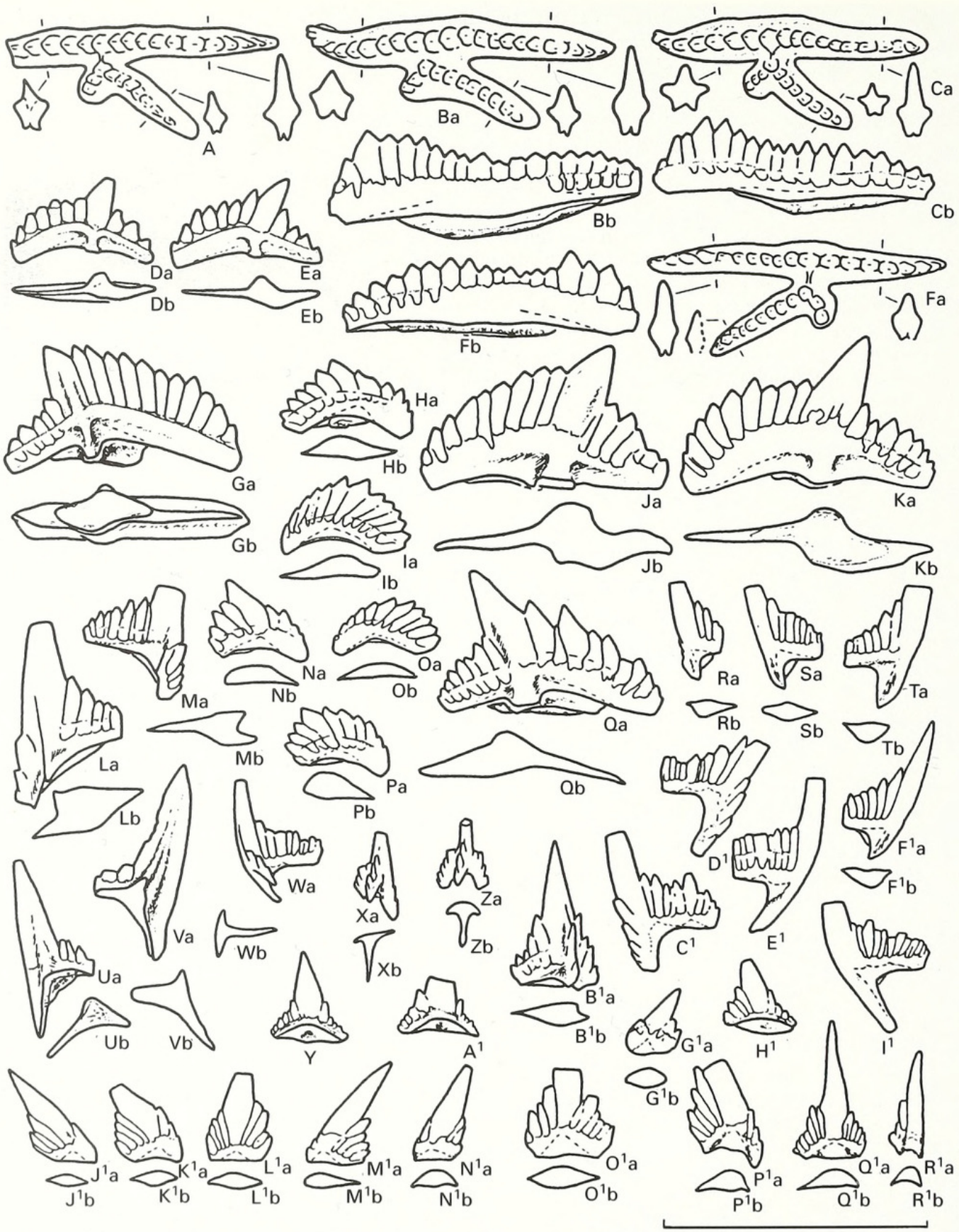


TEXT-FIG. 11. *Pterospathodus amorphognathoides amorphognathoides* Walliser, 1964; Population 1. A–C, F, Pa element. D–E, G, J–K, Q, $Pb_1$ element. H–I, N–P, $Pb_2$ element. L–M, Pc element. R–T, $F^1$, $Sc_3$ element. U–V, $M_1$ element. W, $Sb_2$ element. X, $Sb_1$ element. Y, $A^1$, $H^1$, carniciform element. Z, Sa element. $B^1$, modified carnuliform

lateral denticle(s) may occur at the distal part of the process. Although the fauna is dominated by elements with a bifurcated lateral process, pennate elements may be found quite often. These are easily separated from pennate elements of *P. p. procerus* on the basis of the configuration of the basal platform and cavity.

Based on changes in the morphology of the Pa element, five main temporal populations can be recognized in *P. a. amorphognathoides* (Pls 4–5; Text-figs 3, 11–15).

*Population 1* (Pl. 4, figs 5–20, 22–27; Text-fig. 11). The Pa element possesses a narrow but distinct platform (Pl. 4, figs 6, 8; Text-fig. 11A–C, F). This population also includes rare specimens almost indistinguishable from the elements of *P. a. lithuanicus*. However, in this interval the Pa elements similar to those of *P. a. lithuanicus* possess a short narrow ledge on the outer side of the distal part of the posterior process (Pl. 4, fig. 12). This structure is missing (Pl. 4, figs 29–32, 35), or is very rare (Pl. 4, fig. 34), on the Pa elements of *P. a. lithuanicus*. It is possible that the presence of such Pa elements in Population 1 is evidence that this population forms an evolutionary link between *P. a. lithuanicus* and *P. a. amorphognathoides*. Population 1 is included in *P. a. amorphognathoides* because the subspecies boundary is drawn at the appearance of the new character (platform), not at the point where it was found in all individuals. It is also evident that the initial appearance of platform ledges on the Pa element started on the outer side of the distal part of the posterior process.

Characteristic for Population 1 are at least three morphs of $Pb_1$ elements.

1. Relatively large and long elements without platform ledges (Pl. 4, figs 5, 10; Text–fig. 11J–K), resembling those of *P. a. lithuanicus* (compare Pl. 3, figs 15, 17; Text-fig. 10C, F, O, U).
2. Small straight elements with a distinct high cusp and narrow platform-ledges (Pl. 4, fig. 9; Text-fig. 11D–E).
3. Relatively large straight elements with a short cusp, high denticles on the long anterior process and low denticles on the shorter posterior process (Text-fig. 11G). This morph is almost identical to the holotype of Walliser's '*Ozarkodina gaertneri*' (Walliser 1964, pl. 27, fig. 14). In the collections studied, this type of element is extremely rare, occurring only in few samples and represented, as a rule, by one or two specimens. Rare elements of this type can be found also in younger populations (Text-fig. 13V).

Morphs 1 and 2 dominate in Population 1, the former being more abundant in older strata and morph 2 in younger strata.

*Population 2* (Pl. 4, figs 1–4; Text-fig. 12). The morphologically highly variable platform is widest on the outer proximal side of the Pa element and narrows gradually distally.

*Population 3* (Pl. 5, figs 24–40; Text-fig. 13). The platform on the Pa elements reaches its maximum size in this population. The edges of it, particularly on the posterior process, are strongly undulating and partly turned up. Many specimens possess a triangular or semiquadrate outer lateral lobe/short process which may or may not bear denticle(s) (Pl. 5, fig. 27; Text-fig. 12A, C). In Population 3 platform ledges become well developed on most of the elements of the apparatus.

*Population 4* (Pl. 5, figs 5–9, 11–15, 17–23; Text-fig. 14). On typical Pa elements of this population the platform is wide on the posterior process and becomes rapidly narrow on the anterior process forming a distinct 'bulge' on the outer side of the element, anterior of the point where the inner bifurcated process joins the main blade. Just behind this 'bulge' the platform is widest and possesses an upturned, undulating edge. The structure described above is distinct on the dextral element (Pl. 5, fig. 12; Text-fig. 14A, C) but less well developed on the sinistral one (Pl. 5, fig. 13; Text-fig. 14B).

*Population 5* (Pl. 5, figs 1–4, 10, 16; Text-fig. 15). Most characteristic for this population is a Pa element with the platform widest proximally on the outer side of the element and narrowing equally towards the posterior and anterior ends. Many elements also possess an additional denticle between the main row of denticles and that on the bifurcating lateral process (Text-fig. 15E, G).

Very characteristic of this, the youngest population of *P. a. amorphognathoides*, is the strongly arched (in lateral view) modified carnuliform element (Pl. 5, fig. 10; Text-fig. 15O$^1$–P$^1$). Also, in some sections, a few Pa elements with an extremely wide platform (Text-fig. 15C) were found in the uppermost part of the range of Population 5.

---

element. C$^1$–D$^1$, $Sc_1$ element. E$^1$, I$^1$, $Sc_2$ element. G$^1$, carnuliform element, short morph. J$^1$–N$^1$, carnuliform element, morph a. O$^1$, carnuliform element, morph b(?). P$^1$, curved element, morph c. Q$^1$, curved element, morph a. R$^1$, curved element, morph b. Scale bar represents 1 mm.

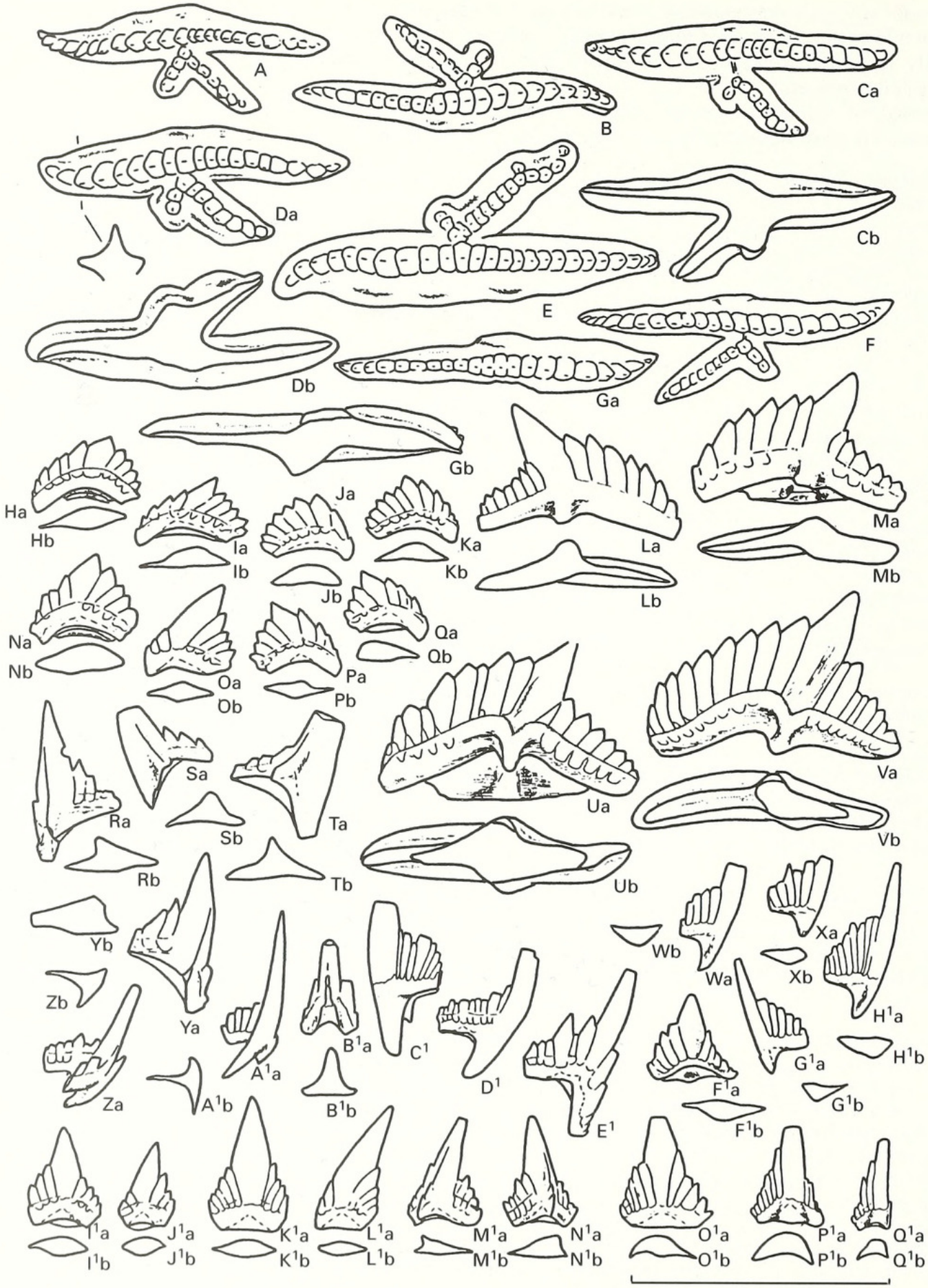


TEXT-FIG. 12. For caption see opposite.

The elements of *P. a. amorphognathoides* in Population 3 are quite similar to those of *P. rhodesi* (see below), differing from them mainly by the less well developed platform/platform ledges. *P. a. amorphognathoides* is abundant and dominates conodont faunas in the open shelf carbonate-terrigeneous facies. Towards the basin it becomes rare and is ecologically replaced by *P. pennatus procerus*.

The populations listed above will in the future probably allow the recognition of several stratigraphically useful subdivisions in the *P. a. amorphognathoides* Zone. However, further studies are needed.

*Occurrence*. *P. a. amorphognathoides*, Lower *Pseudooneotodus bicornis* and Upper *Ps. bicornis* zones. *P. a. amorphognathoides* has been recognized world-wide (see synonymy) except for a few regions: Severnaya Zemlya (Männik 1983) and the Sub-Polar Urals (Melnikov, pers. comm.). It is extremely rare in eastern Canada (Gaspé Peninsula; Nowlan 1983). *P. a. amorphognathoides* is evidently also missing in several other regions (e.g. Greenland – Armstrong 1990; Alaska – Savage 1985; some regions in north-western Canada – McCracken 1991; and Australia – Bischoff 1986) where it is replaced by *P. rhodesi*.

### P. pennatus *lineage*

As was noted above the *P. pennatus* lineage probably appeared, together with the *P. amorphognathoides* lineage, at the end of the *P. eopennatus* Zone. Both lineages evidently originated from the same ancestral taxon: *P. eopennatus* ssp. nov. 2 (Text-fig. 3; Männik 1995). However, some data suggest also another possibility. Morph 5 of *P. eopennatus* ssp. nov. 1 from the *A. irregularis–A. kuehni* subzones is morphologically very similar to *P. p. pennatus* of Walliser (1964, pl. 14, figs 23–26). In the Cellon section *P. p. pennatus* is found together with *P. celloni* in strata considerably younger than the known range of morph 5 in Estonia. Also, the morphologies of elements and co-occurrences of taxa in Cellon indicate that the oldest *P. celloni* fauna described from that section is no older than the latest *P. eopennatus*, but most probably comes from the earliest *P. celloni* chron (Männik 1996).

In Estonia, in open shelf environments morph 5 disappeared during the end-*irregularis* event. That event caused considerable changes in conodont faunas. Several taxa became extinct or disappeared temporarily and *P. eopennatus* ssp. nov. 1 was replaced by *P. eopennatus* ssp. nov. 2. However, it cannot be excluded that *P. eopennatus* ssp. nov. 1 survived the end-*irregularis* event somewhere in offshore regions and gave rise to the *P. p. pennatus – P. p. procerus* lineage. The morphological similarities between the Pa element of *P. p. pennatus* and morph 5 of *P. eopennatus* ssp. nov. 1 suggest a possibility that these two taxa are directly connected. It is possible that the two ecologically restricted lineages might have appeared already at the end of the *A. irregularis* chron. However, no data about the deeper basin lineage is yet available from the interval between the ranges of *P. eopennatus* ssp. nov. 1 and *P. p. pennatus*. Also, *P. p. pennatus* itself has not been found in Estonia. Therefore, in this paper *P. pennatus* is described as a descendant of *P. eopennatus* appearing in the sequence at the same time as *P. amorphognathoides*.

*Pterospathodus pennatus pennatus* (Walliser, 1964)

*1964 *Spathognathodus pennatus pennatus* Walliser, p. 79, pl. 14, figs 23–26; pl. 15, fig. 1.
(?)1968 *Neospathognathodus pennatus* (Walliser, 1964); Nicoll and Rexroad, p. 47, pl. 2, fig. 5.

*Remarks*. *P. p. pennatus* has not been identified in Estonia. In Cellon *P. p. pennatus* has the same

---

TEXT-FIG. 12. *Pterospathodus amorphognathoides amorphognathoides* Walliser, 1964; Population 2. A–G, Pa element. H–K, N–Q, $Pb_2$ element. L–M, U–V, $Pb_1$ element. R, Y, Pc element. S–T, $M_1$ element. W–X, $G^1$–$H^1$, $Sc_3$ element. Z, $Sb_2$ element. $A^1$, $Sb_1$ element. $B^1$, Sa element. $C^1$–$D^1$, $Sc_2$ element. $E^1$, $Sc_1$ element. $F^1$, carniciform element. $I^1$–$J^1$, carnuliform element, short morph. $K^1$–$L^1$, carnuliform element morph a. $M^1$–$N^1$, modified carnuliform element. $O^1$, ?curved element, morph c. $P^1$, curved element, morph a. $Q^1$, curved element, morph b. Scale bar represents 1 mm.

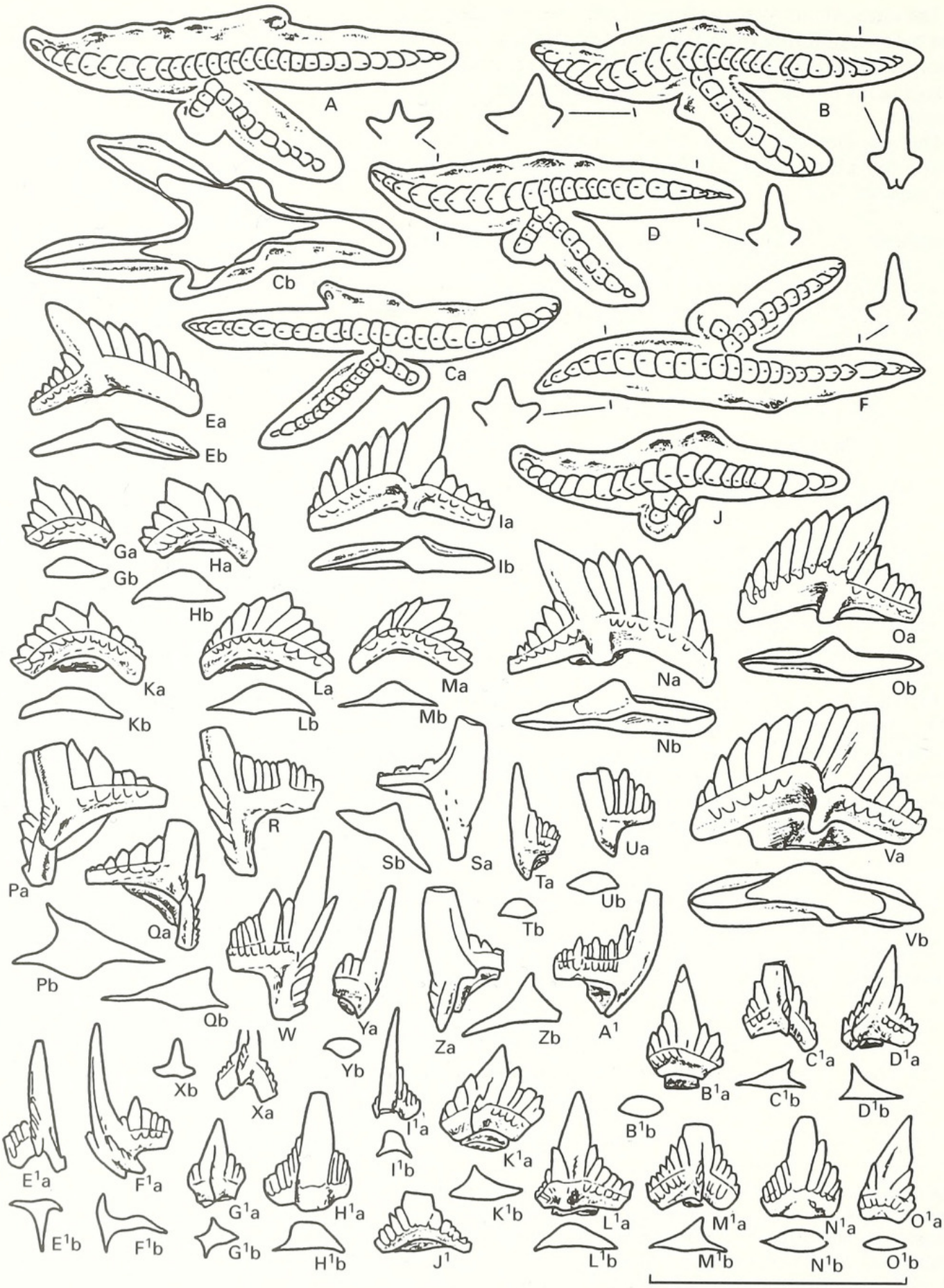


TEXT-FIG. 13. For caption see opposite.

range as *P. celloni* (Walliser 1964). In this section *P. p. pennatus* is very rare in the lowermost sample studied (10 B) which is dominated by elements of *P. a. angulatus*. In sample 10 H/J, I have identified a fragment probably belonging to *P. amorphognathoides lennarti* ssp. nov. together with *P. p. pennatus* and *P. celloni*. In the uppermost sample with *P. p. pennatus* (sample 10 J), a few Pa and Pb elements (Walliser 1964, pl. 15, fig. 1; pl. 27, fig. 5) occur which are morphologically almost identical to those of *P. p. procerus*, indicating a close relationship between these two subspecies.

The morphologically distinct $Pb_1$, $Pb_2$, Pc, $Sc_1$, $Sc_2$ and $Sb_2$ elements, which occur in Estonia with the Pa elements of *P. celloni*, are considered to belong to the apparatus of the latter species (see below). However, '*Neoprioniodus triangularis tenuirameus*' (Walliser 1964, pl. 28, figs 22–24; = $M_1$ element; fig. 21 cannot be identified without direct study of the specimen) and '*Carniodus eocarnicus*' (Walliser 1964, pl. 28, figs 19–20; = $Sc_1$ element) may belong either to *P. celloni* or *P. p. pennatus* – they all are found together in the same strata. Here these elements are tentatively assigned to *P. celloni* (see synonymy). The specimen illustrated by Walliser (1964, pl. 28, fig. 12) as '*N. subcarnus*' is considered to be the $Sc_2$ element of *P. celloni*. The majority of the other *Carniodus*-elements illustrated by Walliser (1964) possess distinct platform ledges and evidently belong to *P. a. amorphognathoides* (see above).

*Occurrence.* *P. celloni* Zone.

## *Pterospathodus pennatus procerus* (Walliser, 1964)

Plate 6, figures 1–25, 27–35; Text-figure 16

v. 1964 *Spathognathodus pennatus procerus* Walliser, p. 80, pl. 15, figs 2–8.
1966 *Spathognathodus pennatus procerus* Walliser, 1964; Spasov and Filipović, p. 50, pl. 1, fig. 6.
p. 1968 *Spathognathodus pennatus procerus* Walliser, 1964; Igo and Koike, pp. 18–19, pl. 2, figs 8–10 (*non* fig. 11 [indet.]).
p. 1968 *Ozarkodina gaertneri* Walliser, 1964; Igo and Koike, p. 14, pl. 1, figs 7–9 (*non* figs 5–6 [= *P. a. amorphognathoides*]).
1968 *Neoprioniodus costatus paucidentatus* Walliser, 1964; Igo and Koike, p. 12, pl. 3, figs 16–17.
.1968 *Neoprioniodus triangularis tenuirameus* Walliser, 1964; Igo and Koike, p. 13, pl. 3, figs 18–19.
p. 1968 *Carniodus* sp. A Igo and Koike, p. 8, pl. 3, fig. 2 (*non* fig. 3 [= *P. a. amorphognathoides*]).
.1968 *Carniodus* sp. B Igo and Koike, p. 8, pl. 3, fig. 20.
.1968 *Roundya*? sp. C Igo and Koike, p. 17, pl. 3, figs 25–28.
p. 1968 *Neoprioniodus* spp. Igo and Koike, p. 14, pl. 3, fig. 24 (*non* fig. 4 [= *P. a. amorphognathoides*]).
1969 *Spathognathodus pennatus procerus* Walliser, 1964; Drygant, p. 50, pl., figs 2–3.
.1976 *Pterospathodus pennatus pennatus* (Walliser, 1964); Barrick and Klapper, p. 86, pl. 1, fig. 19.
v. 1979 *Pterospathodus pennatus procerus* (Walliser, 1964); Jeppsson, p. 235, fig. 71*I–8*.
.1983 *Pterospathodus pennatus procerus* (Walliser, 1964); Savage *et al.*, fig. 2*A–F*.
1984 *Pterospathodus pennatus procerus* (Walliser, 1964); Stouge and Bagnoli Stouge, p. 109, pl. 2, figs 14–17.
1984 *Pterospathodus pennatus procerus* (Walliser, 1964); Drygant, p. 108, pl. 7, figs 17–20.
1985 *Pterospathodus pennatus procerus* (Walliser, 1984); Yu, pl. 1, figs 1–2.
v. 1985 *Pterospathodus pennatus pennatus* (Walliser, 1964); Nehring-Lefeld, p. 637, pl. 1, figs 1–2.
1985 *Pterospathodus pennatus procerus* (Walliser, 1974); Savage, p. 714, fig. 4*A–K*.
vp. 1986 *Pterospathodus procerus* (Walliser, 1964); Bischoff, p. 204, pl. 29, figs 9–10, 15–30 (*non* figs 13–14 [indet.]); pl. 30, figs 1–2 (*non* figs 3–11 [= *P. rhodesi*]).
.1987 *Pterospathodus pennatus procerus* (Walliser, 1964); Over and Chatterton, pl. 4, fig. 4.

---

TEXT-FIG. 13. *Pterospathodus amorphognathoides amorphognathoides* Walliser, 1964; Population 3. A–D, F, J, Pa element. E, I, N–O, V, $Pb_1$ element. G–H, K–M, $Pb_2$ element. P–Q, Pc element. R, W, $Sc_1$ element. S, Z, $M_1$ element. T–U, Y, $Sc_3$ element. X, Sa element. $A^1$, $Sc_2$ element. $B^1$, $L^1$, carniliform element, short morph. $C^1$–$D^1$, $M^1$, modified carniliform element. $E^1$, $Sb^1$ element. $F^1$, $Sb_2$ element. $G^1$, modified carniliform element, short morph. $H^1$, curved element, morph a. $I^1$, curved element, morph b. $J^1$, carniciform element. $K^1$, modified carniliform element, short morph. $N^1$, carniliform element, morph b. $O^1$, carniliform element, morph a. Scale bar represents 1 mm.

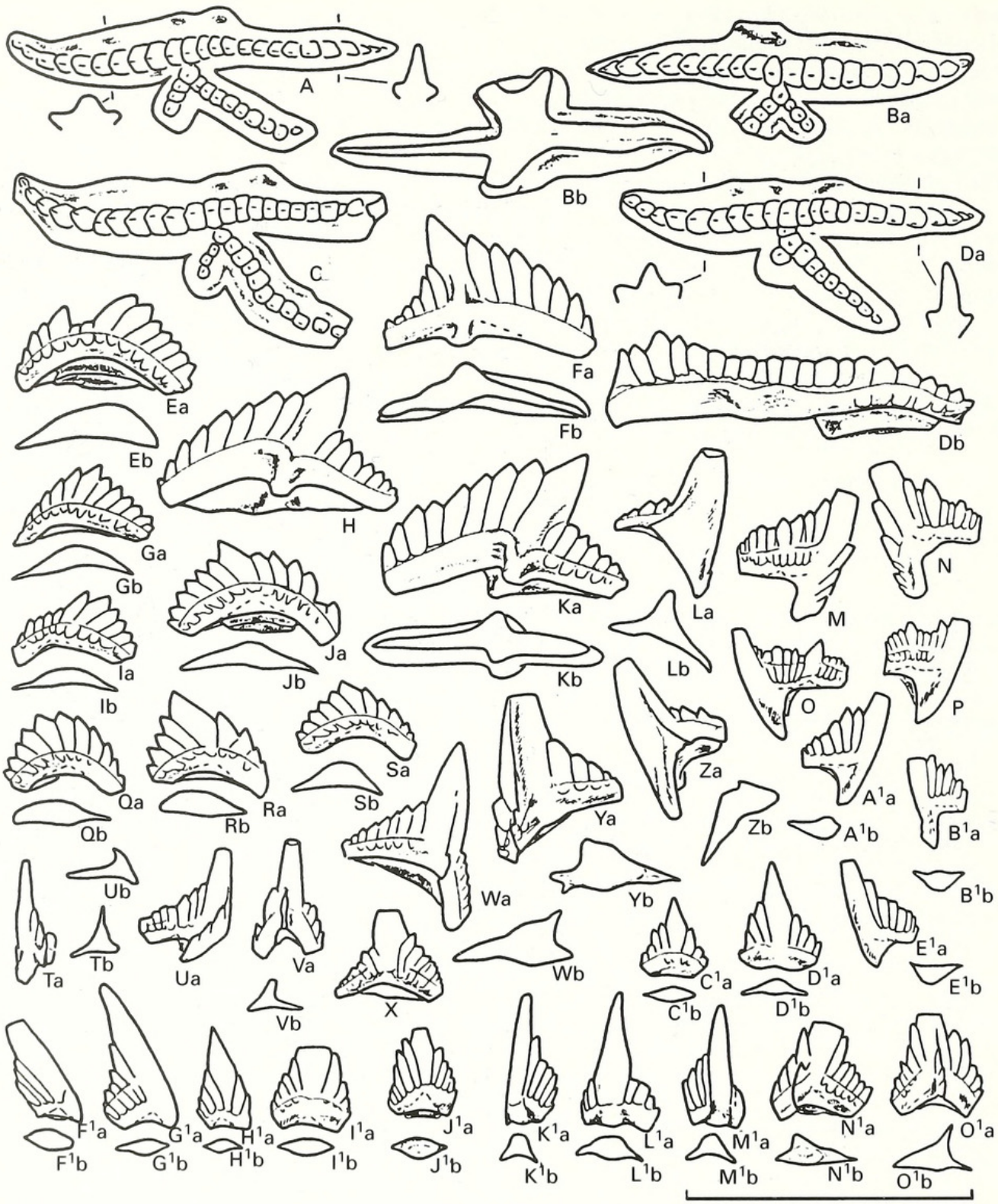


TEXT-FIG. 14. *Pterospathodus amorphognathoides amorphognathoides* Walliser, 1964; Population 4. A–D, Pa element. E, G, I–J, Q–S, $Pb_2$ element. F, H, K, $Pb_1$ element. L, Z, $M_1$ element. M–N, $Sc_1$ element. O–P, $Sc_2$ element. T, $Sb_1$ element. U–V, $Sb_2$ element. W, Y, Pc element. X, carniciform element. $A^1$–$B^1$, $E^1$, $Sc_3$ element. $C^1$–$D^1$, carnuliform element, short morph. $F^1$–$I^1$, carnuliform element, morph a. $J^1$, carnuliform element, morph b(?). $K^1$, $M^1$, curved element, morph b. $L^1$, curved element, morph a. $N^1$–$O^1$, modified carnuliform element. Scale bar represents 1 mm.

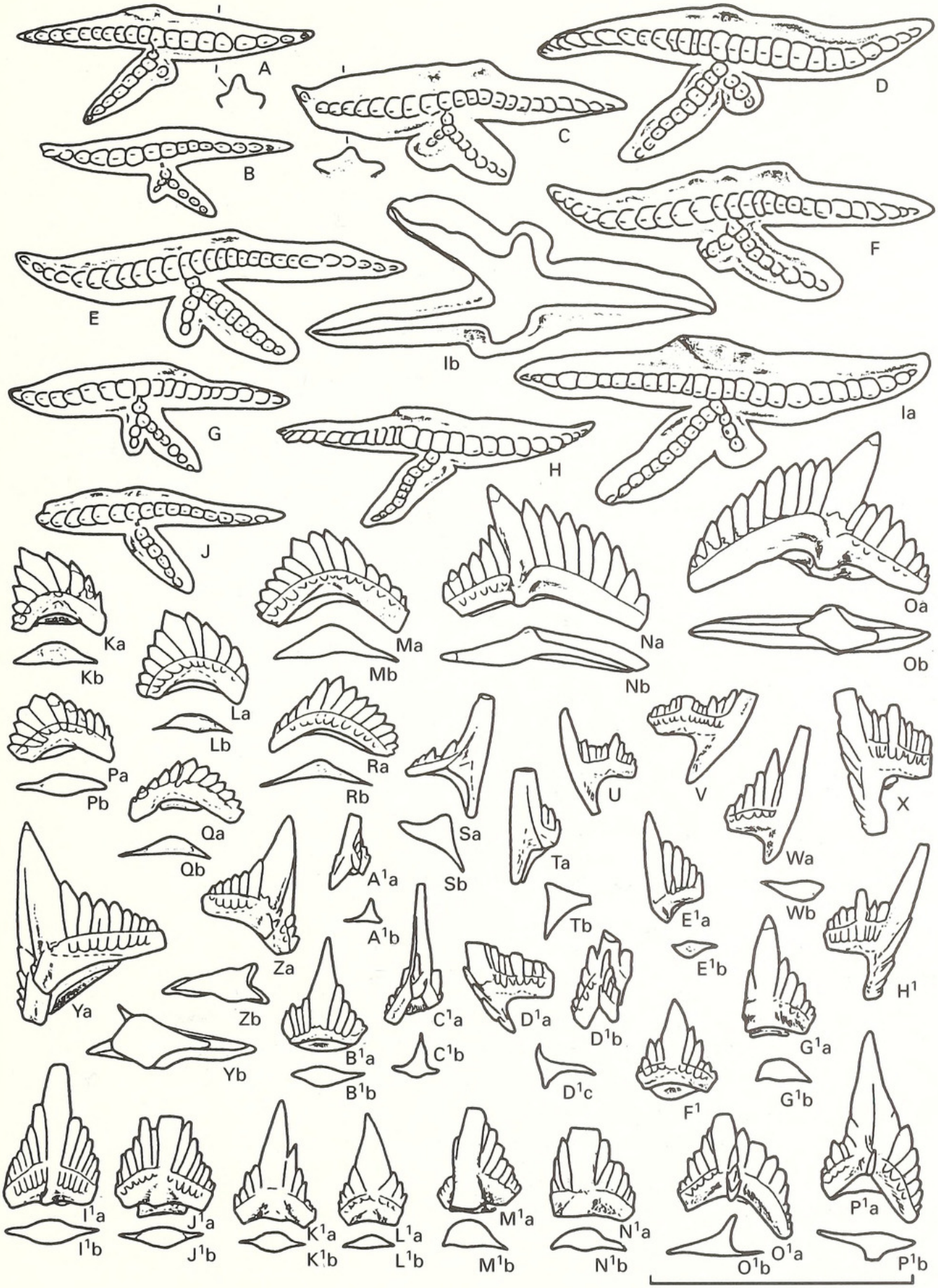


TEXT-FIG. 15. For caption see opposite.

p. 1987 *Pterospathodus pennatus procerus* (Walliser, 1964); An, p. 202, pl. 33, figs 5–6 (*non* figs 4, 7 [= *P. a. amorphognathoides*]).
v. 1990 *Pterospathodus procerus* (Walliser, 1964); Männik and Viira, pl. 17, figs. 29.
p. 1990 *Pterospathodus pennatus procerus* (Walliser, 1964); Uyeno, p. 66, pl. 3, figs 19–20 (*non* fig. 18 [= *P. a. amorphognathoides*]).
.1991 *Pterospathodus procerus* (Walliser, 1964); McCracken, p. 109, pl. 4, figs 12–23.
p? 1991 *Carniodus carnulus* Walliser, 1964; McCracken, p. 108, pl. 3, figs 13–14 (*non* figs 6–12, 15 [= *P. rhodesi*]).
.1992 *Pterospathodus pennatus procerus* (Walliser, 1964); Nehring-Lefeld, pl. 3, figs 1–2.
v. in press *Pterospathodus pennatus procerus* (Walliser, 1964); Männik and Małkowski, pl. 1, figs 6–7, 11–13, 18.

*Material.* Many tens to about a hundred of the Pa and $Pb_1$ elements; few to a few tens of all other elements.

*Remarks.* The apparatus of *P. p. procerus* is well represented in several samples in the studied collections. Pa, $Pb_1$, $Pb_2$, Pc, $M_1$, $M_2$, $Sc_1$, $Sc_2$, $Sc_3$, $Sb_1$, $Sb_2$, Sa, carnuliform morphs a and b, and a possible carniciform element are recognized. The $M_2$ element (Pl. 6, figs 1, 3; Text-fig. 16W–Z) has so far been found only in the *P. p. procerus* apparatus. The $Sc_2$ element seems to be represented by two morphs, one without and the other with denticles on the basal part of the anterior edge of the cusp (Pl. 6, figs 9, 22 and 7, 25 respectively; Text-fig. 16$P^1$–$Q^1$ and $R^1$–$S^1$, $V^1$–$W^1$ respectively). Probable carniciform element (Text-fig. 16$X^1$–$A^2$, $N^2$–$O^2$) of this apparatus possesses a considerably taller cusp than its possible homologues in other apparatuses of *Pterospathodus* (Text-figs 4–15).

The data available allow the recognition of ecological replacement of *P. a. amorphognathoides* by *P. p. procerus* towards offshore environments (Männik 1992). In open shelf environments *P. p. procerus* is extremely rare or completely absent in the *P. a. amorphognathoides* Zone, although in many regions (Estonia – Männik 1992; Gotland – Jeppsson 1979, Jeppsson and Männik 1993; Britain – Männik and Aldridge 1989, Aldridge *et al.* 1993) *P. p. procerus* has been identified from a short interval above the last *P. a. amorphognathoides*. This appearance of *P. p. procerus* in open shelf environments was probably connected with the Ireviken Event, with the extinction of *P. a. amorphognathoides* creating a vacant niche.

*Occurrence. P. a. amorphognathoides* to Upper *P. p. procerus* zones (Jeppsson 1994, 1997) in deeper basin environments; Lower and Upper *P. p. procerus* zones in open shelf facies. *P. p. procerus* has been found in most known sequences world-wide (see synonymy).

### *Pterospathodus celloni* (Walliser, 1964)

Plate 6, figures 26, 36–54; Text-figure 17

v.* 1964 *Spathognathodus celloni* Walliser, p. 73, pl. 14, figs 3–16.
v. 1964 *Ozarkodina adiutricis* Walliser, p. 54, pl. 27, figs 1–10.
vp. 1964 *Carniodus eocarnicus* Walliser, p. 34, pl. 28, fig. 20 (*non* fig. 19 [= *P. amorphognathoides*]).
vp. 1964 *Neoprioniodus subcarnus* Walliser, p. 51, pl. 28, fig. 12 (*non* figs 13–14 [= *P. a. amorphognathoides*]).
v. 1964 *Neoprioniodus triangularis tenuirameus* Walliser, p. 53, pl. 28, figs 21–24.
v. 1964 *Neoprioniodus costatus paucidentatus* Walliser, p. 48, pl. 28, figs 31–35.
v.? 1964 *Roundya brevialata* Walliser, p. 69, pl. 31, figs 8–10.
? 1968 *Ozarkodina adiutricis* Walliser, 1964; Nicoll and Rexroad, p. 48, pl. 2, fig. 8.
? 1968 *Neospathognathodus celloni* (Walliser, 1964); Nicoll and Rexroad, p. 45, pl. 2, figs 1–4.
1971 *Neospathognathodus celloni* (Walliser, 1964); Rexroad and Nicoll, pl. 1, figs 2–4.
1971 *Ozarkodina adiutricis* Walliser, 1964; Rexroad and Nicoll, pl. 1, fig. 5.

---

TEXT-FIG. 15. *Pterospathodus amorphognathoides amorphognathoides* Walliser, 1964; Population 5. A–J, Pa element. K–M, P–R, $Pb_2$ element. N–O, $Pb_1$ element. S–T, $M_1$ element. U–V, $Sc_2$ element. W, $E^1$, $Sc_3$ element. X, $H^1$, $Sc_1$ element. $B^1$, carniciform element. $C^1$, Sa element. $D^1$, $Sb_2$ element. $F^1$, carnuliform element, short morph. $G^1$, $N^1$, curved element, morph a. $I^1$–$J^1$, carnuliform element, morph b. $K^1$–$L^1$, carnuliform element, morph a. $M^1$, curved element, morph b(?). $O^1$–$P^1$, modified carnuliform element. Scale bar represents 1 mm.

1972 *Ozarkodina adiutricis* Walliser, 1964; Rexroad and Nicoll, pl. 1, figs 15–16.
1972 *Spathognathoides celloni* Walliser, 1964; Rexroad and Nicoll, pl. 1, figs 17–19.
1976 *Pterospathodus celloni* (Walliser, 1964); Barrick and Klapper, p. 82, pl. 1, figs 3, 5.
1977 *Ozarkodina adiutricis* Walliser, 1964; Liebe and Rexroad, pl. 1, fig. 11.
1977 *Spathognathodus celloni* Walliser, 1964; Liebe and Rexroad, pl. 1, fig. 12.
1989 *Pterospathodus celloni* (Walliser, 1964); Männik and Aldridge, text-fig. 1*A–F*.
? 1994 *Pterospathodus celloni* (Walliser, 1964); Watkins *et al.*, pl. 10, figs 1–4.

*Material.* Many tens of Pa and Pb elements; a few Pc, $Sc_1$ and $Sc_2$ elements.

*Remarks. P. celloni* is very rare in the Estonian collections, which mainly represent a proximal carbonate-terrigeneous facies. It is mostly represented by Pa and $Pb_1$ elements, with the $Pb_2$ element quite common. However, the identification of the $Pb_2$ element among co-occurring juvenile $Pb_2$ elements of *P. amorphognathoides lennarti* ssp. nov. and *P. a. lithuanicus* is quite problematical. Of the other elements of *P. celloni*, only the $Sc_1$, $Sc_2$ and extremely rare specimens of the $Sb_2$ have been identified. $Sc_1$, $Sc_2$ and $Sb_2$ elements of *P. celloni* are morphologically almost identical to their homologues in *P. eopennatus* apparatuses (Pl. 1, figs 3, 6, 13, 44–45; Text-figs 4F$^2$, H$^2$–K$^2$, 5A$^1$–B$^1$, H$^1$–J$^1$; 6L$^1$–P$^1$, U$^1$–V$^1$). The $Sb_2$ is also almost identical to its homologue in *P. p. procerus* (Pl. 6, figs 10–11, 17–19, 27; Text-fig. 16N$^1$).

Some peculiar carniodiform elements occur together with *P. celloni*. They are here identified as carniciform(?) (Pl. 6, fig. 50; Text-fig. 17L$^1$–N$^1$) and carnuliform (Pl. 6, figs 42, 51–52, 54; Text-fig. 17O$^1$–I$^2$) elements of *P. celloni* apparatus. It is also probable that at least some of the elements described by Walliser (1964) as '*N. triangularis tenuirameus*' and '*N. costatus paucidentatus*' represent, accordingly, the $M_1$ and Pc elements of *P. celloni* (see synonymy).

*P. celloni* seems to have been more abundant in deeper basin environments (graptolite-bearing facies) and was very rare in open shelf regions. Although its origin needs further investigation it is evident that *P. celloni* was closely related to the *P. pennatus* lineage.

*Occurrence.* From the uppermost part of the *P. a. angulatus* Subzone to the *P. a. lithuanicus* Subzone in open shelf facies. The range in deeper facies needs further studies but may be longer. The distribution of *P. celloni* in other regions needs further studies, with revision of collections. However, based on the published data (see synonymy) it seems quite probable that *P. celloni* can be recognized in most known Telychian sequences.

## *Pterospathodus rhodesi* (Savage, 1985)

.1984 *Pterospathodus* n. sp. A Stouge and Bagnoli Stouge, p. 109, pl. 1, figs 1–6.
.1984 *Carniodus carnulus* Walliser, 1964; Stouge and Bagnoli Stouge, p. 108, pl. 1, figs 11–19.
.* 1985 *Pterospathodus amorphognathoides rhodesi* Savage, p. 714, fig. 3*A–T*.
.1985 *Carniodus carnulus* Walliser, 1964; Savage, p. 714, fig. 2*D–N*.
1985 *Xainzadontus dewukaxiaensis* Yu, p. 25, pl. 1, fig. 14.
1985 *Ozarkodina gaertneri* Walliser, 1964; Yu, pl. 1, fig. 8.
1985 *Roundya triangularis* Yu, p. 25, pl. 1, fig. 13.
v. 1986 *Carniodus carnulus* Walliser, 1964; Bischoff, p. 177, pl. 5, figs 18–34; pl. 6, figs 1–37.
v. 1986 *Pterospathodus procerus* (Walliser, 1964); Bischoff, p. 204, pl. 30, figs 3–11.
v. 1986 *Pterospathodus latus* Bischoff, p. 197, pl. 30, figs 15–18, 31; pl. 31, figs 1–14.
v. 1986 *Pterospathodus amorphognathoides* Walliser, 1964; Bischoff, p. 186, pl. 30, figs 19–22; pl. 31, figs 15–39.
.1987 *Pterospathodus pennatus rhodesi* (Savage, 1985); Over and Chatterton, p. 21, pl. 4, figs 5–6.
p. 1987 *Pterospathodus amorphognathoides* Walliser, 1964; Over and Chatterton, pl. 4, fig. 3 (*non* figs 1–2 [= *P. a. amorphognathoides*]).
.1989 *Pterospathodus rhodesi* (Savage, 1985); Männik and Aldridge, text-fig. 4*A–B*.
.1990 *Carniodus carnulus* Walliser, 1964; Armstrong, p. 68, pl. 4, figs 14–29.
.1990 *Pterospathodus amorphognathoides* Walliser, 1964; Armstrong, p. 115, pl. 19, figs 1–5.

.1990 *Pterospathodus pennatus rhodesi* (Savage, 1985); Armstrong, p. 120, pl. 20, figs 6–16.
p. 1991 *Carniodus carnulus* Walliser, 1964; McCracken, p. 108, pl. 3, figs 6–12, 15 (*non* figs 13–14 [= *P. p. procerus*]).
.1991 *Pterospathodus rhodesi* (Savage, 1985); McCracken, p. 109, pl. 5, figs 6–15.

*Remarks.* In some regions (Australia, Alaska, Greenland, Tibet). *P. a. amorphognathoides* is replaced by, or co-occurs with, *P. rhodesi*, all elements of which are characterized by extremely wide platform/platform ledges (see illustrations listed in synonymy). The origin of *P. rhodesi* is not known. In general, the morphology of the elements and the architecture of the apparatus suggest that *P. rhodesi* is closely related to the *P. amorphognathoides* lineage. However, the co-occurrence of *P. a. amorphognathoides* and *P. rhodesi* in some sections (e.g. in the southern Mackenzie

---

EXPLANATION OF PLATE 6

Figs 1–25, 27–35. *Pterospathodus pennatus procerus* (Walliser, 1964). 1, LO 7739t; inner lateral view of dextral $M_2$ element. 2, LO 7740t; inner lateral view of dextral $M_1$ element. 3, LO 7741t; inner lateral view of sinistral $M_2$ element. 4, LO 7742t; inner lateral view of sinistral $M_1$ element. 5, Cn 8065; outer lateral view of dextral $Pb_2$ element. 6, LO 7743t; outer lateral view of sinistral $Pb_2$ element. 7, LO 7744t; inner lateral view of sinistral $Sc_2$ element. 8, Cn 8066; upper view of sinistral Pa element. 9, LO 7745t; inner lateral view of dextral $Sc_2$ element. 10, LO 7746t; posterior view of dextral $Sb_2$ element. 11, LO 7747t; outer lateral view of dextral $Sb_2$ element. 12, LO 7748t; posterior view of dextral $Sb_1$ element. 13, LO 7749t; posterior view of sinistral $Sb_1$ element. 14, Cn 8067; outer lateral view of sinistral $Sc_1$ element. 15, LO 7750t; inner lateral view of sinistral $Sc_1$ element. 16, Cn 8068; outer lateral view of sinistral $Pb_1$ element. 17, LO 7751t; posterior view of sinistral $Sb_2$ element. 18, LO 7752t; outer postero-lateral view of sinistral $Sb_2$ element. 19, LO 7753t; inner antero-lateral view of sinistral $Sb_2$ element. 20, LO 7755t; outer lateral view of dextral Pc element. 21, LO 7755t; inner lateral view of dextral curved(?) element. 22, LO 7756t; inner lateral view of dextral $Sc_2$ element. 23, LO 7757t; inner lateral view of dextral $Sc_3$ element. 24, LO 7758t; inner lateral view of sinistral $Sc_3$ element. 25, LO 7759t; inner lateral view of dextral $Sc_2$ element. 27, LO 7760t; outer lateral view of sinistral $Sb_2$ element. 28, LO 7761t; outer lateral view of dextral carnuliform element, morph a. 29, LO 7762t; outer lateral view of dextral carnuliform element, morph a. 30, LO 7763t; inner lateral view of sinistral carnuliform element, morph b. 31, LO 7764t; outer lateral view of sinistral curved element. 32, LO 7765t; inner lateral view of sinistral carnuliform element, morph a. 33, LO 7766t; outer lateral view of sinistral carnuliform element, morph a. 34, LO 7767t; posterior view of Sa element. 35, LO 7768t; posterior view of Sa element. Figs 1–4, 7, 10–12, 15, 17–21, 25, 27–29, 31–33 and 35 from Nygårdsbäckprofilen-1 section (Gotland), sample G93-977LJ; figs 5, 8, 14 and 16 from Ohesaare core, sample M-935, int. 348·40–348·60 m; figs 6, 9, 13, 22–24, 30 and 34 from Nygårdsbäckprofilen-1 section (Gotland), sample G93-978LJ.

Figs 26, 36–54. *Pterospathodus celloni* (Walliser, 1964). 26, Cn 8069; outer lateral view of dextral $Pb_2$ element. 36, LO 7769t; upper view of sinistral Pa element. 37, Cn 8070; outer lateral view of dextral Pc element. 38, Cn 8071; inner lateral view of dextral $Sc_2$ element. 39, LO 7770t; inner lateral view of sinistral $Sc_2$ element. 40, Cn 8072; outer lateral view of dextral $Pb_1$ element. 41, Cn 8073; inner lateral view of dextral Pa element. 42, Cn 8074; inner lateral view of dextral carnuliform(?) element. 43, LO 7771t; inner lateral view of dextral $M_1$ element. 44, Cn 8075; inner lateral view of sinistral $Sc_1$ element. 45, LO 7772t; inner lateral view of sinistral Pa element. 46, LO 7773t; outer lateral view of sinistral $Pb_1$ element. 47, LO 7774t; inner lateral view of dextral $Sb_2$ element. 48, LO 7775t; outer lateral view of sinistral $Sb_2$ element. 49, LO 7776t; inner lateral view of dextral Pa element. 50, Cn 8076; inner lateral view of dextral carniciform(?) element. 51, Cn 8077; inner lateral view of dextral carnuliform(?) element. 52, Cn 8078; inner lateral view of sinistral carnuliform element. 53, LO 7777t; outer lateral view of dextral $Sb_2$ element. 54, Cn 8079; inner lateral view of sinistral carnuliform(?) element. Figs 26 and 44 from Viki core, sample M-967, int. 153·60–153·72 m; fig. 36 from När core (Gotland), int. 351·60–351·65 m; fig. 37 from Viki core, sample M-360, int. 153·35–153·50 m; figs 38 and 41 from Uulu-330 core, sample M-1070, int. 137·70–137·85 m; figs 39, 43, 45–46 and 48–49 from Själsö section (Gotland), sample G88-637LJ; fig. 40 from Uulu-330 core, sample M-1301, int. 138·05–138·15 m; figs 42, 50–52 and 54 from Viki core, sample M-976, int. 149·95–150·08 m; figs 47 and 53 from När core (Gotland), int. 361·30–361·40 m.

All × 50.


MÄNNIK, *Pterospathodus*

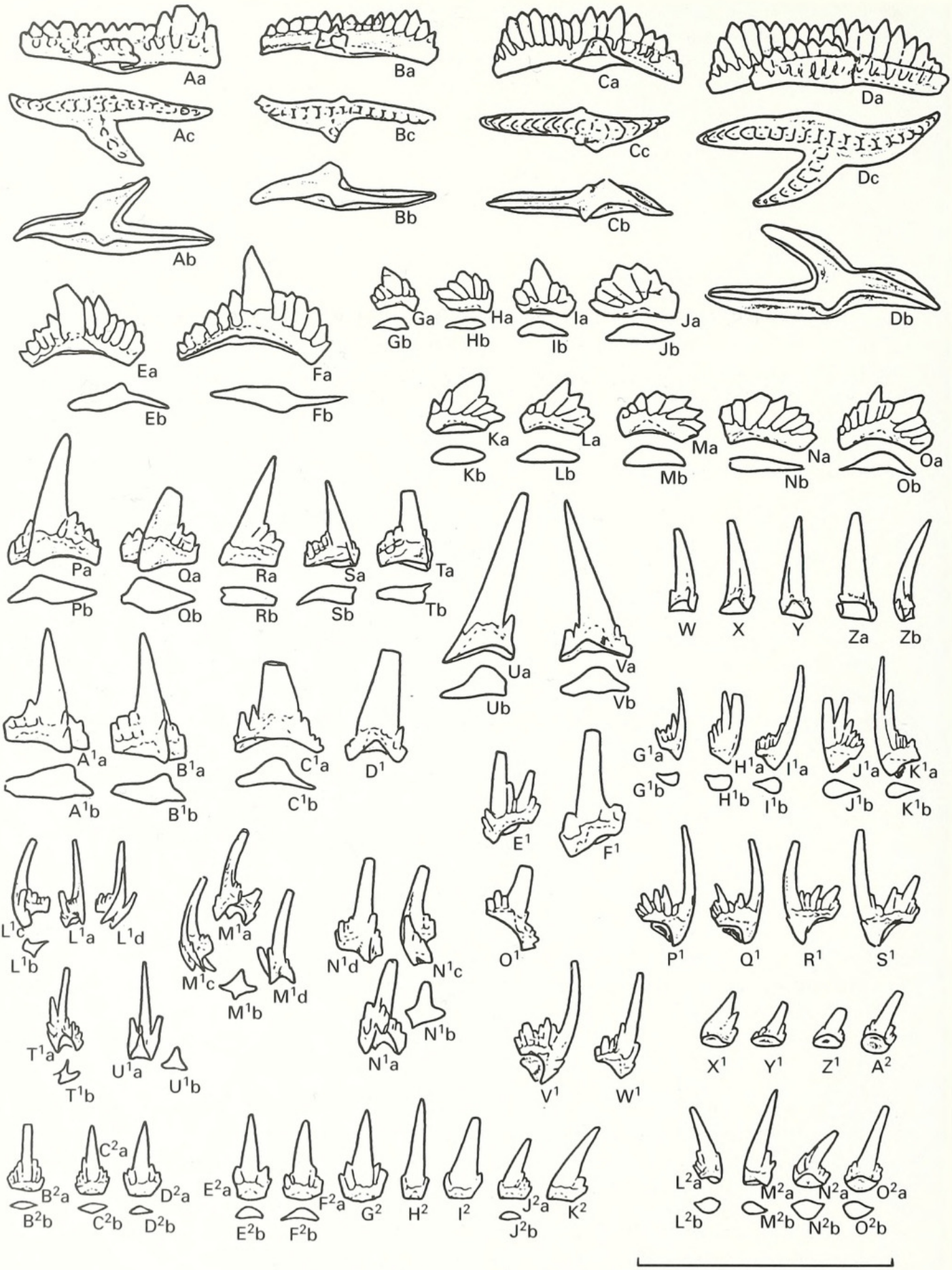


TEXT-FIG. 16. For caption see opposite.

Mountains, Northwest Territories of Canada; Over and Chatterton 1987) indicates that, most probably, they belong to separate species.

The Pa element of *P. rhodesi* is represented at least by two morphs: morph 1 with a bifurcated inner lateral process (Männik and Aldridge 1989, text-fig. 4*A*); and morph 2 with a pennate inner lateral process (Männik and Aldridge 1989, text-fig. 4*B*).

*P. rhodesi* has not been identified in the Baltic or in other parts of Europe.

*Occurrence. P. a. amorphognathoides* Zone (only?).

## ORIGIN

The ancestry of *Pterospathodus* is uncertain. *P. eopennatus* appears widely without a direct antecedent. Bischoff (1986) described a presumed direct ancestor of *P. celloni* (= *P. eopennatus* in this paper) from New South Wales, Australia, which he called *P. cadiaensis*. Elements assigned to this taxon by Bischoff are also known from several other regions (Norway – Aldridge and Mohamed 1982, pl. 1, fig. 33; Severnaya Zemlya – Männik 1983, fig. 4*Y*; Northern Urals – Melnikov, pers. comm.; South China – Aldridge, pers. comm.). Well preserved material from the last region revealed that, in reality, these elements belong to a *Gamachignathus* apparatus, and *P. cadiaensis* was reidentified as *G. macroexcavatus* (Wang and Aldridge, 1996).

The new data presented herein indicate an increased level of similarity between the *Pterospathodus* and *Pranognathus* apparatuses (Männik and Aldridge 1989, text-fig. 5; Uyeno and Barnes 1983, pl. 2, figs 1–11, 14–18, identified as belonging to *Pterospathodus*). However, although the elements of *Pranognathus* can be readily homologized with those of *Pterospathodus* (Pa, $Pb_1$, Pc, $M_1$, $Sc_1$, $Sc_2$, $Sb_1$, $Sb_2$ and Sa can be recognized in *Pranognathus*) there are still too many significant morphological differences between these two apparatuses to allow us to consider *Pranognathus* as a direct ancestor of *Pterospathodus*. In *Pranognathus*, the Pa and $Pb_1$ elements (Männik and Aldridge 1989, text-fig. 5*A–I*, *U–X*) possess deep wide cavities, the Pc element (Männik and Aldridge 1989, text-fig. 5*J–K*, *Y–Z*) has three long processes, the $M_1$ element (Männik and Aldridge 1989, text-fig. 5*L–M*) has a denticulated inner lateral process and a large number of denticles on the anterior and posterior processes, and the anterior process of the $Sc_2$ element (Männik and Aldridge 1989, text-fig. 5*S*) is densely denticulated. Also, several elements known from *Pterospathodus* ($Pb_2$, $Sc_3$, canuliform, carniciform and curved), have not been identified in *Pranognathus*. However, as the ranges of *Pterospathodus* and *Pranognathus* are separated by a considerable time interval, it cannot be excluded that these two taxa are related to each other.

Hence, the origin of *Pterospathodus* remains unknown and needs further studies.

## CONCLUSIONS

1. Elements previously referred to *Carniodus* do not belong to a separate genus, but formed part of the apparatus of *Pterospathodus*.
2. The structure of the *Pterospathodus* apparatus was evidently much more complicated than previously considered. It consists of at least 14 (15) elements: Pa, $Pb_1$, $Pb_2$, Pc, $M_1$, $M_2$ (so far recognized only in the *P. p. procerus* apparatus), $Sc_1$, $Sc_2$, $Sc_3$, $Sb_1$, $Sb_2$, Sa, carnuliform element with five morphs, curved element with three morphs and carniciform element.
3. In the Telychian, at least two distinct *Pterospathodus* lineages: *P. a. angulatus* – *P. a. amorphognathoides*, and *P. p. pennatus* – *P. p. procerus* existed and evolved separately, the former in the open shelf carbonate-terrigeneous facies and the latter in deeper basin graptolite-bearing facies.

---

TEXT-FIG. 16. *Pterospathodus pennatus procerus* (Walliser, 1964). A–D, Pa element. E–F, $Pb_1$ element. G–O, $Pb_2$ element. P–T, $A^1$–$B^1$, Pc element. U–V, $C^1$–$D^1$, $M_1$ element. W–Z, $M_2$ element. $E^1$–$F^1$, $O^1$, $Sc_1$ element. $G^1$–$K^1$, $Sc_3$ element. $L^1$–$M^1$, $Sb_1$ element. $N^1$, $T^1$, $Sb_2$ element. $P^1$–$S^1$, $V^1$–$W^1$, $Sc_2$ element. $U^1$, Sa element. $X^1$–$A^2$, carniciform element. $B^2$–$C^2$, carnuliform element, morph b. $D^2$–$M^2$, carnuliform element morph a. $N^2$–$O^2$, ?carniciform element. Scale bar represents 1 mm.

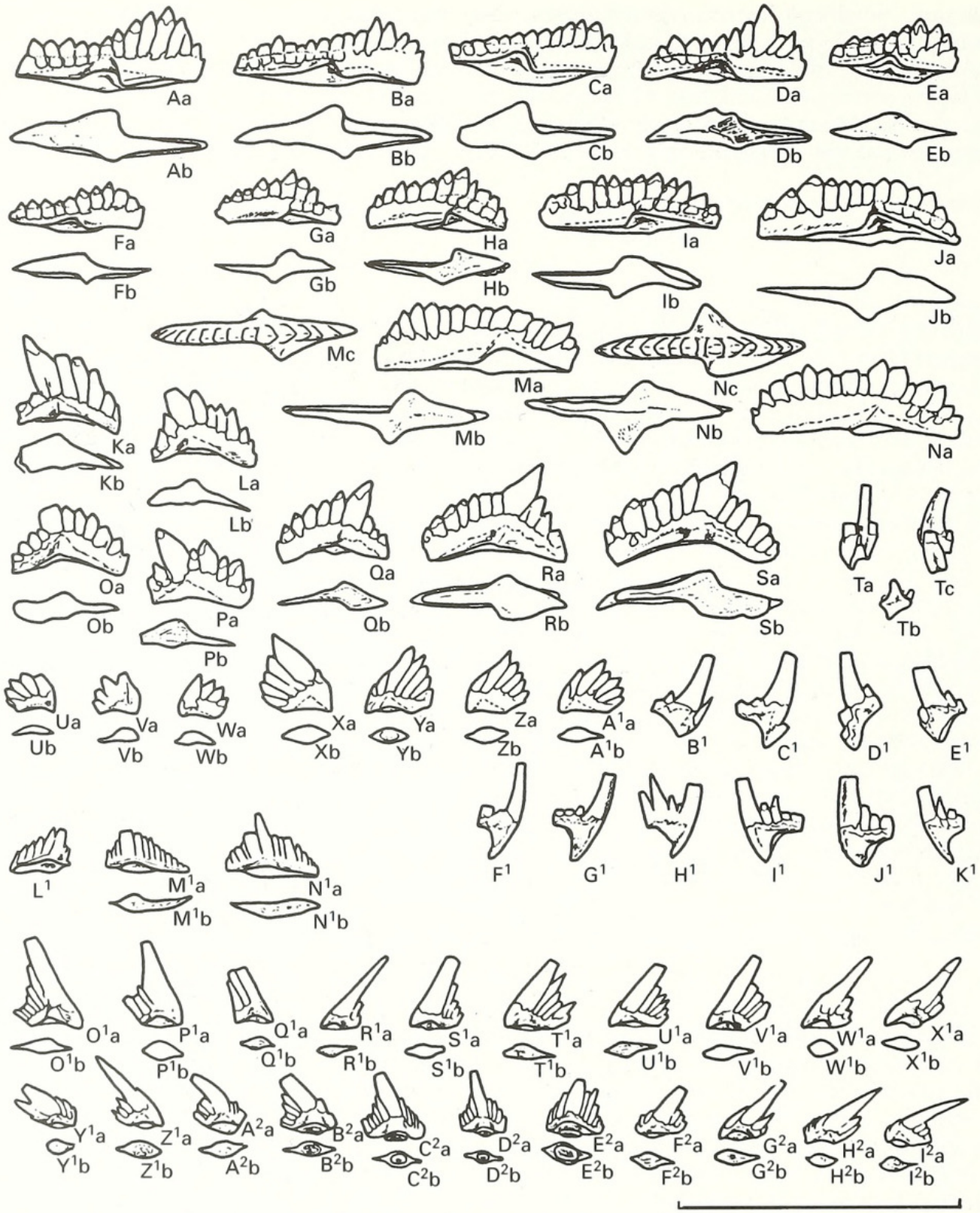


TEXT-FIG. 17. *Pterospathodus celloni* (Walliser, 1964). A–J, M–N, Pa element. K–L, O–S, $Pb_1$ element. T, $Sb_2$ element. U–$A^1$, $Pb_2$ element. $B^1$–$E^1$, $Sc_1$ element. $F^1$–$K^1$, $Sc_2$ element. $L^1$–$N^1$, carniciform(?) element. $O^1$–$I^2$, carnuliform(?) element. Scale bar represents 1 mm.

Both probably originated from a common ancestral taxon at the end of the *P. eopennatus* Zone, although they may have appeared in the upper part of the *A. irregularis* Subzone.

4. Evolution was more rapid, and the morphological variation within each population greater, in open shelf environments.

5. Three main intervals of evolution are recognized in the *Pterospathodus* sequence. The boundaries between them are marked by distinct morphological changes in the elements.
6. *P. celloni* was restricted to deeper basin environments, and was closely related to the *P. pennatus* lineage.
7. The appearance of *P. celloni* and *P. p. procerus* in open shelf environments occurred during times when the usual conditions there were partially (or completely – Ireviken Event) altered causing temporary disappearances or the final extinction of several lineages.
8. The evolutionary steps in the *Pterospathodus* lineage, together with changes shown by the rest of the Telychian conodont fauna, provide excellent potential for high resolution stratigraphy (Männik 1995, 1996).

*Acknowledgements*. Richard J. Aldridge, Howard A. Armstrong, Günther C. O. Bischoff, Antanas Brazuaskas, Lennart Jeppsson, Hans A. Nakrem, Hans P. Schönlaub and Otto H. Walliser kindly gave me free access to their collections of conodonts. Lennart Jeppsson and Richard J. Aldridge read the manuscript critically and suggested many improvements. Claes Bergman and Fredrik Jerre assisted with the SEM, Gennadi Baranov made the prints and Kaie Ronk the drawings of conodonts.

The research was carried out in the Institute of Geology, Tallinn (financed by the Institute of Geology and The Estonian Science Foundation), and in the Department of Historical Geology and Palaeontology, Lund University, Lund (financed by The Swedish Natural Science Research Council). My sincere thanks to everybody.

## REFERENCES

ALDRIDGE, R. J. 1972. Llandovery conodonts from the Welsh Borderland. *Bulletin of the British Museum (Natural History), Geology Series*, **22**, 127–231, pls 1–9.

—— 1974. An *amorphognathoides* Zone conodont fauna from the Silurian of the Ringerike area, south Norway. *Norsk Geologisk Tidsskrift*, **54**, 295–303.

—— 1975. The stratigraphic distribution of conodonts in the British Silurian. *Journal of the Geological Society, London*, **131**, 607–618, 3 pls.

—— 1979. An upper Llandovery conodont fauna from Peary Land, eastern North Greenland. *Rapport Grønlands Geologiske Undersøgelse*, **91**, 7–23, pls 1–2.

—— 1980. Notes on some Silurian conodonts from Ireland. *Journal of Earth Sciences of the Royal Dublin Society*, **3**, 127–132.

—— 1985. Conodonts of the Silurian System from the British Isles. 68–92. *In* HIGGINS, A. C. and AUSTIN, R. L. (eds). *A stratigraphical index of conodonts*. Ellis Horwood, Chichester, 263 pp.

—— JEPPSSON, L. and DORNING, K. J. 1993. Early Silurian episodes and events. *Journal of the Geological Society, London*, **150**, 501–513.

—— and MOHAMED, I. 1982. Conodont biostratigraphy of the early Silurian of the Oslo Region, 109–120, 2 pls. *In* WORSLEY, D. (ed.). Subcommission on Silurian Stratigraphy. Field Meeting, Oslo Region, 1982. *Paleontological Contributions from the University of Oslo*, **278**, 175.

AN TAI-XIANG 1987. [*The Lower Palaeozoic conodonts of South China.*] Beijing University Press, Beijing, 238 pp., 35 pls. [In Chinese.]

ARMSTRONG, H. A. 1990. Conodonts from the Upper Ordovician–Lower Silurian carbonate platform of North Greenland. *Grønlands Geologiske Undersøgelse*, **159**, 1–151, pls 1–23.

BARCA, S., FERRETTI, A., MASSA, P. and SERPAGLI, E. 1992. The Hercynian Arburese Tectonic Unit of SW Sardinia. New stratigraphic and structural data. *Rivista Italiana di Paleontologia e Stratigrafia*, **98**, 119–136, pls 1–4.

BRAZAUSKAS, A. Z. 1983. Conodont zones of Lithuanian Llandovery facies. *Nauchnye Trudy Vysshih Uchebnyh Zavedenij Litovskoj SSR, Geologija*, **4**, 41–66. [In Russian, with English and Lithuanian summaries].

BARRICK, J. E. 1983. Wenlockian (Silurian) conodont biostratigraphy, biofacies, and carbonate lithofacies, Wayne Formation, Central Tennessee. *Journal of Paleontology*, **57**, 208–239.

—— and KLAPPER, G. 1976. Multielement Silurian (late Llandoverian–Wenlockian) conodonts of the Clarita Formation, Arbuckle Mountains, Oklahoma, and phylogeny of *Kockelella*. *Geologica et Palaeontologica*, **10**, 59–100, pls 1–4.

BISCHOFF, G. C. O. 1986. Early and middle Silurian conodonts from midwestern New South Wales. *Courier Forschungsinstitut Senckenberg*, **89**, 337, pls 1–34.

COOPER, B. J. 1977. Toward a familial classification of Silurian conodonts. *Journal of Paleontology*, **51**, 1057–1071.

DRYGANT, D. M. 1969. [Konodonty Restevskogo, Kitajgorodskogo i Mukshinskogo gorizontov Silura Podolii.] *Paleontologicheskij Sbornik*, **6** (1), 49–54, 1 pl. [In Russian].

—— 1984. [*Korrelyaciya i konodonty silurijskih-nizhnedevonskih otlozhenij Volyno-Podolij.*] Naukova Dumka, Kiev, 192 pp., 16 pls. [In Russian].

DUMOULIN, A. and HARRIS, A. G. 1987. Off-platform Silurian sequence in the Ambler River Quadrangle. *Geologic Studies in Alaska by the U.S. Geological Survey during 1987*, 35–38.

HELFRICH, C. T. 1980. Late Llandovery–early Wenlock conodonts from the upper part of the Rose Hill and the basal part of the Mifflintown formations, Virginia, West Virginia, and Maryland. *Journal of Paleontology*, **54**, 557–569, 2 pls.

IGO, H. and KOIKE, T. 1968. Ordovician and Silurian conodonts from the Langkawi Island, Malaya, Part 2. *Geology and Palaeontology of Southeast Asia*, **4**, 1–21, pls 1–3.

JIANG WU, ZHANG FANG, ZHOU XIYUN, XIONG JIANFEI, DAI JINYIE and ZHONG DUAN 1986. [*Conodonts – palaeontology.*] Southwestern Petroleum Institute, Sichuan, 264 pp, pls 265–287. [In Chinese].

JEPPSSON, L. 1979. Conodonts. 225–248. *In* JAANUSSON, V., LAUFELD, S. and SKOGLUND, R. (eds). Lower Wenlock faunal and floral dynamics – Vattenfallet section, Gotland. *Sveriges Geologiska Undersökning Avdhandlingar och Uppsatser*, **C762**, 1–294.

—— 1987. Lithological and conodont distributional evidence for episodes of anomalous oceanic conditions during the Silurian. 129–145. *In* ALDRIDGE, R. J. (ed.). *Palaeobiology of conodonts*, Ellis Horwood, Chichester, 180 pp.

—— 1994. A new standard Wenlock conodont zonation. 133. *In* SCHÖNLAUB, H. P. and KREUZER, L. H. (eds). IUGS Subcommission on Silurian Stratigraphy – Field Meeting Eastern + Southern Alps, Austria 1994 in mem. H. Jaeger. *Berichte der Geologischen Bundesanstalt*, **30**, 1–156.

—— 1997. A new latest Telychian, Sheinwoodian and early Homerian (early Silurian) Standard Conodont Zonation. *Transactions of the Royal Society of Edinburgh: Earth Sciences*, **88**, 91–114.

—— and MÄNNIK, P. 1993. High-resolution correlations between Gotland and Estonia near the base of the Wenlock. *Terra Nova*, **5**, 348–358.

KLAAMANN, E. 1990. Locality 8:3. Valgu outcrop. 181–182. *In* KALJO, D. and NESTOR, H. (eds). *Field Meeting, Estonia* 1990. *An excursion guidebook*. Tallinn, 209 pp.

KLEFFNER, M. A. 1985. Conodont biostratigraphy of the stray 'Clinton' and 'Packer Shell' (Silurian, Ohio subsurface) and its bearing on correlation. 219–229, 2 pls. *In* GRAY, J., MASLOWSKI, A., McCULLOUGH, W. and SHAFER, W. E. (eds). *The new Clinton collection – 1985*. Ohio Geological Society, Columbus, Ohio, 243 pp.

—— 1987. Conodonts of the Estill Shale and Bisher Formation (Silurian, southern Ohio): biostratigraphy and distribution. *Ohio Journal of Sciences*, **87** (3), 78–89.

—— 1991. Conodont biostratigraphy of the upper part of the Clinton Group and the Lockport Group (Silurian) in the Niagara Gorge Region, New York and Ontario. *Journal of Paleontology*, **65**, 500–511.

KUWANO, Y. 1976. Finding of Silurian conodont assemblages from the Kurosegawa tectonic zone in Shikoku, Japan. *Memoirs of the National Science Museum*, **9**, 17–22, 2 pls. [In Japanese with English summary].

LIEBE, R. M. and REXROAD, C. B. 1977. Conodonts from Alexandrian and early Niagaran rocks in the Joliet, Illinois, area. *Journal of Paleontology*, **51**, 844–857, pls 1–2.

MABILLARD, J. E. and ALDRIDGE, R. J. 1983. Conodonts from the Coralliferous Group (Silurian) of Marloes Bay, south-west Dyfed, Wales. *Geologica et Palaeontologica*, **17**, 29–43, pls 1–4.

MANARA, C. and VAI, G. B. 1970. La sezione e i conodonti del costone sud del M. Rauchkofel (Paleozoico, Alpi Carniche). *Giornale di Geologia*, **36**, 441–503, pls 59–63.

McCRACKEN, A. D. 1991. Silurian conodont biostratigraphy of the Canadian Cordillera with a description of new Llandovery species. 97–127, 5 pls. *In* ORCHARD, M. J. and McCRACKEN, A. D. (eds). Ordovician to Triassic conodont paleontology of the Canadian Cordillera. *Bulletin of the Geological Survey of Canada*, **417**, 1–335.

MILLER, R. H. 1976. Revision of upper Ordovician, Silurian, and lower Devonian stratigraphy, southwestern Great Basin. *Bulletin of the Geological Society of America*, **87**, 961–968.

—— 1978. Early Silurian to early Devonian conodont biostratigraphy and depositional environments of the Hidden Valley Dolomite, southeastern California. *Journal of Paleontology*, **52**, 323–344, pls 1–4.

MÄNNIK, P. 1983. Silurian conodonts from Severnaya Zemlya. *Fossils and Strata*, **15**, 111–119, 1 pl.

—— 1992. [Upper Ordovician and lower Silurian conodonts in Estonia.] Unpublished Ph.D. thesis, University of Tartu, Estonia. [In Russian].

—— 1995. The evolution of selected conodont lineages and an improved zonation for the Telychian (late Llandovery). 52–54. *In* BROCK, G. A. (ed.). First Australian Conodont Symposium (AUSCOS-I) and the

Boucot Symposium, 18–21 July, 1995, Abstracts and Programme. *Special Publications of the Macquarie University Centre for Ecostratigraphy and Palaeobiology* (*MUCEP*), **1**, 1–108.

—— 1996. Telychian (Early Silurian) conodont *Pterospathodus*: evolution and taxonomy. 35. *In* DZIK, J. (ed.). *Sixth European Conodont Symposium* (*ECOS VI*), *Abstracts*. Institut Paleobiologii PAN, Warszawa, 70 pp.

—— and ALDRIDGE, R. J. 1989. Evolution, taxonomy and relationships of the Silurian conodont *Pterospathodus*. *Palaeontology*, **32**, 893–906.

—— and MAŁKOWSKI, K. 1998. Silurian conodonts from the Gołdap core, Poland. *Palaeontologia Polonica*, **58**, 139–149.

—— and VIIRA, V. 1990. Conodonts. 84–89, pls 16–18. *In* KALJO, D. and NESTOR, H. (eds). *Field Meeting, Estonia 1990. An excursion guidebook*. Tallinn, 209 pp.

NAKREM, H. A. 1986. Llandovery conodonts from the Oslo Region, Norway. *Norsk Geologisk Tiddskrift*, **66**, 121–133.

NEHRING-LEFELD, M. 1985. Conodonts of the *amorphognathoides* Zone (Silurian) from eastern part of the Podlasie Depression. *Kwartalnik Geologiczny*, **29** (3/4), 625–652, pls 1–6. [In Polish with English and Russian summaries].

—— 1992. Biostratigraphy of the Old Paleozoic carbonates in the Zawiercie area (NE margin of the Upper Silesian Coal Basin). *Geological Quarterly*, **36**, 171–198, pls 1–5.

NICOLL, R. S. and REXROAD, C. B. 1968. Stratigraphy and conodont paleontology of the Salamonie Dolomite and Lee Creek Member of the Brassfield Limestone (Silurian) in southeastern Indiana and adjacent Kentucky. *Bulletin of the Department of Natural Resources of the Geological Survey of Indiana*, **40**, 1–73, pls 1–7.

NOWLAN, G. S. 1981. Late Ordovician – early Silurian conodont biostratigraphy of the Gaspé Peninsula – a preliminary report. 257–291, 7 pls. *In* LESPÉRANCE, P. J. (ed.). *Subcommission on Silurian Stratigraphy, Ordovician-Silurian Boundary Working Group. Field Meeting, Anticosti–Gaspé, Québec 1981, Vol. 2: stratigraphy and paleontology*. University of Montreal, 321 pp.

—— 1983. Early Silurian conodonts of eastern Canada. *Fossils and Strata*, **15**, 95–110.

OVER, D. J. and CHATTERTON, D. E. 1987. Silurian conodonts from the southern Mackenzie Mountains, Northwest Territories, Canada. *Geologica et Palaeontologica*, **21**, 1–49, pls 1–8.

PICKETT, J. 1978. Silurian conodonts from Blowclear and Liscombe Pools, New South Wales. *Journal and Proceedings of the Royal Society of New South Wales*, **111**, 35–39.

QIU HONGRONG 1985. Silurian conodonts in Xizang (Tibet). *Bulletin of the Institute of Geology of the Chinese Academy of the Geological Science*, **11**, 23–38, pls 1–2. [In Chinese with English summary].

—— 1988. Early Palaeozoic conodont biostratigraphy of Xizang (Tibet). *Symposium on Stratigraphy and Paleontology*, 185–202, 6 pls.

REXROAD, C. R. and NICOLL, R. S. 1971. Summary on conodont biostratigraphy of the Silurian System of North America. *Memoir of the Geological Society of America*, **127**, 207–225, pls 1–2.

—— —— 1972. Conodonts from the Estill Shale (Silurian, Kentucky and Ohio) and their bearing on multielement taxonomy. *Geologica et Palaeontologica*, **SB1**, 57–74, pls 1–2.

SALADŽIUS, V. 1975. Conodonts of the Llandoverian (lower Silurian) deposits of Lithuania. 219–225, pls 1–2. *In* GRIGELIS, A. A. (ed.). *The fauna and stratigraphy of Palaeozoic and Mesozoic of Baltic and Byelorussia*. 'Mintis', Vilnius, 249 pp. [In Russian, with English summary].

SAVAGE, N. M. 1985. Silurian (Llandovery–Wenlock) conodonts from the base of the Heceta Limestone, southeastern Alaska. *Canadian Journal of Earth Sciences*, **22**, 711–727.

—— POTTER, A. W. and WYATT, G. G. 1983. Silurian and Silurian to early Devonian conodonts from West Central Alaska. *Journal of Paleontology*, **57**, 873–875.

SCHÖNLAUB, H. P. 1969. Das Paläozoikum zwischen Bischofalm und Hohem Trieb (Zentrale Karnische Alpen). *Jahrbuch der Geologischen Bundesanstalt*, **112**, 265–320, pls 1–2.

—— 1971. Zur Problematic der Conodonten-Chronologie an der Wende Ordoviz/Silur mit besonderer Berücksichtigung der Verhältnisse im Llandovery. *Geologica et Palaeontologica*, **5**, 35–57, pls 1–3.

—— 1975. Conodonten aus dem Llandovery der Westkarawanken (Österreich). *Verhandlungen der Geologischen Bundesanstalt*, **2–3**, 45–65, pls 1–2.

SPASOV, H. and FILIPOVIĆ, I. 1966. The conodont fauna of the older and younger Palaeozoic in southeastern and northwestern Bosnia. *Geološki Glasnik*, **11**, 33–53, pls 1–3.

STOUGE, S. and BAGNOLI STOUGE, G. 1984. An upper Llandovery conodont fauna from Eastern Hall Land, North Greenland. *Bolletino della Società Paleontologica Italiana*, **23**, 103–112, pls 1–2.

SWEET, W. C. 1981. Morphology and composition of elements. W5–W20. *In* ROBINSON, R. A. (ed.). *Treatise on invertebrate paleontology. Part W. Miscellanea. Supplement 2. Conodonta*. Geological Society of America and University of Kansas Press, Boulder, Colorado and Lawrence, Kansas, 202 pp.

—— 1988. The Conodonta. Morphology, taxonomy, paleoecology, and evolutionary history of a long-extinct animal phylum. *Oxford Monographs on Geology and Geophysics*, **10**, 1–212.

UYENO, T. T. 1990. Biostratigraphy and conodont faunas of Upper Ordovician through Middle Devonian rocks, eastern Arctic Archipelago. *Bulletin of the Geological Survey of Canada*, **401**, 1–210, pls 1–20.

—— and BARNES, C. R. 1981. A summary of Lower Silurian conodont biostratigraphy of the Jupiter and Chicotte formations, Anticosti Island, Québec. 173–184, 1 pl. *In* LESPÉRANCE, P. J. (ed.). *Subcommission on Silurian Stratigraphy, Ordovician-Silurian Boundary Working Group. Field Meeting, Anticosti–Gaspé, Québec 1981, Vol. 2: stratigraphy and paleontology*. University of Montreal, 321 pp.

—— —— 1983. Conodonts of the Jupiter and Chicotte formations (lower Silurian), Anticosti Island, Québec. *Bulletin of the Geological Survey of Canada*, **355**, 1–48, pls 1–9.

WALLISER, O. H. 1964. Conodonten des Silurs. *Abhandlungen des Hessischen Landesamtes für Bodenforschung*, **41**, 1–106, pls 1–32.

WANG CHEN-YUAN and ALDRIDGE, R. J. 1996. Conodonts. 46–55, pls 1–3. *In* CHEN XU and RONG JIA-YU (eds). [*Telychian* (*Llandovery*) *of the Yangtze Region and its correlation with British Isles*.] Science Press, Beijing, 157 pp. [In Chinese].

WATKINS, R., KUGLITSCH, J. J. and McGEE, P. E. 1994. Silurian of the Great Lakes Region, Part 2: paleontology of the Upper Llandovery Brandon Bridge Formation, Walworth County, Wisconsin. *Milwaukee Public Museum Contributions in Biology and Geology*, **87**, 1–71, pls 1–4.

YU HONGJIN 1985. Conodont biostratigraphy of Middle–Upper Silurian from Xainza, Northern Xizang (Tibet). *Contribution to the geology of the Qinghai-Xizang* (*Tibet*) *Plateau*, **16**, 15–31, pls 1–3. [In Chinese with English summary].

PEEP MÄNNIK
Institute of Geology
Tallinn Technical University
Estonia pst. 7
EE0001 Tallinn, Estonia
e-mail mannik@gi.ee

Typescript received 3 July 1997
Revised typescript received 25 March 1998

## APPENDIX

List of localities cited in text (see also Text-fig. 1).

A. Exposures

1. Valgu – a drainage canal; studied section corresponds to Point 1 in Klaamann (1990, p. 181).
2. Velise-Kõrgekalda – low cliff on the left bank of the Päärdu (on some maps indicated as Velise) River; *c.* 2·5 km west-south-west of a bridge across the river in Velise village, central Estonia.
3. Själsö – shore exposure; *c.* 4·3 km west of Väskinde church, Gotland, Sweden.
4. Överstekvarn 2 – several small exposures in the southern brook about 200 m north-west of Överstekvarn; *c.* 4·45 km (south-)south-west of Lummelunda church, Gotland, Sweden.
5. Nygårdsbäckprofilen 1 – a brook section at the mouth of Nygårdsbäcken (bäcken = brook) and shore section south-west of it; *c.* 2·97 km north-west of Västerhedje church, Gotland, Sweden.

B. Cores

1. The Nurme, Uulu-330, Viki and Ohesaare cores are housed in the Särghaua field station (central Estonia), Institute of Geology, Tallinn Technical University.
2. The Pahapilli core is housed in the Turja field station (southern Saaremaa, Estonia), Geological Survey of Estonia.
3. The När core is housed in the Geological Survey of Sweden, Uppsala, Sweden.